NLRC5

An NLR member with impact on adaptive and innate immune mechanisms and its protective role in the progression of colitis

Dissertation

zur Erlangung des Doktorgrades
der Mathematisch-Naturwissenschaftlichen Fakultät
der Christian-Albrechts-Universität zu Kiel

Vorgelegt
von
Manja Ehmke

Kiel, 2015

Diese Dissertation wurde angefertigt unter der Leitung von Prof. Dr. Philip Rosenstiel am Institut für Klinische Molekularbiologie (IKMB).

1. GUTACHTER:	PROF. DR. PHILIP ROSENSTIEL
2. GUTACHTER:	PROF. DR. THOMAS ROEDER
DATUM DER DISPUTATION:	11. JANUAR 2015
ZUM DRUCK GENEHMIGT:	11. JANUAR 2015

DER DEKAN DER MATHEMATISCH-NATURWISSENSCHAFTLICHEN FAKULTÄT

gez. Prof. Dr. Wolfgang J. Duschl

EIDESSTATTLICHE ERKLÄRUNG

Hiermit versichere ich, Manja Ehmke, geboren am 09. Oktober 1982 in Stralsund, dass ich die vorliegende Dissertation mit dem Titel

„NLRC5 – An NLR member with impact on adaptive and innate immune mechanisms and its protective role in the progression of colitis“

selbst und selbständig gemäß den Regeln der guten wissenschaftlichen Praxis der Deutschen Forschungsgemeinschaft und ausschließlich unter Verwendung der hier angegebenen Hilfsmittel angefertigt habe.
Darüber hinaus versichere ich, dass ich zeitgleich mit diesem Thema nicht an einer anderen Fakultät im In- oder Ausland die Zulassung zur Promotion beantragt habe oder beantragen werde.
Dies ist mein erstes Promotionsvorhaben an einer Hochschule. Ich habe weder eine missglückte Promotion hinter mir, noch wurde mir je ein akademischer Grad entzogen.

.....

Manja Ehmke

NLRC5 – An NLR member with impact on adaptive and innate immune mechanisms and its protective role in the progression of colitis

TABLE OF CONTENTS

1 Introduction 6

1.1 The Immune System 6
1.2 Innate Immunity 6

1.2.1 Early Induced Responses: Inflammation & Cytokines 7
1.2.2 Pattern Recognition Receptors – Innate Immune Sensors 8
1.2.3 TLRs – TOLL-like Receptors 9
1.2.4 NLRs – Nucleotide-Binding Domain And Leucine-Rich Repeats-Containing Receptors 9

1.2.4.1 Discovery & Plant Homologues 9

1.2.4.2 Structure & Subfamilies 9

1.2.4.3 Signaling 10

1.2.4.4 NLR Ligands & Expression 11

1.2.4.5 NLRs and Disease 11

1.2.5 NLRC5 – An NLR Member With Ambiguous Functions 12

1.2.5.1 Expression & Induction 12

1.2.5.2 Structure 12

1.2.5.3 Proposed Functions 13

1.3 Adaptive Immunity 15

1.3.1 Generation & Maturation Of Lymphocytes 15
1.3.2 Variant Lymphocyte Antigen Receptors 16
1.3.3 B Lymphocytes & Humoral Adaptive Immunity 16
1.3.4 T Lymphocytes & Cell-Mediated Adaptive Immunity 16
1.3.5 Antigen Presentation 17

1.3.5.1 MHC Class II Complex 17

1.3.5.2 MHC Class I Complex 18

1.4 Inflammatory Bowel Disease 19

1.4.1 Clinical Manifestation 19
1.4.2 Pathogenesis 20
1.4.3 Therapy 20
1.4.4 DSS-Induced Colitis 21

1.5 Objective 22

2 Materials & Methods 23

2.1 Experimental Mice 23

2.1.1 Generation of *Nlrc5* Knockout Mice 23
2.1.2 Animal Husbandry 24
2.1.3 Genotyping 24

2.1.4 Withdrawal of Murine Material for *ex vivo* Analyses 25
2.1.5 Experimental DSS Colitis 25
2.2 Histology 25
2.2.1 Hematoxylin & Eosin Staining 25
2.2.2 Periodic Acid – Schiff Stain 26
2.2.3 Microscopy 26
2.3 Cell Culture 26
2.3.1 Cell lines & Passage 26
2.3.2 Primary Cell Culture 27
2.3.3 Harvesting Cultured Cells 28
2.3.4 Cell Stimulations 28
2.4 Flow Cytometry 28
2.5 Enzyme-Linked Immunosorbent Assay 29
2.6 Multiplex Assay 30
2.7 Isolation & Analyses of DNA 30
2.7.1 DNA Extraction 30
2.7.2 Polymerase Chain Reaction 30
2.7.3 Agarose Gel Electrophoresis 31
2.8 Isolation & Analyses of RNA 31
2.8.1 RNA Isolation & Determination of Concentration 31
2.8.2 Genomic DNA Contaminations & RNA Clean Up 32
2.8.3 Reverse Transcription PCR 32
2.8.4 Quantitative Real Time PCR 33
2.9 Isolation & Analyses of Proteins 34
2.9.1 Protein Isolation & Determination of Concentration 35
2.9.2 SDS–PAGE 35
2.9.3 Western Blotting (Immunoblotting) 36
2.10 Statistical Analyses 38
2.11 Tissue Panels 38
2.12 Software 38
3 Results 39
3.1 NLRC5 – Expression and Induction 39
3.1.1 *NLRC5* RNA is highly expressed in human and murine immune tissues 39
3.1.2 NLRC5 protein was detected in various cell lines and is upregulated by IFNγ 40
3.2 Analysis of Secondary Immune Organs in *Nlrc5* ko Mice 41
3.2.1 No changes in spleen weight 41
3.2.2 No structural alterations in secondary lymphoid organs 41
3.2.3 Altered immune cell populations in the spleen 43
3.3 The Expression of MHC Molecules on *Nlrc5*-Deficient Cells 43
3.3.1 Diminished MHC class I expression on *Nlrc5*-deficient leukocytes 43

3.3.2 Two MHC class I expressing leukocytes populations exist 45
3.3.3 Enlarged population of MHC class II$^+$ cells in the spleen 47
3.3.4 MHC Class I is still inducible in *Nlrc5*-deficient lymphocytes 47
3.4 Altered Cytokine Expression in *Nlrc5*-Deficient Cells 48
3.4.1 Impaired induction of type I and II IFNs 48
3.4.2 Impaired induction of Il-1β 51
3.4.3 Altered expression of pro-inflammatory cytokines 52
3.5 The Impact of Nlrc5 on Experimental Murine Colitis 53
3.5.1 Increased severity of acute colitis in *Nlrc5* ko mice 53
3.5.1.1 Decreased survival during acute DSS treatment 54
3.5.1.2 Elevated disease activity index 54
3.5.1.3 Comparable colon shortening 56
3.5.1.4 Altered colonic inflammation and epithelial damage 57
3.5.1.5 Increased goblet cell hypoplasia in the colon 59
3.5.1.6 Elevated expression of distinct cytokines 60
3.5.1.7 Altered spleen weight in *Nlrc5* ko and wt mice 62
3.5.1.8 Elevated myeloperoxidase expression 62
3.5.1.9 Reduced *Cd8* expression in murine spleen 63
3.5.2 Increased Severity of Chronic Colitis in *Nlrc5* ko Mice 63
3.5.2.1 Decreased survival during chronic DSS treatment 64
3.5.2.2 Progression of body weight loss and diarrhea during chronic colitis 64
3.5.2.3 Severe colon shortening in *Nlrc5* ko mice 66
3.5.2.4 Elevated crypt loss in an *Nlrc5* ko subgroup 66
3.5.2.5 Elevated expression of distinct cytokines 68
3.5.2.6 Altered spleen weight in *Nlrc5* ko and wt mice 69
3.5.2.7 Elevated myeloperoxidase expression 70
3.5.2.8 Expression of *Cd4* and *Cd8* in murine spleen and colon tissue 70
4 Discussion 72
4.1 NLRC5 expression – Implications for potential functions 72
4.2 The expression of MHC molecules is altered on *NLRC5* deficient cells 74
4.2.1 NLRC5-dependent MHC class I expression on immune cells 74
4.2.2 NLRC5-independent MHC class I expression on immune cells 75
4.2.3 *NLRC5* deficiency affects the expression of MHC class II 77
4.3 *NLRC5* deficiency leads to a diminished CD8$^+$ T cell population 78
4.4 *NLRC5* deficiency does not affect CD4$^+$ T cell numbers 79
4.5 NLRC5 has a complex influence on cytokine responses in primary immune cells 79
4.6 Influence of NLRC5 on experimental colitis *in vivo* 81

4.6.1 Mice lacking *Nlrc5* are more susceptible to DSS-induced colitis 82
4.6.2 The production of inflammatory cytokines was elevated in *Nlrc5*-deficient mice upon DSS treatment 83
4.6.3 The enhanced epithelial destruction in the colon of *Nlrc5* ko mice is not due to an elevated influx of inflammatory cells 85
4.6.4 An altered MHC expression in *Nlrc5*-deficient mice can favor intestinal inflammation by different means 87
4.6.5 *Nlrc5* ko mice are susceptible to develop an aggravated chronic colitis accompanied by hyposplenism 89

5 Clinical Relevance & Future perspectives 91

5.1 NLRC5 is potently involved in innate and adaptive defense against intracellular pathogens 91
5.2 NLRC5: a new susceptibility gene for IBD or inflammatory diseases? 91
5.3 NLRC5 might be a promising target to enhance tumor immunity 92
5.4 Functional NLRC5 defects might induce a clinical picture comparable to BLS I 92
5.5 Future perspectives & Concluding remarks 93

6 Summary 94
7 Zusammenfassung 96
8 Appendix 98

8.1 Bibliography 98
8.2 Figure Directory 111
8.3 Table Directory 112
8.4 Abbreviations 113

1 INTRODUCTION

1.1 THE IMMUNE SYSTEM

Organisms are in constant contact to potentially harmful exogenous influences. Therefore, mechanisms have evolved that aim to protect the host. They are referred to as the immune system.
The word “immune” is derived from the Latin *in munos* meaning “to be unaffected”. As biological term the designation “immune” describes the insusceptibility of an organism towards foreign or abnormal structures. Protozoa as well as metazoa possess an inbred innate immune system, which comprises various immediate nonspecific defense mechanisms, but do not lead to an immunological memory. Vertebrates developed additional, more complex immune processes that adapt to the specific stimulus. This acquired immunity persists as immunological memory after stimulus removal and allows a faster and more efficient response in case of a reinfection.

1.2 INNATE IMMUNITY

Innate immune responses are characterized by a rapid onset, a limited specificity and no formation of an immunological memory.

Microorganisms, which summarize bacteria, viruses, fungi and multicellular eukaryotic parasites, are permanently in contact with the human body on external and internal epithelial surfaces. The epithelial barrier is a first protection shield that keeps away the vast majority of potentially harmful environmental agents. Next to mechanical protection, epithelia also possess chemical defense mechanisms to protect against microorganisms by secreting antimicrobial peptides e.g. defensins or lysozyme onto external epithelial surfaces. Microorganisms that overcome the epithelial barrier and invade the organism, e.g. through epithelial lesions, face a first line of specialized phagocyting cells, namely macrophages (Mϕ) and dendritic cells (DCs), that reside in the underlying tissues. Both carry special inherited receptors on their outer surface that recognize evolutionary conserved pathogen-associated molecular patterns (PAMPs) and are therefore called pattern recognition receptors (PRR).
Ligand recognition by distinct PRRs activates Mϕs as well as DCs to phagocytose the encountered microorganism. Other PRRs are secreted into the extracellular fluids and are part of the humoral innate immunity. They bind foreign pattern and thereby opsonize invading microorganisms for subsequent phagocytosis. The elimination by phagocytosis starts immediately upon microorganism invasion and is the prominent innate mechanism within the first four hours after microbial penetration. The response is able to remove invading microorganisms before any signs of infection might even develop (Janeway, 2005).

Microorganisms that cannot be repelled at this immediate early stage lead to the induction of early induced responses and are called pathogenic microorganisms or pathogens. These responses are the main defense at 4-96 hours post infection. They are also induced by PRRs. These do not only induce phagocytosis, but also generate intracellular signals that lead to the expression of pro-inflammatory cytokines and chemokines, which in turn initiate a local inflammation.
Inherited innate responses are further indispensable for the induction of precise adaptive mechanisms (Janeway, 2005).

1.2.1 EARLY INDUCED RESPONSES: INFLAMMATION & CYTOKINES

Inflammation is a physiological reaction towards potentially harmful stimuli like invading microorganisms or irritating substances. It can also be directed against self molecules leading to auto-inflammatory disorders.
Under steady state conditions, monocytes from the blood migrate into the tissues, where they differentiate into Mϕs and phagocytose self and foreign material within the extracellular compartment. Mϕs can initiate an inflammation via their PRRs. Activated Mϕs produce and secrete pro-inflammatory cytokines especially tumor necrosis factor alpha (TNFα), interleukin 1 beta (IL-1β) and IL-6. TNFα and IL-1β potently activate the surrounding endothelial cells leading to vasodilatation and hence an upregulation of blood flow into the infected area. The increased perfusion causes redness (*rubor*) and heating (*calor*), two of the five cardinal features of inflammation. Vessels increase their permeability allowing the leakage of fluid and plasma proteins from the blood into the infected tissues. This causes tissue swelling (*tumor*) and the sensation of pain (*dolor*). Aching is further induced by prostaglandins, which are rapidly produced by activated Mϕs together with other lipid mediators as leukotrienes and platelet activating factor (PAF). PAF mediates increased coagulation in the surrounding efferent vessels, which prevents that the infection spreads through the blood stream. Moreover, inflammation is characterized by a functional loss within the affected area (*functio laesa*).
Activated Mϕs produce chemoattractant cytokines, so called chemokines. These drive a chemotactic invasion of specific leukocytes into the inflamed area. TNFα induces an increased vessel diameter and the expression of special adhesion molecules on the endothelium. In combination with the chemokines CXCL8 (IL-8, murine: KC) and CCL2 this enables leukocyte extravasation. Within the tissue leukocytes move further along a chemokine gradient towards the origin of inflammation. CXCL8 is a very early induced chemokine mediating the attraction and extravasation of neutrophil granulocytes and naïve T lymphocytes. Later, CCL2 is secreted to attract monocytes and immature DCs into the inflamed tissue. These cell types do not only phagocytose, but also present antigen and therefore convey a pivotal role in the developing adaptive responses.

Mϕs and neutrophils are part of the cellular innate immunity and potently phagocytose and digest foreign material. Neutrophils are the most abundant type of polymorphnuclear leukocytes in the bloodstream making up about 50% of all circulating leukocytes, but are never seen in the tissue unless an inflammatory response is induced. During an inflammation neutrophils are recruited to the site of infection or injury and make up the most frequent cell type. Neutrophils are short lived and die during the inflammatory response within the tissue thereby leading to pus formation. Mϕs do not only destroy pathogens by digestion, but also initiate adaptive responses by antigen presentation. Mϕs do not die during the infection, but can convey subsequent immune responses (Janeway, 2005).

The induced pro-inflammatory cytokines TNFα, IL-1β and IL-6 initiate various further mechanisms, which aim to efficiently remove invading pathogens by acting on different local as well as distant cell types and tissues throughout the body.
They for instance initiate the generation and mobilization of neutrophils in the bone marrow and function as endogenous pyrogens, which accelerates the formation of adaptive responses. Locally secreted TNFα and IL-1β activate endothelial cells to express altered cellular adhesion molecules, which initiates immune cell extravasation. TNFα induces intravascular coagulation. Moreover, IL6 induces an acute phase response that leads to the secretion of collectins, which are secreted PRRs that opsonize microorganisms.

Interferons (IFNs) comprise a cytokine subgroup with potent antiviral functions. Accordingly, they are predominantly produced during viral infections. IFNα is mainly secreted by leukocytes, IFNβ by fibroblasts. Secreted type I IFNs induce an antiviral state in the producing cell itself (autocrine) as well as in neighboring cells (paracrine).
IFNs signal via the JAK-STAT signaling pathway and lead to the induction of IFN-stimulated genes (ISG). These turn on mechanisms that interfere with viral replication and block a spreading of the infection to uninfected cells. Type I IFNs induce e.g. 2´-5´oligoadenylate syntethase (OAS), an enzyme that activates the internal RNase L to degrade intracellular viral, but also host ribonucleic acids (RNAs). Furthermore, protein kinase R (PKR) is induced, which phosphorylates the eukaryotic translation initiation factor 2 alpha (eIF2α) and thereby inactivates the viral and host protein synthesis within the cell. Type I IFNs also initiate the production of interferon gamma (IFNɣ), a type II IFN, which is mainly secreted by T lymphocytes and natural killer (NK) cells. IFNɣ potentiates the antiviral mechanisms of type I IFNs, but has its greatest importance by shaping adaptive responses.
Beyond the induction of cytokines and chemokines pathogens recognition via PRRs also leads to the expression of co-stimulatory molecules on Mϕs and DCs. Surface molecules like CD80 (B7.1) and CD86 (B7.2) are indispensable co-receptors for the activation of adaptive responses (Janeway, 2005).

1.2.2 Pattern Recognition Receptors – Innate Immune Sensors

In 1989 Charles Janeway postulated the concept of distinct microbial pattern that are recognized by specific receptors of the innate immune system (Janeway, 1989). Until then, innate immunity was thought to be basically composed of nonspecific phagocytosis and the main immunological research focused on adaptive mechanisms. Today we know that there are evolutionary conserved patterns on microbes, so called pathogen-associated microbial patterns (PAMPs) that are recognized by germline-encoded receptors termed pattern recognition receptors (PRRs). Next to PAMPs PRRs also recognize endogenous danger-associated molecular patterns (DAMPs) that originate e.g. from injury or cell death.
A great variety of PRRs has been discovered until now. There are phagocytosis-inducing PRRs (e.g. scavenger receptors and C-type lectin receptors (CLRs) and signaling PRRs, which convey downstream signals that initiate early induced innate responses as inflammation. Four major families of these signaling PRRs have been classified: the TOLL-like receptor (TLR), RIG-I like receptor (RLR), AIM2-like receptor (ALR) and NOD-like receptor (NLR) family.
All PRRs have inherited and invariable receptor specificity. Therefore, innate mechanisms can react immediately to invading microorganisms, but they can only recognize a limited spectrum of PAMPs in contrast to the antigen receptors of the adaptive immune system, which can bind an infinite multiplicity of antigens. However, PRRs can recognize a broad spectrum of pathogens as PAMPs are shared by several microorganisms e.g. viral double stranded RNA (dsRNA), flagellin in the bacterial flagellum as well as lipopolysaccharid (LPS) in the cell wall of gram negative bacteria. Moreover, PAMPs are vital microbial structural or nucleic acid components that cannot be altered to escape this PRR immune recognition.
A combination of different PRRs is expressed on immune as well as on non immune cells. The composition is cell type-specific. Different receptors elicit diverse innate responses and shape the innate as well as the developing adaptive immune response (Janeway, 2005; Mogensen, 2009).

1.2.3 TLRs – TOLL-LIKE RECEPTORS

TLRs are membrane bound PRRs that scan the extracellular and luminal fluids for microbial patterns. These are recognized by the leucine-rich repeats (LRR)-containing ectodomain, while the intracellular TOLL/IL-1 receptor (TIR) domain exerts the downstream signal transduction. All TLR members except TLR3 signal via the adaptor protein myeloid differentiation primary response gene 88 (MyD88) to induce nuclear factor kappa-light-chain-enhancer of activated B cells (NF-κB) as well as mitogen-activated protein kinases (MAPK) signaling. Both result in the induction of pro-inflammatory cytokines. TLR3 signals MyD88-independent via the adaptor TIR-domain-containing adapter inducing IFNβ (TRIF). This TRIF-dependent TLR signaling pathway leads to the activation of NF-κB as well as IFN regulatory factor 3 (IRF3), which next to NF-κB target genes also induces type I IFNs. TLR4 is the only TLR protein that can signal spatially separated via both pathways (Kawai and Akira, 2010).
The TLR members TLR3, TLR7, TLR8 and TLR9 are located on intracellular membranes of endosomes, lysosomes and endolysosomes as well as the endoplasmic reticulum, while all other TLRs are located at the plasma membrane. TLR4 is unique as it switches between both localizations upon activation. The plasma membrane bound TLRs recognize mainly microbial membrane components (e.g. TLR5 recognizes flagellin of the bacterial flagellum), while TLRs on intracellular membranes recognize microbial nucleic acids (e.g. TLR3 recognizes dsRNA) (Kawai and Akira, 2010).

1.2.4 NLRs – NUCLEOTIDE-BINDING DOMAIN AND LEUCINE-RICH REPEATS-CONTAINING RECEPTORS

1.2.4.1 DISCOVERY & PLANT HOMOLOGUES

The nucleotide-binding domain (NBD) and leucine-rich repeat (LRR)-containing gene family is the largest known family of intracellular PRRs so far. It was initially found by database search for homologous structures to plant resistance genes (R genes). R genes-encoded proteins detect the presence of pathogens within plants and induce defense responses via MAPK signaling or cell death. The encoded proteins are either cytosolic or membrane bound and their largest know subgroup contains a nucleotide-binding site as well as an LRR domain and is therefore called NB-LRR subfamily of R genes (Jones and Takemoto, 2004).
In the human genome 22 R gene homologues were found that share strong structural and functional similarities to NB-LRR genes (Aravind et al., 2001; Tschopp et al., 2003). To emphasize the evolutionary conserved domains and the similarity to plant NB-LRR genes, the new gene family was named NBD and LRR-containing (NLR; also NOD-like receptor) gene family (Ting et al., 2008).

1.2.4.2 STRUCTURE & SUBFAMILIES

All NLRs have a typical tripartite domain structure (Fig. 1-1). Two domains, the LRR and the NBD, are conserved among plants and vertebrates and shared by almost all NLR members. The LRR domain at the carboxy-terminal end of the NLR protein senses specific ligands in analogy to the TLRs LRR domain.
The centrally located NBD is also referred to as NOD (nucleotide-binding and oligomerization domain) or NACHT domain, which is an acronym for NAIP, CIITA, HET-E and TP1 (see table of abbreviations). The NBD is required for NLR oligomerization and hence activation. It is part of a P-loop NTPase with nucleotide triphosphatase activity (Martinon and Tschopp, 2004).
The NLR amino-terminus harbors the effector domain, which upon NLR oligomerization leads to homotypic protein-protein interactions. These interactions link the receptor to downstream adaptor and

effector proteins that convey signal transduction. Four different effector domains are known today that are shared by various NLR members. NLR members are subclassified by these N-terminal effector domains. NLRAs contain an acidic activation domain (AD; also: acidic transactivation or acidic domain), NLRBs a baculoviral inhibitory repeat-like domain (BIR), NLRCs a caspase activation and recruitment domain (CARD) and NLRPs a pyrin domain (PYD). NLRs that do not share any effector domain homology are classified as NLRX (Tab. 1).

N-terminal effector domains	NLR subfamilies	Former classified as	Representatives
Acidic activation domain (AD)	NLRA		CIITA
Baculoviral inhibitory repeat-like domain (BIR)	NLRB	NAIPs, BIRC	NAIP
Caspase activation and recruitment domain (CARD)	NLRC	NODs, CARDs	NOD2, NLRC5
Pyrin domain (PYD)	NLRP	NALPs, PAN, PYPAF	NLRP3
No strong homology to other NLR subfamilies	NLRX		NLRX1

Tab. 1: NLR subfamilies classified by effector domain homology.

Until the agreement on a generally accepted nomenclature of the NLR members in 2008 there was a confusing diversity of names for individual NLR members. CARD-containing NLR members were referred to as NODs or CARDs, while PYD-containing NLRs were denoted NALPs. Four NLR members were not renamed according to the new classification due to intense research and a vast amount of publications ahead of the consensus of a common NLR nomenclature. These are the NLRA protein CIITA (MHC class II transactivator), the NLRB protein NAIP (neuronal apoptosis inhibitory protein) and the NLRC proteins NOD1 and NOD2 (nucleotide-binding oligomerization domain-containing protein 1 and 2), respectively (Ting et al., 2008).
Up to date there are 22 known human and 34 murine NLR members. Not for all of them ligands have been identified so far and despite structural similarities some family members might actually not even have receptor functions (Martinon and Tschopp, 2005).

1.2.4.3 SIGNALING

In the inactive state, NLRs are autorepressed by the LRR domain, which hinders the NBD sterically from oligomerization. This prevents spontaneous oligomerization and activation in the absence of proper ligands. Furthermore, endogenous NLR concentrations are low to prevent activation by aggregations. Ligand sensing induces a conformational change that exposes the NBD and hence allows NLR oligomerization. Depending on the NLR member, homo- as well as hetero-oligomers are known. Effector domains become exposed and corresponding adaptor proteins are recruited via homotypic interactions. Adaptors are mutually activated by close vicinity and a signal is conveyed downstream (Martinon and Tschopp, 2005).
CARD-containing NLR members (NLRCs) recruit CARD-containing adaptors as the serine threonine kinase RIP2, which is recruited e.g. to NOD1 and NOD2. Subsequently, this activates NF-κB and MAPK signaling and the production of inflammatory cytokines (Girardin et al., 2001; Inohara et al., 2000; Park et al., 2007). In contrast, PYD-containing NLRs (NLRPs) recruit PYD-containing adaptors. NLRPs that lead to the formation of caspase-1 activating inflammasomes (e.g. NLRP1, NLRP3, NLRP4) associate e.g. with the PYD-containing inflammasome adaptor apoptosis-associated speck-like protein containing a CARD (ASC), which is encoded by the *PYCARD* gene. ASC recruits caspase-1 via a CARD-CARD interaction. Oligomerization of NLRPs and their interaction with adaptors and effectors brings inflammatory caspases close together and leads to the activation of the inflammasome complex, cleaves IL-1 and IL-18 propeptides into their active forms (Martinon et al.,

2002). IL-1 and IL-18 subsequently bind to their receptor complexes at the plasma membrane. These (like TLRs) have intracellular TIR domains and recruit TIR adaptors as MyD88 to activate NF-κB and other inflammatory signaling pathways.

1.2.4.4 NLR LIGANDS & EXPRESSION

Diverse ligands of foreign (PAMPs), but also endogenous (DAMPs) nature can be sensed by NLRs. NOD1 and NOD2 homo-oligomers e.g. sense fragments of the bacterial cell wall component peptidoglycan (PGN). NOD1 detects γ-D-glutamyl-mesopimelic acid (*meso*-DAP) present in PGN of all gram negative and certain gram positive bacteria (Chamaillard et al., 2003a), while NOD2 recognizes muramyl dipeptide (MDP) present in all (gram negative and positive) bacteria (Girardin et al., 2003). NLRP3 instead was shown to form an inflammasome that is activated by a decline in the intracellular K^+ concentration (Muñoz-Planillo et al., 2013) and therefore by a great variety of structurally unrelated ligands that all induce K^+ efflux. Among these are e.g. bacterial and viral RNA (Kanneganti et al., 2006a, 2006b), monosodium urate (Martinon et al., 2006), nigericin (Mariathasan et al., 2006) as well as reactive oxygen species (ROS) that are produced after exposure to silica or asbestos (Dostert et al., 2008). The NLRP3 inflammasome leads to activation of caspase-1. Due to the variety of ligands NLRP3 is thought to be a general cellular stress receptor.
NLRs are defined as cytosolic PRRs, but they can also associate to other cellular compartments. NOD1 and NOD2 for instance are usually cytoplasmic, but were also found to be attached to the plasma membrane upon activation, which seems to be involved in downstream signaling (Barnich et al., 2005; Kufer et al., 2008). Furthermore, NLRX1 locates at the mitochondrial membrane (Moore et al., 2008) and CIITA within the nucleus (Harton et al., 1999).

1.2.4.5 NLRS AND DISEASE

Mutations in NLR genes were found to be involved in the development of a variety of inflammatory disorders.
Missense mutations in the NBD of *NLRP3* can e.g. cause different autosomal dominant autoinflammatory syndromes: familial cold autoinflammatory syndrome, Muckle–Wells syndrome or chronic infantile neurological cutaneous and articular syndrome. These are characterized by periodic fever and skin rashes (McDermott, 2002).
In contrast, loss of function mutations in the *CIITA* gene severely impede the expression of major histocompatibility complex class II (MHC class II, MHC II) receptors. This subsequently causes a severe combined immunodeficiency with impaired B and T cell responses towards extracellular pathogens and consequently leads to strong inflammations. The vulnerability due to decreased MHC class II levels is referred to as Bare Lymphocyte Syndrome (BLS) type II.
Mutations in NOD2 are associated with two different inflammatory disorders: Blau syndrome and Crohn´s disease (CD, Morbus Crohn). CD is a chronic inflammatory disorder of the intestine associated with mutations in the NOD2 LRR domain (Hampe et al., 2001; Hugot et al., 2001; Ogura et al., 2001). CD-associated mutations impair NOD2-mediated MDP recognition and the subsequent NF-κB activation in the presence of bacterial infection (Chamaillard et al., 2003b; Inohara et al., 2003). Further clinical aspects of CD are introduced below (see 1.4). The rare autosomal dominant Blau syndrome is caused by mutations in the NOD2 nucleotide binding domain instead (Miceli-Richard et al., 2001; Wang et al., 2002), which leads to an overactivation of NOD2 even in the absence of bacterial insults (Chamaillard et al., 2003b; Kanazawa et al., 2005). The disease is characterized by granulomatouse arthritis, uveitis as well as skin lesions.

1.2.5 NLRC5 – An NLR Member With Ambiguous Functions

NLRC5 was previously also referred to as NOD4, NOD27 or CLR16.1 until the NLR nomenclature classified the protein to the NLRC subfamily due to structural means (Ting et al., 2008). The *NLRC5* gene is located on chromosome 16q13 and covers a region of 93980 base pairs (bp). It encodes a messenger RNA (mRNA) with a length of 6775 bp containing 52 exons (NCBI ID: 84166). This mRNA is translated into a 1866 amino acid long peptide chain with a molecular weight of 204,6 kDa (Uniprot ID: Q86WI3).

1.2.5.1 Expression & Induction

Initially NLRC5 was reported to be expressed in brain, lung and prostate tissue and only little amounts were found in immune tissues (Kuenzel et al., 2010). In contrast, other groups reported NLRC5 to be highly expressed in immune tissues and hematopoietic cells (Benko et al., 2010; Neerincx et al., 2010).
The protein was found to be strongly upregulated by IFNɣ in hematopoietic as well as non-hematopoietic cells (Benko et al., 2010; Kuenzel et al., 2010; Neerincx et al., 2010).
Secreted IFNɣ binds to the IFNɣ receptor complex on the plasma membrane and induces intracellular JAK-STAT signaling. This leads to the phosphorylation of STAT 1 and the formation of phosphoSTAT 1 homodimers. These can enter the nucleus and are believed to bind the NLRC5 promoter region and induce the transcription of NLRC5 (Kuenzel et al., 2010).
It was also reported that NLRC5 can be moderately induced by IFNβ as well as LPS and the synthetic dsRNA analogue polyinosinic acid‑polycytidylic acid (poly(I:C)). The last two are TLR ligands capable of inducing IFNβ either via TRIF-dependent TLR4 or TLR3 signaling. Furthermore, some viruses were reported to induce NLRC5 by inducing IFNɣ e.g. *Sendai virus* (Neerincx et al., 2010), a single stranded (ss) RNA virus, as well as *Cytomegalovirus* (Kuenzel et al., 2010), a double stranded (ds) deoxyribonucleic acid (DNA) virus.

1.2.5.2 Structure

NLRC5 shares the NLR-typical tripartite domain structure consisting of a C-terminal LRR domain, a centrally located nucleotide binding domain and a N-terminal effector domain (Fig. 1-1).
The extended LRR region harbors 26 LRR motifs and makes NLRC5 the largest of all known NLR members. Alternative mRNA splicing within the LRR region generates five distinct NLRC5 isoforms, one of them is missing the entire LRR region. Alterations in the length of the LRR region are supposed to yield conformational variants and might thereby allow the recognition of different ligands. The isoforms could furthermore regulate specific NLRC5 functions in a cell type- or tissue-specific manner. Although NLRC5 belongs to the family of PRRs, it is unknown if the protein is capable of recognizing a specific yet unknown ligand and if this would occur in a direct or indirect manner (Neerincx et al., 2010).
The NLRC5 NBD region contains a Walker A motif (also called a phosphate or P-loop), which is a nucleoside triphosphate (NTP) binding site. It is not known so far if ATP or GTP nucleosids are bound to the NLRC5 Walker A motif. Furthermore, the NTP hydrolysis site, called Walker B motif, is located within the NBD (Neerincx et al., 2010).
The N-terminal effector domain of NLRC5 comprises the tertiary structure of a death fold domain with its typical α-helical repeats, although it doesn´t share much structural similarities to the known death fold domains of other NLRs as e.g. the CARD and PYD domains. Therefore, the NLRC5 protein is assigned to the NLRC subfamily and the effector domain is referred to as atypical CARD domain.

Wagner and colleagues found that this atypical CARD neither homotypically interacts with the CARD of the adaptor protein RIPK2, which is known to activate pro-inflammatory pathways in NOD1 and NOD2 signaling; nor did it interact with the CARD or PYD domain of ASC (Wagner et al., 2009). In contrast, the group around Davis later reported the interaction of NLRC5 with ASC, an observation that links NLRC5 to inflammasomes (Davis et al., 2010). There is only little knowledge on further adaptors that interact with the atypical NLRC5 CARD domain. Consequently, there is not much known about potential NLRC5 downstream signaling pathways.

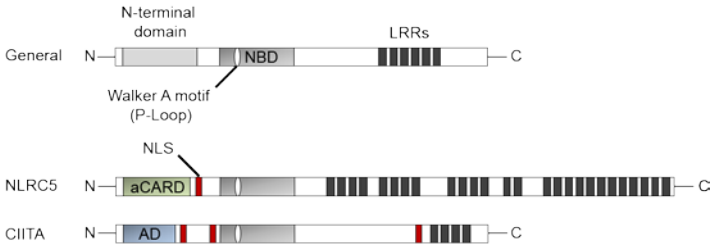

Fig. 1-1: Tripartite NLR structure
Depicted is a simplified illustration of the tripartite NLR structure as well as the human NLRC5 and CIITA domain structure. The N-terminal structure can be constituted by AD, BIR, CARD or PYD domains and account for the classification into NLR subfamilies. Length and composition of the LRR region varies between individual NLR members. Moreover, accessory domains and motifs exist. The CIITA isoform expressed in DCs furthermore bears an N-terminal CARD domain upstream the AD.
Abbreviations: NBD (nucleotide-binding domain), LRR (leucine-rich repeat), CARD (caspase activation and recruitment domain), aCARD (atypical CARD), AD (acidic activation domain), NLS (nuclear localization signal)

1.2.5.3 PROPOSED FUNCTIONS

The proposed NLRC5 functions are shortly summarized below and reflect the contradictory results published.

Antiviral Function
Initially NLRC5 was reported to potentiate antiviral signaling, which supports a pro-inflammatory role of the protein.
The infection of human foreskin fibroblasts with CMV induced IFNɣ, which led to an upregulation of NLRC5 via the JAK/STAT signaling pathway. NLRC5 subsequently activated the nuclear promoter sites IFNɣ activation sequence (GAS) and Interferon-specific response element (ISRE) and mediated the transcription of certain antiviral proteins e.g. IFNα (Kuenzel et al., 2010).
NLRC5 was further necessary for efficient antiviral responses against SeV. When NLRC5 was silenced only diminished amounts of IFNβ as well as CXCL10, 'regulated on activation, normal T cell expressed and secreted' (RANTES, CCL5) and macrophage inflammatory protein 1α (MIP1α, CCL3) were induced in infected THP-1 cells. All of these are crucial to initiate a proper antiviral response. However, autoactivation experiments could not confirm an activation of the ISRE promoter regions by NLRC5 nor detect an activation of the NF-κB, IFNβ, IRF3 or IRF7 promoter regions (Neerincx et al., 2010).

Inhibition of NF-κB and IFN signaling pathways
In contrast, other groups describe NLRC5 be a negative regulator of inflammation as the protein limits the duration and intensity of an inflammatory event.
Benko and colleagues reported that NLRC5 overexpression in HEK293 cells leads to a diminished NF-κB, ISRE and AP-1 promoter activity. Furthermore, they observed that the silencing of NLRC5 by short hairpin RNAs (shRNAs) in the murine macrophage cell line RAW264.7 reduces the expression

of the anti-inflammatory IL-10, while pro-inflammatory cytokines like IL-6, IL-1β and TNFα were significantly upregulated (Benko et al., 2010). These results are supported by Cui et al. who reported that NLRC5 is a potent negative regulator of the NF-κB signaling pathway supposedly by binding to the IκB kinase complex (IKKα/IKKβ). Furthermore, they found NLRC5 to inhibit IFNβ promoter activity via an interaction with retinoic acid‑inducible gene 1 (RIG-I) and melanoma differentiation associated gene 5 (MDA5). Consequently, the group around Cui (in contrast to others) proposes NLRC5 to negatively regulate type I IFN responses. A transient knockdown of NLRC5 by small interfering RNAs (siRNAs) enhanced innate immune responses as the induction of pro-inflammatory mediators e.g. TNFα as well as IFNβ was elevated (Cui et al., 2010). In accordance, the group around Kumar found NLRC5 to suppress NF-κB activation using reporter gene assays (Kumar et al., 2011). These results collectively support an anti-inflammatory NLRC5 function.
However, *in vivo* and *ex vivo* experiments based on *Nlrc5*-deficient mice could not verify any of the *in vitro* overexpression and silencing data described by any group before. *Nlrc5*-deficient primary cell cultures showed a normal generation of pro-inflammatory cytokines, chemokines and type I IFNs if stimulated with various TLR or RLR ligands as well as dsDNA. Neither viral infections with *Newcastle disease virus* (NDV, ssRNA) or *Herpes simplex virus 1* (HSV-1, dsDNA) nor bacterial infections with the gram positive *Francisella tularensis*, *Salmonella enterica ssp. enterica ser. Typhimurium* or the gram negative *Listeria monocytogenes* led to an altered production of pro-inflammatory mediators in *Nlrc5*-deficient cells (Kumar et al., 2011).

Inflammasome Activation
Kumar and colleagues further observed that NLRC5 overexpression activates caspase-1 and induces the production of IL-1β *in vitro*. Activation of the NLRP3, NLRC4 and absent in melanoma 2 (AIM2) inflammasome was tested in *Nlrc5*-deficient primary cultures using various specific ligands, but no effect on the IL-1β production was found. Therefore, they concluded that NLRC5 does not participate in the formation of any of these inflammasomes, but might rather comprise an own NLRC5 inflammasome with yet unassigned ligands (Kumar et al., 2011). The group around Jenny Ting also found implications for NLRC5 in inflammasome activation. They observed a reduced production of IL-1β in NLRC5-silenced cells during infections with different bacteria and proposed NLRC5 has a pro-inflammatory function as it promotes the generation of mature IL-1β. The tested bacterial strains *Escherichia coli*, *Shigella flexneri* and *Staphylococcus aureus* typically lead to inflammasome activation in an NLRP3- and ASC-dependent fashion, which was impaired upon NLRC5 deletion. Other NLRP3 activators like monosodium urate or alum also lead to a diminished IL-1β production in NLRC5-silenced cells, while the activation of the NLRP3 inflammasome by the pore forming toxins nigericin and α-hemolysin was not altered. Co-immunoprecipitation studies found NLRC5 to interact directly with the NBD of NLRP3 and the adaptor protein ASC (in contrast to observations made by (Wagner et al., 2009). Hence, it was concluded that NLRC5 is possibly a component of the NLRP3 inflammasome or a newly discovery inflammasome itself (Davis et al., 2010).

NLRC5 As Transcriptional Regulator In The Nucleus
While NLRC5 was initially described to be located within the cytosol (Kuenzel et al., 2010; Neerincx et al., 2010), a shuttling mechanism was discovered between the cytosol and the nucleus later on (Benko et al., 2010; Meissner et al., 2010). Using sequence analysis and deletion mutants Meissner et al. discovered a nuclear localization signal at the transition between CARD and NBD domain, which controls the subcellular localization of NLRC5. Nuclear import is conveyed by importin α, while the export was found to depend on exportin 1, also known as chromosome maintenance region (Crm1 or CrmA) (Meissner et al., 2010). A comparable mechanism is used by another NLR member, CIITA,

which also shuttles in an exportin 1-dependent fashion between the cytosol and the nucleus acting as a transcriptional coactivator for MHC class II coding genes within the nucleus (Spilianakis et al., 2000; Steimle et al., 1994).
Accordingly, the group around Meissner postulated a rather nuclear NLRC5 function and identified genes that were differentially regulated by the NLR member. Most strikingly NLRC5 was found to influence the expression of those *human leukocyte antigen* (*HLA*) genes that code for MHC class I molecules (*HLA-A, -B, -C, -E*) as well as genes that are associated with MHC class I antigen presentation and processing (e.g. *β2M, LMP2, TAP1*). They further identified NTP binding within the Walker A motif to be required for the induction of MHC class I, while NTP hydrolysis at the Walker B site was not. Mutations in the Walker A motif prevented NTP binding, while mutations within the nuclear localization signal (NLS) prevented proper importin α binding. Both abrogated the nuclear import of NLRC5 and thereby gene induction. Using reporter gene and chromatin precipitation assays it was further discovered that NLRC5 directly binds and transactivates the promoter regions of *HLA* and *HLA*-associated genes (Meissner et al., 2010, 2012a).

1.3 Adaptive Immunity

Adaptive defense mechanisms are precise and combat intruding pathogens efficiently if innate responses alone fail to entirely clear the infection. They start delayed, approximately 4-7 days post infection, because antigen-specific adaptive effector cells need to be generated first (Janeway, 2005).

1.3.1 Generation & Maturation Of Lymphocytes

Adaptive responses are initiated in secondary lymphoid organs, namely the spleen that collects antigens from the blood, the lymph nodes that collect antigens from the tissues and the mucosa-associated lymphoid tissues (MALTs) that encounter antigen from epithelial surfaces.
Key players of adaptive responses are the lymphocytes, which derive from lymphoid precursors in the bone marrow and mature in the central (primary) lymphoid organs. Two types of lymphocytes exist: T lymphocytes (T cells, TCs) that mature in the thymus and B lymphocytes (B cells, BCs) that mature in the bone marrow. During lymphocyte development a single lymphoid progenitor gives rise to a vast number of naïve lymphocytes that all bear antigen receptors, either T (TCR) or B cell receptors (BCR) with a unique specificity. Developing immature lymphocytes that strongly bind self antigens are potentially self-reactive and are therefore removed from the lymphocytes receptor repertoire, a process termed clonal depletion. Naïve T and B lymphocytes leave the primary lymphoid organs to circulate continuously through the blood and the peripheral (secondary) lymphoid organs until their surface bound lymphocyte antigen receptors encounters their specific antigen. Upon antigen recognition naïve lymphocytes stop migrating. They start to proliferate and differentiate into distinct effector cells, which clonally expand to generate progeny with identical antigen receptor specificity as well as equal effector functions.
Next to the recognition of their specific antigen naïve lymphocytes need a second, co-stimulatory signal to be activated for maturation. This controls the initiation of adaptive responses and prevents the onset of defense mechanisms against harmless antigens. Missing co-stimulation leads to the induction of anergy as the presented antigen is considered as “self”. This loss of reactivity towards the presented peptide cannot be restored if the antigen is encountered again (Janeway, 2005).

1.3.2 VARIANT LYMPHOCYTE ANTIGEN RECEPTORS

A vast variety of innate PRRs can be expressed on different cell types to convey innate immune responses. In contrast, lymphocytes express only one type of adaptive antigen receptor that possesses only one particular antigen-binding specificity to initiate adaptive responses. All naïve lymphocytes recognize different antigens, but several lymphocytes can encounter diverse antigens on the same pathogen.

Contrary to the invariant innate pathogen receptors (PRRs) lymphocyte antigen receptors are not germline-encoded. They have individual variant antigen-binding properties and recognize only a very distinct antigen on a precise pathogen. A vast variety of TC and BC receptor specificities (1×10^8 in humans) exist, because a huge individual receptor repertoire is generated by somatic recombination during lymphocyte development.

However, different from PRRs there is only a limited number of naïve lymphocytes that bear a particular antigen-binding receptor. Clonal expansion upon antigen recognition is therefore essential for an effective adaptive response.

The majority of effector cells undergo apoptosis after the antigen has been successfully cleared from the system, but some effector cells bearing that receptor specificity persist. These constitute the immunological memory and facilitate a faster response towards this exact antigen in case of reinfection (Janeway, 2005).

1.3.3 B LYMPHOCYTES & HUMORAL ADAPTIVE IMMUNITY

T and B lymphocytes differ in the architecture of their antigen receptors, in the way they recognize antigens and the effector functions they mediate.

B cells, DCs and Mϕs are professional antigen presenting cells (APCs). They constitutively express MHC class II receptors on their surface and present extracellular antigens to T lymphocytes (see 1.3.4). Furthermore, naïve B lymphocytes recognize unprocessed antigens in the extracellular space via their BCRs.

Simultaneous signaling of the BCR and a surfacial MHC class II induces the maturation of naïve B lymphocytes to antibody secreting plasma cells. These antibodies are directed against the native BCR-bound antigen (antigen: *anti*body *gen*erating).

Antibody-binding neutralizes extracellular pathogens and bacterial toxins and prevents a spreading of the infection. It further tags pathogens for phagocytosis, a process known as opsonization.

Intracellular infections are not recognized by the adaptive humoral responses, because antibodies are only directed against native antigens and bacterial-derived toxins in the extracellular room. Additional cell-mediated adaptive mechanisms are required for a proper immune surveillance, which depends on the effector functions of T lymphocytes (Janeway, 2005).

1.3.4 T LYMPHOCYTES & CELL-MEDIATED ADAPTIVE IMMUNITY

Naïve T lymphocytes detect processed peptide antigens that are presented by MHC molecules on the surface of APCs. Co-stimulatory signals, which are needed for T lymphocyte activation, are also delivered by APCs. Their expression is induced by innate mechanisms e.g. upon PRR recognition. Accordingly, innate immunity plays a pivotal role in the generation of adaptive responses.

The presentation of endogenous and exogenous peptides by MHC receptors and their recognition by T lymphocytes is essential for the generation of adaptive responses. Accordingly, T lymphocytes are screened for their ability to bind self peptides on MHC molecules during development in the primary

lymphoid organs. Immature T cells receive survival signals if their TCR is able to interact with MHC-peptide complexes (positive selection). Cells that strongly interact with MHC-bound self-peptides are retrieved these survival signals (negative selection) to prevent the development of autoreactive T lymphocytes.
MHC class I molecules, which present intracellular peptides, are bound by the TCR in combination with the CD8 co-receptor. $CD8^+$ T lymphocytes mature to cytotoxic effector cells. These cytotoxic T lymphocytes (CTLs) convey a cell-specific killing towards attached cells if the particular antigen is encountered again. CTLs thereby eliminate infected, but also malignant cells.
Extracellular peptides are presented on MHC class II molecules and recognized by TCRs that carry a CD4 co-receptor. $CD4^+$ T lymphocytes mature to T helper cells, which are activated to convey their effector function upon encounter of the particular antigen on a MHC class II receptor. Different $CD4^+$ T cell populations exist that encompass distinct effector functions.
For instance, Th1 cells mainly secret IFNγ, TNFα and IL-2. They potently induce Mϕ activation and differentiation. In contrast, Th2 cells are not involved in cell-mediated innate responses. They convey the co-stimulatory signal to activate naïve BCs and are therefore indispensable for the adaptive humoral immunity (Janeway, 2005).

1.3.5 Antigen Presentation

Antigens are generated inside the cell and presented on major histocompatibility complexes (MHC) at the plasma membrane. They are recognized by T lymphocytes via their TCR. Two distinct MHC classes exist called MHC class I and II (also MHC I and MHC II), which both share a comparable three dimensional structure as well as similar biological functions. MHC class I and II components are collectively encoded within the *HLA* gene cluster. Their heavy chains are highly polymorphic. Both classes differ in their expression pattern and in the origin, generation and loading of bound peptides. Both MHC complexes induce different adaptive defense mechanisms (Neefjes et al., 2011) (see also 1.3.4).

1.3.5.1 MHC Class II Complex

MHC class II molecules are heterodimers that consist of two homogenous heavy chains (designated α and β). Each of these chains is encoded by one of the highly polymorphic genes *HLA-DR*, *HLA-DQ* or *HLA-DP*. The α and β chain are assembled in the ER and associate with an invariant chain, Ii, which mediates a rapid transport of the MHC II-Ii complex to the late endosomal compartment for peptide loading. MHC class II complexes present exogenous antigens, which are derived from the extracellular space or the endosomal compartment. Self or foreign proteins are taken up by phagocytosis and degraded to peptides by proteases in the late endosome. The invariant chain binds the MHC II peptide binding groove that forms between the α and β chain. This prevents ER peptides from binding to the MHC II molecule. In the late endosomal compartment Ii is digested by cathepsins, just the class II-associated Ii peptide (CLIP) region is preserved within the MHC II peptide binding groove. It is exchanged with a suitable peptide by HLA-DM, an MHC-like molecule that acts as a chaperone. The late endosomal compartment containing the MHC II α/β complex, HLA-DM and cathepsins is also termed the MHC class II peptide loading compartment (MIIC) (Hartman et al., 2010). Peptide-loaded MHC class II complexes are transported from the late endosome to the plasma membrane for antigen presentation (Neefjes et al., 2011).
The expression of the MHC class II α and β chain and proteins involved in MHC II presentation e.g. Ii and HLA-DM is regulated by the NLR family member CIITA. CIITA is strongly induced by IFNγ. It

does not directly bind to the DNA, but is recruited to the enhanceosome that assembles around the SXY motif within the MHC class II promoter region. CIITA recruits the transcription machinery and thereby regulates the transcriptional regulation of MHC class II expression (Reith et al., 2005).
The expression of MHC class II is restricted to professional APCs in the steady state, but IFNγ induces MHC class II molecules also on other cell types like fibroblasts, endothelial and epithelial cells during the course of inflammation or infection (Bland, 1988; Geppert and Lipsky, 1985). MHC class II-peptide complexes are bound by $CD4^+$ T lymphocytes and initiate their maturation to effector cells as well as their subsequent activation.

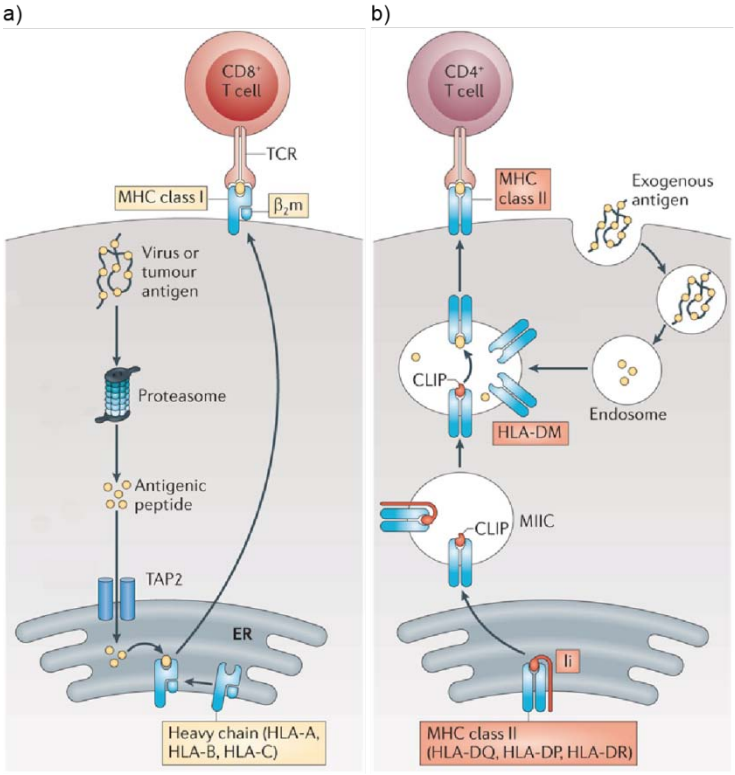

Fig. 1-2: Generation and presentation of antigenic peptides
a) Intracellular proteins are degraded by proteasomes within the cytosol, imported into the ER and bound onto MHC class I:β2M complexes. Loaded MHC class I:peptide complexes are presented to $CD8^+$ T cells at the plasma membrane. **b)** Extracellular proteins are degraded within endosomes and loaded onto MHC class II complexes in the MIIC, which is part of the late endosomal compartment.
Figure adapted after: "NLRC5: a key regulator of MHC class I-dependent immune responses." Kobayashi & van den Elsen, Nature Reviews Immunology, 2012 December
Abbreviations: β2M (beta-2- microglobulin), CLIP (class II-associated li peptide), HLA (human leukocyte antigen), MIIC (MHC class II peptide loading compartment), MHC (major histocompatibility complex), TAP2 (transporter associated with peptide binding 2), TCR (T cell receptor)

1.3.5.2 MHC Class I Complex

MHC class I molecules are ubiquitously expressed on the surface of all nucleated cells. NF-κB and ISRE binding sites are located in the promoter regions of MHC class I coding genes. Accordingly, MHC I expression is further upregulated during inflammatory responses (Gobin et al., 1998a, 1999).
The MHC class I complex predominantly presents cytosolic and nuclear peptides to the T cell receptor of $CD8^+$ T lymphocytes. Cytosolic proteins are either endogenous or derived from intracellular pathogens. They are mainly degraded by the cytosolic 26S proteasome, while nuclear proteins are degraded by nuclear proteasomes and generated peptides diffuse through the nuclear pores into the cytosol (Reits et al., 2003). Besides the 26S proteasome immune cells express an immune proteasome. Its proteolytic subunits are incorporated into the 20S core barrel of the 26S proteasome and alter the

degradation pattern. The immune proteasome selectively generate immunogenic peptides and thereby improve the antigen presentation by MHC class I complexes (Toes et al., 2001). Immune proteasomes exhibit an enhanced activity to better cope with the increasing amounts of misfolded proteins generated during immune stress or IFNɣ responses (Seifert et al., 2010).
MHC class I molecules are heterodimers that consist of a polymorphic transmembrane heavy chain encoded by either *HLA-A*, *HLA-B* or *HLA-C* and a light chain called beta-2-microglobulin (β2M). Both chains assemble in the ER. They are stabilized by chaperones until a suitable 8 – 9 aa long peptide is bound in their peptide binding groove. Approximately 8 – 16 aa long peptides are pumped from the cytosol into the ER lumen by the transporter associated with peptide binding (TAP), which is located in the ER membrane. These peptides are further N-terminally trimmed until they adequately fit the peptide binding groove. The MHC class I peptide loading complex ensures efficient peptide binding. It is constituted of the MHC class I heterodimer, TAP and various chaperons e.g. TAP-associated glycoprotein (tapasin) that stabilize the complex until a proper peptide is bound. Upon peptide binding the complex achieves intrinsic stability, the chaperones dissociate and the MHC I-peptide complex is transported via the Golgi network toward the plasma membrane where MHC class I exposes its bound peptide to the extracellular room (Neefjes et al., 2011).
CIITA was reported to induce the transcription of MHC class I in addition to MHC class II molecules *in vitro* (Gobin et al., 1997, 1998b, 2001; Martin et al., 1997), but a major role of CIITA in regulating MHC I transcription could not be confirmed *in vivo* as *Ciita* ko mice showed normal basal MHC class I expression (Itoh-Lindstrom et al., 1999). NLRC5 has recently been reported to be the master regulator of the transcription of genes coding for MHC class I molecules as well as proteins involved in MHC class I loading (Meissner et al., 2010).

1.4 Inflammatory Bowel Disease

The term inflammatory bowel disease (IBD) summarizes a group of intestinal inflammatory disorders of which ulcerative colitis (UC) and Crohn´s disease (CD) are the most frequent and best characterized forms. Both diseases are highly prevalent in the western civilization (Kaser et al., 2010).

1.4.1 Clinical Manifestation

UC and CD are recurrent or chronic inflammatory conditions that typically have their onset in the 2nd and 3rd decade of life. They are characterized by similar clinical signs e.g. abdominal pain, cramps, vomiting, diarrhea and rectal bleeding followed by anemia and body weight loss. Both forms are diagnosed via inflammatory markers in the stool and the endoscopic examination of the large intestine (coloscopy). UC and CD are mainly distinguished by the location of the inflammation and the kind of inflammatory changes (Podolsky, 2002).
CD can affect the entire gastrointestinal tract from the mouth to the anus. The inflammation is transmural, involving all layers of the bowel wall, and occurs discontinuous with segmental inflammatory patches (so called skip lesions) that are separated by healthy tissue. CD affects the colon and the terminal part of the small intestine, the ileum. In contrast, UC is characterized by a continuous inflammation in the mucosal and submucosal tissue. It is usually restricted to the colon and the rectum and histologically characterized by neutrophil influx into the lamina propria, goblet cell depletion and crypt abscesses (Xavier and Podolsky, 2007).

1.4.2 PATHOGENESIS

IBD is an idiopathic disease. Its pathogenesis is supposedly multifactorial. A general genetic susceptibility in combination with a dysregulated immune system, an altered microbial gut flora as well as other environmental factors are thought to favor the development of disease (Kaser et al., 2010).

Genome-wide association studies (GWAS) discovered more than 163 IBD susceptibility regions related to 300 known genes so far (Jostins et al., 2012), but individual IBD risk loci confer only a modest risk for disease development.

Sporadic occurring IBD results from an accumulation of a great quantity of interacting single nucleotide polymorphisms (SNPs), which alone only have minor biological effects. In contrast, a familial heritability of IBD is due to rare genetic variants, which have a major biological impact and are modified by further SNPs (Kaser et al., 2010). Mutations in the autophagy gene ATG16L1 (Hampe et al., 2007; Rioux et al., 2007) as well as the NLR gene family member NOD2 were e.g. identified as major risk loci for the development of CD in the Caucasian population (Hampe et al., 2001; Hugot et al., 2001; Ogura et al., 2001).

Cytokines are involved in the pathogenesis of IBD as they drive and control the inflammation and convey the clinical symptoms (Strober et al., 2002). Several IBD risk loci were found to encode for cytokines as well as their receptors or signaling pathways (Jostins et al., 2012). Th1-associated cytokines like IFNɣ and IL-2 are upregulated in CD patients, while UC rather favors a Th2 phenotype with an elevated secretion of IL-5 and IL-13 (Fuss et al., 1996). The neutralization of cytokines during the course of IBD has been an intense field of research and the antibody-mediated blockage of TNFα is a successful therapeutical option today (Danese and Fiocchi, 2011).

An important environmental factor in the development of IBD is the composition of the gut microbiota. Intestinal microorganisms usually coexists in balance with the immune system of the host (Round and Mazmanian, 2009). Defects in mucosal immune mechanisms as well as an altered enteric colonization can disrupt this balance. This can favor excessive responses towards commensals, colonization with potentially pathogenous microorganisms or bacterial invasion. IBD patients were found to have a less complex microbial pattern within the gut (Frank et al., 2007). The composition of the enteric microbiota can be affected by diet, antibiotic treatment or gut infection, facts that have also been associated with the onset of IBD (Kaser et al., 2010).

1.4.3 THERAPY

UC and CD are not medically curable. Both diseases need to be treated individually with immunosuppressive and anti-inflammatory drugs to relief symptoms and control the inflammation. UC can be eliminated by the removal of the large bowel, as the disorder is strictly limited to colon tissue. In contrast, surgery will not abolish CD as it affects the entire gastrointestinal tract and often flares up again after the removal of severely affected parts at the junction of the combined healthy intestinal sites (Karimuddin, Gilles, 2015; Tresca, 2015).

Due to its clinical manifestations IBD restricts the life quality of affected patients. The disease is rarely fatal, but complications can occur like toxic megacolon or gut perforation, which can be lethal. Furthermore, patients have an elevated risk to develop colorectal cancer (Berg et al., 2002; Itzkowitz et al., 2005).

1.4.4 DSS-Induced Colitis
A Murine Model To Initiate Innate And Adaptive Immune Processes

Dextran sodium sulphate (DSS), a sulphated polysaccharide, induces experimental colitis in rodents when administered orally (Chassaing et al., 2014; Perse et al., 2012). DSS is directly cytotoxic to intestinal epithelial cells (IEC) of the basal crypts. Thereby it disrupts the epithelial barrier and allows the infiltration of microorganisms and antigens from the gut lumen into the bowel wall, which subsequently induces an inflammatory response (Ni et al., 1996).
The induction of experimental colitis by DSS is simple, inexpensive, has an immediate onset and a well controllable progression of inflammation. Accordingly, it is a very common method. Acute, chronic or relapsing disease can be induced depending on the concentration, duration and frequency of DSS administration. Furthermore, the model is dependent on the depicted mouse strain (Mähler et al., 1998) and the bacterial colonization of the gut (Bylund-Fellenius et al., 1994; Nell et al., 2010).
DSS-induced colitis shares common clinical and histological features of human IBD. Therefore, it is used as an animal model to investigate IBD pathogenesis and potential therapies. Acute murine DSS colitis is mainly characterized by diarrhea, weight loss and traces of blood in the feces. Intestinal inflammation is histologically characterized by neutrophil influx into the lamina propria and submucosa, cryptitis as well as crypt abscesses and the subsequent necrosis within the epithelial layer. Epithelial degeneration is further accompanied by mucin depletion. Upon chronification the inflammation becomes transmural, lymphoid follicles appear in the subserosa and especially mononuclear leukocytes infiltrate the bowel wall. Preceding erosions can regenerate and reepithalize with squamous epithelium that is normally only found in the anal mucosa (Perse et al., 2012).
DSS-induced colitis affects especially the rectum similar to UC. However, focal lesions, disseminated lymphoid follicles and transmural inflammation found in the chronic state rather reassemble the pathogenesis of CD (Perse et al., 2012).
Innate immune mechanisms are indispensable for the genesis of DSS-induced colitis in mice. In contrast, adaptive responses, which also evolve and exacerbate disease, are dispensable for the onset and progression of the DSS-induced intestinal inflammation (Dieleman et al., 1994; Garrett et al., 2007).

1.5 OBJECTIVE

This project focused on the characterization of a specific NLR gene family member that was barely characterized when this work started: the 'NLR family, CARD domain containing 5' (NLRC5).
The aim was to investigate and characterize the role of NLRC5 in immune processes.

In detail, the following questions were addressed:

I. Does the expression pattern of NLRC5 indicate a functional relevance of the protein in immune organs, tissues or cells?

   Is the expression of NLRC5 regulated during immune responses?

II. Is NLRC5 involved in innate immune processes comparable to other NLR members?
    a. Is the protein involved in innate signaling pathways and the induction of cytokines?
    b. Has NLRC5 an impact on the generation and / or migration of innate immune cells?

III. Is NLRC5 involved in adaptive responses?
    a. Has it an effect on the generation and differentiation of lymphocyte populations?
    b. Is the protein implicated in antigen presentation as reported for CIITA?

IV. What is the phenotype of *Nlrc5*-deficient (ko) mice?
    a. Does the ko affect viability and fertility?
    b. Does the ko influence the normal development of tissues and organs?
    c. Do ko mice show an altered susceptibility or progression towards DSS-induced intestinal inflammation?

2 MATERIALS & METHODS

Used abbreviations are listed in alphabetical order in the appendix.

2.1 EXPERIMENTAL MICE

Genetically engineered mice are an important method to study the function of genes e.g. those that were identified by sequencing, but whose biological roles have not been elucidated. Their specific protein functions might be evaluated by observing an altered phenotype upon gene inactivation. The knockout technique was first published in 1989 and is best established for laboratory mice until now (Thomas and Capecchi, 1987).

2.1.1 GENERATION OF *NLRC5* KNOCKOUT MICE

A constitutive *Nlrc5* knockout mouse line (*Nlrc5* ko, *Nlrc5*$^{-/-}$) was generated by the company genOway to obtain a model organism to investigate the biological function of the *Nlrc5* gene *ex vivo* and *in vivo*. The ko mouse has a targeted gene deletion. Due to the extensive size of the *Nlrc5* gene (~56 kb) it was not possible to delete the entire gene using homologous recombination. Only the exons 4–7 were removed. Exon 4 contains the ATG start codon necessary for the initiation of transcription. Furthermore the CARD and NACHT domain are encoded within the deleted region. The deletion resulted in the absence of any *Nlrc5* transcript.
A targeting vector was designed in which the exons 4-7 were replaced by a *loxP*-flanked neomycin resistance cassette. It contained two homology arms isogenic to the used embryonic stem (ES) cell line 129Sv/Pas. This facilitated homologous recombination and therefore the targeting and replacement of the coding sequence at exons 4–7 with the manipulated vector construct. The two *loxP* sites allowed the later deletion of the neomycin selection cassette using Cre recombinase. A diphtheria toxin A (DTA) negative selection marker reduced the isolation of non-homologous recombined ES cell clones.

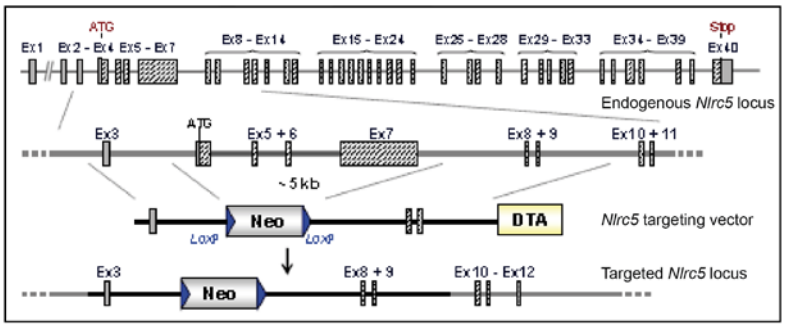

Tab. 2: *Nlrc5* knockout strategy
Displayed is the *Nlrc5* targeting strategy for the deletion of exon 4–7. The diagram is not depicted to scale. Hatched rectangles represent putative *Nlrc5* coding sequences (Ex1-40), grey rectangles indicate non coding exon portions, the solid line represents the chromosome sequence. LoxP sites are represented by blue triangles. The size of the *Nlrc5* sequence to be deleted is shown. (Figure adapted after genOway)

ES cells were obtained from the blastocyst of 129Sv/Pas mice and the designed linearized targeting vector was inserted by electroporation. A positive selection was carried out by gentamicin (G418) to identify recombinant ES cell clones. These were injected into the blastocyst of C57BL/6J mice and reimplanted into pseudo pregnant females. Chimeras were born and the males mated with C57BL/6J

females to generate the F1 generation that was imported into the central animal facility (ZTH; Zentrale Tierhaltung) of the University Hospital Schleswig Holstein in Kiel.
The generated *Nlrc5* knockout mice were further back crossed on C57BL/6N background (B6;129Sv/Pas-*Nlrc5*^{tm1geno}). Genotypes were analyzed by polymerase chain reaction (PCR). Heterozygous offspring was crossed to yield $^{-/-}$ and $^{+/+}$ genotypes, which will be referred to as *Nlrc5* knockout (ko; $^{-/-}$) and wild type (wt; $^{+/+}$) below.

2.1.2 ANIMAL HUSBANDRY

Animals were bred and kept in individually ventilated cages (IVC) in the ZTH under specific pathogen-free (SPF) standard conditions as defined by the Federation of European Laboratory Animal Science Associations (FELASA) (Nicklas et al., 2002) with a light/ dark rhythm of 12/12 h and temperatures of 20-24 °C. Water and food were given *ad libitum*. Mice were separated from the mother at the age of 4 weeks and tail- or ear-clipped to allow genotyping.
During colitis experiments mice were kept under SPF conditions in the Victor Hensen animal facility (VHH) on the university campus, Kiel.
All experiments were approved by the Ministry of Agriculture and Environment Schleswig-Holstein and the commissary of animal welfare of the Christian Albrechts University, Kiel.

License number	Designation
V 312-72241.121-33 / 554	Characterization of the *Nlrc5* knockout mouse - killing for tissue withdrawal
V 312-72241.121-33 (26-3/10)	Characterization of the *Nlrc5* knockout mouse - acute and chronic DSS-induced colitis

Tab. 3: Animal experiment license numbers
(From the Ministry of Agriculture and Environment Schleswig-Holstein for conducted animal experiments)

2.1.3 GENOTYPING

Mouse DNA was isolated from tail or ear clips (DNA extraction 2.7.1) and endpoint PCRs were performed using DreamTaq Green DNA Polymerase (Fermentas) and primers recommended by genOway to evaluate murine genotypes (Tab. 4, Tab. 5, PCR 2.7.2).

Gene	Name	Sequence	Species	Amplicon (bp)
Nlrc5 ko	ROS2-I2_PCR#1_F	GCCAGACAGCATAGACCAGATAGTGG	*Mus musculus*	2197
	ROS2-H2_PCR#1_R	CTACTTCCATTTGTCACGTCCTGCACG	*Mus musculus*	
Nlrc5 wt	ROS2-I3_PCR#2_F	GAGTCACTCACTCTCCAGGGACAGTGG	*Mus musculus*	2113
	ROS2-N_PCR#2_R	CTGTTGAGCTGACGGTGGATGACC	*Mus musculus*	

Tab. 4: *Nlrc5* Genotyping Primer Sequences

Dream Taq PCR Reaction Mix

Components	*Quantity*
Template DNA	1 µg
Primer Fw	0.25 µl
Primer Rev	0.25 µl
dNTP Mix	0.5 µl
Buffer	2 µl
DEPC H_2O	15.8 µl
Polymerase	0.2 µl

PCR Cycler Program

Temperature	*Time*	
95 °C	4 min	
95 °C	30 s	35x
65 °C	1 min	
72 °C	3 min	
72 °C	8 min	
4 °C	∞	

GT Amplicons on Agarose Gel

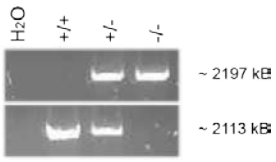

Tab. 5: Genotyping of *Nlrc5*$^{-/-}$ mice

2.1.4 WITHDRAWAL OF MURINE MATERIAL FOR *EX VIVO* ANALYSES

Animals were sacrificed by cervical dislocation before organs were removed. During experimental colitis experimental animals were anaesthetized by a mixture of ketamine (Ketavet, Pfizer) and xylazine (Rompun, Bayer) given intraperitoneally. A maximal volume of blood was taken by cardiac puncture. Blood was given immediately into blood collection tubes filled with lithium heparin-gel (Microvette 500 LiHepGel; Sarstedt) and centrifuged for 5 min at 10 000 x g at RT to obtain the serum for further analyses.
Organs were either fixed in 10% formalin for histological embedding or deep-frozen in liquid nitrogen for later RNA, DNA or protein isolation. Frozen tissues were homogenized in the corresponding lysing buffers using the tissue homogenizer (Tissue Lyser II, QIAGEN) and the desired compounds were extracted after standard protocols (2.7.1; 2.8.1; 2.9.1).

2.1.5 EXPERIMENTAL DSS COLITIS

Dextran sodium sulfate (DSS) chemically induces intestinal inflammation in rodents if applied orally (Ohkusa, 1985; Okayasu et al., 1990) and is therefore a widely used model to study IBD, in specific Colitis ulcerosa or Morbus Crohn.
Male wt and *Nlrc5* ko mice at comparable ages were given DSS dissolved in autoclaved drinking water at indicated concentrations, while control groups were given autoclaved water only. Beverages were renewed every second day to prevent bacterial contamination especially in the DSS-containing bottles. Weight, stool consistency, rectal bleeding and overall behavior were monitored every 1-2 days to study disease progression and to meet animal welfare conventions. Mice were excluded from the experiment if weight loss exceeded 20% of the initial body weight or if the overall health conditions were unacceptable after FELASA guidelines. Stool samples were collected from each mouse and smeared on paper to evaluate consistency. Intestinal bleeding was evaluated by testing for occult blood in stool with the Guajak test modified after Greegor (Greegor, 1971) as instructed by the manufacturer (Haemoccult, Beckman Coulter). The study design was double blind until the end of data analyses. All experimental groups were handled and analyzed equally. The precise treatment plan for the acute as well as the chronic colitis were modified after the *"Chemically induced mouse models of intestinal inflammation"* (Wirtz et al., 2007) to adapt disease progression to the individual conditions in the VHH animal facility as well as the C57BL/6J mouse strain and the laboratory DSS lot. An overview of DSS treatment is given prior to the results (Fig. 3-15, Fig. 3-26). After successful induction of colitis, mice were sacrificed and blood as well as organs were removed and prepared as described above (2.1.4).

2.2 HISTOLOGY

Organs were removed from the sacrificed mice, fixed in 10% formalin for 24 h, dehydrated by an increasing alcohol–xylol series (STP 120; Thermo Scientific) and embedded in paraffin (TES 99; MEDITE). Paraffin blocks were cut into 3.5 µl thick sections with a microtome (RM2255; Leica Microsystems) and deposed on microscopic slides. Prior to staining, slides were deparaffinized and rehydrated in a decreasing xylol–alcohol dilution series.

2.2.1 HEMATOXYLIN & EOSIN STAINING

Hematoxylin and eosin (HE) staining is a widespread staining technique for the evaluation of tissue slides. It is a combination of two different staining methods. Hematoxilin is a natural dye. Oxidized to

hemalaun it stains basophile cellular structures blue like e.g. the DNA-containing nucleus and the rough endoplasmic reticulum, which is rich in ribosomes. In contrast, the synthetic acidic dye eosin stains acidophil cellular structures red like e.g. proteins within the cytoplasm and mitochondria.
Deparaffinized tissue sections were stained with hemalaun (Carl Roth, #T865.3) and blued in tap water. Subsequently, sections were stained with eosin (Carl Roth, #X883.2) and washed briefly under tap water. Slides were dehydrated in an ascending ethanol series and finally preserved under a cover lid using Roti®-Histokitt (Carl Roth, 6638.1).

2.2.2 Periodic Acid – Schiff Stain

The Periodic Acid–Schiff (PAS) reaction stains polysaccharides and mucosubstances. Glycol groups in polysaccharides are oxidized by periodic acid to aldehyde groups. These can bind sulfite from Schiff´s reagent to generate fuchsins, which give the red color to the mucopolysaccharides.
Deparaffinized tissue sections were stained with 0.5% periodic acid (Merck, #1.00524.0025) and washed in tap water. Then sections were stained with 0.5% Schiff´s reagent (Sigma-Aldrich, #3952016) and washed thoroughly with tap water. Afterwards sections were counterstained with hemalaun (see 2.2.1), blued with tap water, dehydrated in an ascending ethanol series and preserved under a cover lid using Roti®-Histokitt (Carl Roth, 6638.1).

2.2.3 Microscopy

Slides were examined with the Axio Imager.Z1 (Zeiss) and pictures taken using the AxioVision Rel.4.8 software supplied by the manufacturer. Magnifications are indicated in the results section.

2.3 Cell Culture

Immortal as well as primary mortal cells were cultured, stimulated and analyzed.

2.3.1 Cell lines & Passage

Cell lines were cultured in the indicated formats and media (Tab. 6). Full media were supplemented with 10% fetal calf serum (FCS) at 37 °C and 5% CO_2. Cells were washed and diluted in fresh media twice a week. Adherent cell lines were pretreated with trypsin/ EDTA for 5-10 minutes at 37 °C in order to detach cells from cell culture dishes. This is further referred to as “culture under standard conditions”.

Cell Line	Description	Basic Media	DSZM No.
Immortal Cell Lines			
DB-2	Human B cell	RPMI 1640	
HEK-293	Human embryonic kidney	DMEM	ACC-305
HeLa	Human cervix carcinoma (from **He**nrietta **La**cks)	RPMI 1640	ACC-57
HT-29	Human colon adenocarcinoma	DMEM	ACC-299
Jurkat	Human T cell leukemia	RPMI 1640	ACC-282
THP-1	Human acute monocytic leukemia	RPMI 1640	ACC-16
Generated Primary Cell Lines			
BMDM	Murine bone marrow-derived macrophages	MMM + DMEM*	
Splenocytes	Murine mixed splenocytes	RPMI 1640*	

Tab. 6: Cultured immortal and primary cell lines
*see Tab. 7 for medium details

2.3.2 PRIMARY CELL CULTURE

Primary splenocyte culture

Mice were sacrificed and spleens removed immediately. All further steps were performed under sterile conditions. Spleens were grinded through a 70 µm cell strainer (Sarstedt) and taken up in splenocytes medium (Tab. 7). Gained single cell suspensions were carefully layered on an equal volume (5 ml) of room tempered Ficoll gradient (Pancoll mouse, PAN-Biotech) and centrifuged in 15 ml reaction tubes for 20 min at 1200 x g without bracket. The interphase, containing the leukocytes, was isolated, washed in PBS and the mixed murine splenocytes were seeded into the desired format.

Standard Culture Media
RPMI 1640 / MEM / DMEM; all from PAA Laboratories GmbH 10% (v/v) FCS Gold, PAA Laboratories GmbH
Splenocyte & BMDC Medium
RPMI 1640 + L-Glutamin + 25 mM HEPES, PAA Laboratories GmbH 10% (v/v) FCS Gold, PAA Laboratories GmbH 1% (v/v) Penicillin/Streptomycin, PAA Laboratories GmbH 1% (v/v) Amphotericin B, PAA Laboratories GmbH 0.01% (v/v) β-Mercaptoethanol, Sigma Only for BMDCs: Add fresh: 20 ng/ml rmGM-CSF, Immunotools
BMDM Medium
44% (v/v) MMM, PAA Laboratories GmbH 44% (v/v) DMEM, PAA Laboratories GmbH 10% (v/v) FCS Gold, PAA Laboratories GmbH 1% (v/v) Penicillin/Streptomycin , PAA Laboratories GmbH 1% (v/v) Fungizone®Antimycotic, Gibco® Add fresh: 20 ng/ml recombinant mouse (rm) M-CSF, Immunotools

Tab. 7: Cell culture media

Primary Bone Marrow-Derived Macrophages (BMDMs)

After sacrificing the mice, the bone marrow was isolated by flushing ice cooled BMDM-medium through the bones of the hind legs under sterile conditions. Afterwards bone marrow was pipetted through a cell strainer (Sarstedt) to gain single cell suspensions that were seeded in large 25 ml cell culture plates. Medium was supplemented with fresh M-CSF (macrophage colony-stimulating factor; 20 ng/ml; Immunotools) and changed regularly. Mϕs were harvested, counted and seeded into the desired experimental formats, when plate bottoms were filled with adherent differentiated Mϕs (approximately after 10 days). Mϕs were not trypsinized but scraped off culture plates for passage.

Primary Bone Marrow-Derived Dendritic Cells (BMDCs)

Bone marrow was gathered and prepared as described in the BMDM protocol above. Cells were cultured in BMDC medium supplemented with fresh GM-CSF (granulocyte macrophage colony-stimulating factor; 20 ng/ml; Immunotools) until DCs were generated (10–21 days). Medium was changed regularly. Adherent mature DCs were scraped off the cell culture plate, counted and seeded into the desired format prior to the experiments.

2.3.3 HARVESTING CULTURED CELLS

Medium was taken off and cells were washed with PBS. After PBS was removed thoroughly cells were broken up by specific lysing buffers to extract DNA, RNA or proteins (see 2.7.1, 2.8.1, 2.9.1). Non adherent (suspension) cells were spun down, the supernatant was removed and the pellet lysed with the desired buffer.

2.3.4 CELL STIMULATIONS

Stimuli were diluted in culture-specific media before they were given onto cells.

Stimulus	Product name	Company	Catalog number
rm M-CSF	Recombinant Mouse Macrophage Colony Stimulating Factor	Immunotools	12343118
rm GM-CSF	Recombinant Mouse Granulocyte Macrophage Colony Stimulating Factor	Immunotools	12343125
rh IFNγ	Recombinant Human Interferon gamma	Biosource	aa24-166
rh TNFα	Recombinant Human Tumor Necrosis Factor alpha	R&D systems®	210-TA
rm IL-2	Recombinant Mouse Interleukin 2	Immunotools	12340024
PHA	Phytohemagglutinin PHA-L	Sigma	L2769
PMA	Phorbol 12-myristate 13-acetate	Sigma-Aldrich	79346
Iono	Ionomycin calcium salt	Sigma-Aldrich	I0634
ATP	Adenosine 5′-triphosphate disodium salt	Sigma-Aldrich	A65509
LPS	Lipopolysaccharid from *Escherichia coli* Nissle 1917 DMSO	Provided by the Research Center Borstel	
ssRNA	Single stranded (ss) RNA40 / LyoVec™	InvivoGen	tlrl-lrna40
poly(I:C)	Polyinosinic Acid - Polycytidylic Acid	Calbiochem	528906
Brefeldin A	Brefeldin A	Sigma-Aldrich	B6542

Tab. 8: List of utilized stimuli

2.4 FLOW CYTOMETRY

Flow cytometry is used to characterize high quantities of single cells within a liquid medium. It is a rapid multiparameter laser-based technology to analyze cell numbers and cell properties like size and granularity, cell death status as well as extracellular and intracellular markers.
Cell size and granularity can be determined by the scattering of visible light. The diffraction of light at a single cell is expressed in the forward scatter (FSC) and depends on cell volume, while the refraction is expressed in the sideward scatter (SSC) and depends on cell granularity. Further information can be collected by excitation of fluorescent dyes using different lasers and detection of the emitted fluorescent light of every individual cell passed by the laser e.g. information about cell death and cell cycle can be gained if cells were pretreated with DNA intercalators like propidium iodide (PI). Here, fluorophore-bound antibodies were used to bind specific cell-associated molecules.
Cultured cells were harvested and transferred to 96-well plates (2×10^5 cells per well; BD Falcon 96-well 340 µl storage plate V bottom; BD Bioscience). All further steps were conducted at 4 °C. Cells were washed with flow cytometry washing buffer (FWB; Tab. 16). Fc receptors, which are present especially on Mϕs and DCs were blocked for 20 min with anti mouse (α ms) CD16/ CD32 (BD Pharmingen) to reduce nonspecific immunoglobulin binding. Afterwards, cells were stained with target-specific fluorophore coupled antibodies diluted in FWB (30 min). Additional samples were stained with isotype controls to evaluate nonspecific antibody binding that generates nonspecific fluorescence signals. In advance of intracellular staining, cells were fixed and permeabilized with the

BD Cytofix/ Cytoperm™ Kit (BD Bioscience) as indicated by the manufacturer. To prevent fluorophore bleaching, stainings and all following steps were conducted in the dark. Before the flow cytometric measurement cells were washed thoroughly with FWB.

Data Analysis

Cells were analyzed using the BD FACS Calibur™ flow cytometer (BD Bioscience). They were measured either in FACS tubes (Sarstedt) or directly in the 96-well format using the High Throughput Sampler (BD Bioscience). Data analysis was performed with the BD CellQuest Pro™ Software (BD Bioscience) and the Flowing Software 2.5.1 (Perttu Terho, University of Turku, FI; Turku Bioimaging).

Geometric Mean

The geometric mean is defined as the *n*th root of the product of n numbers and was used – instead of the mean – to describe the "mean fluorescence intensity" if data were scaled logarithmically. It can also be denoted as geometric mean fluorescence intensity (gMFI) and was used to compare fluorescence intensities when the focus of the analysis was not on the number of stained cells, but the fluorescence intensity of individual cells.

2.5 Enzyme-Linked Immunosorbent Assay

The enzyme-linked immunosorbent assay (ELISA) is an antibody based technique used to detect and quantify e.g. proteins, hormones and viruses in liquid media like culture supernatants or blood serum. Here, sandwich ELISAs were performed. Thereby target-specific "capture" antibodies were attached via their Fc part to adsorbing 96-well plates. Then samples were incubated on the antibody coated plate before a second biotin-labeled "detection" antibody was added.

The target protein is immobilized at the plate bottom by the capture antibody. The detection antibody binds the target protein. Subsequently, horseradish peroxidase (HRP)-coupled streptavidin is added, which binds and crosslinks the biotins coupled to the detection antibody. 3,3',5,5'-Tetramethylbenzidine (TMB) substrate is added, a chromogen that is oxidized by the bound HRP leading to a color change from colorless to blue. The reaction is stopped with acid and the absorption measured with a spectrophotometer at a wavelength of 450 nm. The absorption is proportional to the amount of bound target protein and measured protein concentrations can be calculated in relation to a standard curve.

All performed ELISAs were conducted according to the manufacturer's protocol. See also product sheets (Tab. 9).

Target	Product	Company	Cat. No
ms IFNγ	IFN-gamma Mouse Antibody Pair	Invitrogen	CMC4033
ms IL1-β	IL1-beta Mouse Antibody Pair	Invitrogen	CMC0813
ms TNFα	TNF-alpha Mouse Antibody Pair	Invitrogen	CMC3013

Tab. 9: Enzyme-linked immunosorbent assays

2.6 Multiplex Assay

Bead-based multiplex immunoassays were performed to measure multiple mediators within the same sample of serum or supernatant.
Color-coded beads are precoated with mediator-specific capture antibodies and added to the sample. Due to differently coded beads, several mediators can be detected in the same sample. Capture antibodies bind the specific mediator of interest. A secondary biotinylated detection antibody is added that is specific for the mediator to be analyzed. Antibody–antigen complexes form, similar to the ELISA technique. Afterwards phycoerythrin (PE)-conjugated Streptavidin is added and binds the biotinylation sites. Samples are measured in a dual-laser flow-based detection instrument. The bead and therefore the analyte detected is evaluated by one laser, while the second laser determines the PE signal intensity, which is proportional to the amount of detected analyte.
The assays were purchased from Bio-Rad and technically performed as well as analyzed by the Bioglobe GmbH, Hamburg.

2.7 Isolation & Analyses of DNA

Deoxyribonucleic acid (DNA) is extracted to analyze individual genetic and epigenetic features. Here genetic analyses were mainly performed to identify murine genotypes, which is required for animal breeding and animal experiments.

2.7.1 DNA Extraction

DNA was extracted using the DNeasy Blood & Tissue Kit (QIAGEN) according to the manufacturer´s instructions. Tissues were lysed with Proteinase K, afterwards DNA was precipitated by adding ethanol and bound to a silica membrane in a spin column. After several washing steps the DNA was eluted by DNA Elution buffer (Tab. 16).

2.7.2 Polymerase Chain Reaction

The polymerase chain reaction (PCR) is used to exponentially amplify genetically material, which can subsequently be further analyzed. It is a cyclic process based on a repeated enzymatic reaction with three major steps today carried out in fully automated thermocylers (Saiki et al., 1985):

1. Denaturation of the double stranded genetic material (DNA, RNA, cDNA) into single stranded templates at 95 °C. A longer denaturation step for initial break up is necessary, especially for genomic DNA.
2. Annealing of specific short single stranded oligonucleotides (primers) on complementary DNA templates. The annealing temperature is dependent on the melting temperature of the specific primers.
3. Primer extensions by a DNA-dependent DNA polymerase, which is stable at high temperatures. For instance, the Taq polymerase has its enzymatic optimum at 72 °C. The enzyme was originally found in the thermophile bacteria *Thermus aquaticus*, hence its name. There are also other thermostable enzymes, which can amplify templates of varying length thereby making more or less mistakes. Depending on the initial template and the desired amplicon also RNA-dependent DNA polymerase (reverse transcriptases) or RNA-dependent RNA polymerases are used. A prolonged terminal extension phase yields more products.

These three consecutive PCR steps are repeated 25–35 times. The amount of amplicon approximately doubles during each cycle until the capacity on free dNTPs and primers or polymerase activity is exhausted and the accumulation of product terminates. PCR amplicons can be separated on an agarose gel by electrophoresis. Different amplicons can be compared by size. Amplicons can also be isolated for sequencing and sequential cloning. The signal strength of an amplicon band after gel electrophoresis describes only the "endpoint" of the amplification process (endpoint PCR) and does not provide information about the initially inserted amount of template. Therefore, quantifications are only possible in comparison with an amplicon of a housekeeping template.
There are more specialized PCR methods used for quantifications, which are called quantitative PCRs were template amplification is monitored during the entire cycling process, virtually in "real time". Therefore, these specialized quantitative PCR forms are called real-time quantitative PCR (RT–qPCR; see also 2.8.4).
Here end-point PCRs were performed to evaluate RNA contaminations with genomic DNA (gDNA), to test the successful synthesis of complementary DNA (cDNA) and to determine the genotype of the experimental animals. The exact protocols are given in the referring method sections.

2.7.3 Agarose Gel Electrophoresis

PCR products were separated by size on agarose gels. The polymer agarose builds a gel matrix after been heated up in an aqueous solution. The gel matrix is used for separating macromolecules like nucleic acids (DNA, RNA, cDNA) by electrophoresis. Nucleic acids move to the anode (+) within an electrical field due to their negatively charged phosphate backbone. Because their base pair content is proportional to the chain length and approximately proportional to the molecular mass shorter bp chains can move faster through the agarose meshwork than longer ones. So nucleic acids are separated by size during electrophoresis and the molecular mass is determined in comparison to a DNA marker with nucleic acids of know sizes
Here, PCR products were separated on gels containing 1% (w/v) agarose, 0.5x TAE (Tris–Acetat–EDTA) buffer and 0.5x Sybr®Safe DNA Gel Stain (Life Technologies), a DNA intercalator excitable by ultra violet (UV) light. The gel was covered with TAE puffer, pockets were loaded with either 15 µl amplicon or 5 µl marker (SmartLadder, Eurogentec) and a voltage of 120 V was applied until samples were separated to the desired extent. Amplified nucleic acid bands were visualized under UV light in the BioDocAnalyze (Biometra).

2.8 Isolation & Analyses of RNA

Ribonucleic acids, in specific mRNAs, are transcribed from DNA templates and are translated into amino acid chains. Gene expression was studied by analyzing mRNA quantities.

2.8.1 RNA Isolation & Determination of Concentration

Total RNA was isolated with the RNeasy®Mini kit (QIAGEN) from cell pellets or tissue homogenates following the instructions of the manufacturer. Cells were lysed and homogenized on the QIAGEN shredder columns in the presence of a highly denaturing guanidine–thiocyanate-containing buffer that immediately inactivates RNA-degrading enzymes called RNases. Ethanol was added for precipitation before the mixture was given on spin columns with silica based membranes. Genomic DNA contaminations were digested by DNases on the column as described by the manufacturer using the RNase-Free DNase set (QIAGEN). The high salt buffer system allowed RNA with more than 200 bp

to bind to the membrane. Therefore, especially mRNAs were enriched in the eluate, while smaller RNA molecules were mostly lost in the process. After the elution of RNA from the columns by nuclease-free water RNA, concentrations were measured using the NanoDrop®ND1000 spectrophotometer (Thermo Fisher Scientific) and stored at –80 °C.

2.8.2 GENOMIC DNA CONTAMINATIONS & RNA CLEAN UP

Extracted RNAs were tested for contamination with genomic DNA (gDNA) using endpoint PCR. Exon-intron spanning glyceraldehyde 3-phosphate dehydrogenase (GAPDH) primers were used, which only anneal to DNA templates as RNA does not contain intros anymore. Therefore, only gDNA-encoded GAPDH will amplify during a PCR and can be visualized on an agarose gel.
Upon gDNA detection RNA clean up was performed as described in the RNeasy®Mini kit manual (QIAGEN). The RNA sample was bound again onto a silica column and DNase digestion was repeated using the RNase-Free DNase set (QIAGEN).

Go Taq PCR Reaction Mix

Components	*Quantity*
Template	1 µg
Primer Fw	0.25 µl
Primer Rev	0.25 µl
dNTP Mix	0.5 µl
Buffer	4 µl
H_2O*	13.8 µl
Polymerase	0.2 µl

PCR Cycler Program

Temperature	*Time*	
94 °C	4 min	
94 °C	30 sec	20-25x
58 °C	30 sec	
72 °C	1 min	
72 °C	4 min	
4 °C	∞	

Tab. 10: Endpoint PCR
*****nuclease-free water

2.8.3 REVERSE TRANSCRIPTION PCR (RT-PCR)

The amounts of isolated RNA are low and very fragile. Therefore, mRNA is reverse transcribed to the more stable cDNA for further analyses.
The cDNA synthesis was performed with the RevertAid™Premium First Strand cDNA Synthesis Kit (Fermentas) as instructed by the manual and with the quantities listed below. The supplied reverse transcriptase enzyme is an RNA-directed DNA polymerase obtained from the retrovirus *Moloney Murine Leukemia Virus* (MMLV). The used oligo(dT_{18}) primer anneals selectively to the 3'poly(A) tail of eukaryotic mRNAs and initiate them to be reverse transcribed into single stranded cDNAs.

Reverse Transcription Reaction Mix

	Components	*Quantity*
Step 1	RNA	1 µg
	Oligo(dT_{18}) Primer	0.125 µl
	dNTP Mix	0.5 µl
	H_2O*	ad 7.5 µl
Add for Step 2	RT Buffer	2 µl
	Reverse Transcriptase	0.5 µl

PCR Cycler Program

Temperature	*Time*
Step 1:	
65 °C	5 min
4 °C	∞
Step 2:	
25 °C	10 min
50 °C	15 min
85 °C	5 min
4 °C	∞

Tab. 11: Reverse Transcription
*****nuclease-free water

After reverse transcription, cDNAs were diluted with nuclease-free water to a concentration of 10 ng/µl and preserved at –20 °C. Successful cDNA synthesis was tested by endpoint PCR using GAPDH primers, followed by agarose gel electrophoresis. Samples that had no or just very few amplicons of the house keeping gene were not used for further analyses.

2.8.4 QUANTITATIVE REAL TIME PCR (RT-qPCR)

The quantitative real time PCR (RT-qPCR) is an advanced PCR technique were the amplification is directly (in "real time") measured by light emission and the template can be quantified as it is proportional to the amount of product in the exponential phase of amplification. Therefore, either a fluorescing DNA intercalator or FRET (Förster or fluorescence resonance energy transfer) probes are added to the reaction mix.

TaqMan Assay

RT-qPCRs were performed using TaqMan® Gene Expression Assays as suggested by the manufacturer (Life Technologies; Tab. 13). Two specific unlabeled primers and a specific FRET labeled probe were added to the reaction mix that also contained the cDNA sample and TaqMan master mix. Temperature cycles were performed in a light cycler (7900HT Fast Real Time PCR System, 384-well format, Applied Biosystems; software SDSv2.4; Tab. 12) that continuously measures the fluorescence within the samples.

Primers and the labeled probe bind the cDNA template after denaturation. The probe is labeled with a fluorophore at the 5' end and with a quencher at the 3' end. As long as both are in close vicinity there is no fluorescence detectable as the light emitted at the 5' end is taken up (quenched) at the 3' end.

As the primer is prolonged toward the assay probe during the elongation cycle, the probe is hydrolyzed from the template by the exonuclease function of the DNA polymerase. Therefore, the fluorophore is set free from the quencher and the emitted light is now detectable by the light cycler. The fluorescence intensity is proportional to the amount of template just amplified. As a new cycle starts a new probe binds to the specific template section to be hydrolyzed in the course of primer elongation.

TaqMan Reaction Mix

Component	*Quantity*
cDNA (5-10 ng)	0.5 µl
TaqMan probe and primer (see Tab. 13; Life Technologies)	0.5 µl
TaqMan mastermix (MM 4370074; Life Technologies)	4.5 µl

Light Cycler Program

Temperature	*Time*	
50 °C	2 min	
95 °C	10 min	
95 °C	15 sec	45x
60 °C	1 min	

Tab. 12: TaqMan Assay Procedure

The TaqMan® Gene Expression Assays were performed as suggested by the manufacturer (Life Technologies; Tab. 13).

Target	Full name	Species	ID
Actb	Actin beta	Mouse	Mm00607939_s1
Cd4	CD4 antigen	Mouse	Mm00442754_m1
Cd8	CD8 antigen, beta chain 1	Mouse	Mm00438116_m1
Ciita	Class II transactivator	Mouse	Mm00482914_m1
Cxcl1	Chemokine (C-X-C motif) ligand 1; KC (keratinocyte-derived chemokine)	Mouse	Mm00433859_m1
Cxcl2	Chemokine (C-X-C motif); Gro2, MIP-2	Mouse	Mm00436450_m1
Gapdh	Glyceraldehyde-3-phosphate dehydrogenase	Mouse	Mm99999915_g1
Ifnb1	Interferon beta	Mouse	Mm00439552_s1
Ifng	Interferon gamma	Mouse	Mm01168134_m1
Il10	Interleukin 10	Mouse	Mm00439614_m1
Il12a	Interleukin 12a; IL-12p35	Mouse	Mm00434165_m1
Il1b	Interleukin 1 beta	Mouse	Mm00434228_m1
Il6	Interleukin 6	Mouse	Mm99999064_m1
Mhc class II	histocompatibility 2, class II antigen A, beta 1; IAb	Mouse	Mm00439216_m1
Mpo	Myeloperoxidase	Mouse	Mm01298424_m1
Nlrc5	NLR family, CARD domain containing 5	Mouse	Mm01243039_m1
Tnfa	Tumor necrosis factor alpha	Mouse	Mm00443258_m1

Tab. 13: TaqMan Assays obtained from Life Technologies™

RT-qPCR Data Analyses

After the RT-qPCR is terminated, a threshold is defined within the exponential phase of the gained fluorescence data. Further data analyses use the so called Ct value (cycle threshold), which is the defined number of cycles required for the fluorescent signal of one sample to cross this threshold. The Ct level is inversely proportional to the amount of initial target nucleic acid within a sample. The relative target gene expression in comparison to a housekeeping gene ($\Delta Ct = 2^{-Ct\ Target} / 2^{-Ct\ Housekeeper}$) as well as the relative and absolute expression of the target gene in comparison to an internal reference can be calculated from the Ct values ($\Delta\Delta Ct = \Delta Ct_{target} / \Delta Ct_{reference}$).

2.9 Isolation & Analyses of Proteins

Proteins are extracted and analyzed e.g. to obtain information about their expression or interacting partners.

2.9.1 PROTEIN ISOLATION & DETERMINATION OF CONCENTRATION

Cells or homogenized tissues were lysed using a Nonidet P-40 (Octylphenolethoxylat, NP40; Fluka)-containing buffer (Tab. 16). Lysates were sonicated (3 x 5 s) and incubated on ice for 1 h before they were spun down (4 °C, 10 min, 16 000 x g) to sediment cell debris. The concentration of protein within the supernatant was measured using DC™ Protein Assay (Bio-Rad) as indicated by the manufacturer. The assay is based on the Lowry protein assay (Lowry et al., 1951), a biochemical assay used to assess the total protein concentration. It combines the Biuret test, where peptide bonds form a complex with copper II (Cu II) ions under alkaline conditions, with the oxidation of aromatic protein residues. Cu II ions are reduced to Cu I, which can subsequently reduce the yellow Folin–Ciocalteu reagent to molybdenum blue. After a colorimetric measurement at 490 nm concentrations can be defined in comparison to a standard curve.

2.9.2 SDS–PAGE (SODIUM DODECYL SULFATE–POLYACRYLAMIDE GEL ELECTROPHORESIS)

SDS is an anionic detergent that can dissolve hydrophobic molecules. It binds proteins, denatures and linearizes them to their primary structure and transfers an even distribution of negative charge per unit mass. Therefore, all SDS-treated proteins are negatively charged (anions) and move to the positively charged anode (+) in an electrical field. To separate the proteins by size a gel electrophoresis is carried out in a polymerized acrylamide gel (PAGE, polyacrylamide gel electrophoresis). Smaller proteins will move faster trough the polyacrylamide meshwork than larger molecules on their way to the anode (Laemmli, 1970; Shapiro et al., 1967).

Proteins were set to equal concentrations before protein lysates were diluted with sodium dodecyl sulfate (SDS)-containing loading buffer (5x SDS loading buffer; Tab. 16). Samples were heated at 95 °C for 5 min, spun down and supernatants were separated on polyacrylamide gels.

12 µg total protein per sample was loaded on two-parted polyacrylamide gels consisting of an upper stacking gel (3% w/v polyacrylamide), which bundles samples within the lanes at the beginning of the electrophoresis, followed by a separating gel, which contained 7–15% (w/v) polyacrylamide, depending on the protein sizes to be separated (Tab. 14). Gels were run in an ionic Tris/ Glycine/ SDS (TGS; Bio-Rad) buffer system at 15 mA per gel for 30 min for stacking and with 30 mA per gel for 45–75 minutes for separation.

Sample protein sizes were estimated in comparison to a protein standard (PageRuler Plus Prestained Protein Ladder, 10–250 kDa, Thermo Fisher Scientific), which is a mix of proteins with known molecular mass, that was loaded on the same gel.

		Stacking Gel	**Separation Gels**		
Protein size			50–200 kDa	30–120 kDa	20–100 kDa
Acrylamide % (w/v)		3%	7.5%	10%	12%
Aqua bidestillata	(ml)	1.95	5	4.15	3.5
4x Stacking buffer	(ml)	0.75			
4x Separation buffer	(ml)		2.5	2.5	2.5
(Bis) Acrylamide; Bio-Rad	(ml)	0.3	2.5	3.35	4
TEMED; Sigma-Aldrich	(µl)	3	10	10	10
10% APS	(µl)	30	100	100	100

Tab. 14: Self-casted polyacrylamide gels

2.9.3 WESTERN BLOTTING (IMMUNOBLOTTING)

Protein Transfer

After proteins were isolated and subsequently separated by SDS-PAGE, they were transferred (blotted) vertically from the polyacrylamide gel onto a polyvinylidene fluoride membrane (Immun-Blot®PVDF Membrane; Bio-Rad). PVDF membranes were activated in methanol.

Then a stack was assembled, by surrounding the polyacrylamide gel and the underlying PVDF membrane with buffer soaked Whatman filter papers (Extra Thick Filter Paper, Bio-Rad) in the following order: cathode buffered filter – polyacrylamide gel – PVDF membrane – anode I buffered filter – anode II buffered filter. For protein transfer the western blot stack was blotted for 20 minutes at 1 A/ 25 V (TransBlot Turbo Transfer System; Bio-Rad).

Name	Target	Origin	Dilution	Company	# Cat. No.
Primary antibodies					
αNLRC5 3H8	hu Nlrc5	rat	1:250	Courtesy of T. Kufer	
αGAPDH	hu/ms GAPDH	mouse	1:1000	Santa Cruz Biotechnology, Inc.	Sc-59541
Secondary antibodies (HRP-coupled)					
αRat IgG HRP	rat immunoglobulins	goat	1:2000	SIGMA-ALDRICH	A9037
α ms HRP	ms immunoglobulins	sheep	1:2000	GE Healthcare	NA931-1ML
Flow cytometric antibodies (Fluorophore coupled)					
α ms CD8 FITC	ms CD8	rat	1:6	Immunotools	22220083
α ms CD4 PE	ms CD4	rat	1:6	Immunotools	22150044
α ms CD3ε FITC	ms CD3	hamster	1:6	Immunotools	22150033
α ms CD19 PE	ms CD19	rat	1:4	Immunotools	22220194
α ms CD11b FITC	ms CD11b	rat	1:4	Immunotools	22159113
α ms Gr-1 FITC	ms Gr-1	rat	1:2	Immunotools	22155243
α ms H-2Kb APC	ms MHCI (H-2Kb)	mouse	1:100	eBioscience	17-5958
α ms H-2Db FITC	ms MHCI (H-2Db)	mouse	1:50	eBioscience	11-5999
α ms MHC II (I-A) PE	ms MHCII (I-A)	rat	1:40	eBioscience	12-5322
α ms CD25 FITC	ms CD25	rat	1:6	Immunotools	22150253
α ms IL-1β/ IL-1F2 PE	ms IL-1 beta	rat		R&D Systems®	IC4013P
α ms CD16/CD32	Fc receptors; Fc Block	rat	1:100	BD Pharmingen	553142
ms IgG2a K Isotype APC	Isotype ctrl	mouse		eBioscience	17-4724
ms IgG2a Isotype FITC	Isotype ctrl	mouse		Immunotools	21275523
rat IgG2a, κ Isotype FITC	Isotype ctrl	rat		Biolegend	400506
rat IgG2b, κ Isotype PE	Isotype ctrl	rat		BD Pharmingen	555848

Tab. 15: Antibody List

Blocking & Antibody Detection

After western blotting PVDF membranes were incubated with 5% non fat dry milk (NFDM; blocking buffer; Tab. 16) for at least 1 h at room temperature (RT) to block all nonspecific protein binding sites and prevent nonspecific antibody binding.

Afterwards membranes were probed with target protein-specific primary antibodies diluted in blocking buffer and incubated for 1 h at RT or overnight (o/n) at 4 °C. The primary antibody was washed off carefully with TTBS (Tab. 16) and membranes were probed with corresponding HRP-coupled secondary antibodies (45 min at RT). Secondary antibodies bind species-specific antigens on primary antibodies and lead to signal amplification. Unbound secondary antibodies were

washed of carefully with TTBS before membranes were incubated with enhanced chemiluminescent substrate (ECL; RPN2134; GE Healthcare). The substrate was activated by the HRP enzyme, which generates chemiluminescence. Chemiluminescent signals were detected on light sensitive film (Hyperfilm, GE Healthcare; table top film processor Curix 60, AGFA). After the detection of the target protein membranes were covered with stripping buffer and incubated in a water bath at 65 °C for 45 min to strip off all bound antibodies. After intensive washing in TTBS PVDF membranes can be blocked and probed again with a different antibody. Usually membranes are reprobed and developed for a housekeeping protein, usually β-ACTIN or GAPDH, which serves as loading control and allows a normalization of protein contents in the subsequent densitometric analyses.

Buffer	Composition
Flow Cytometry	
Flow Cytometry Washing Buffer (FWB)	0.5% (w/v) BSA in PBS
DNA isolation	
DNA Elution buffer	Tris/Cl 10 mM; EDTA 0.5 mM; pH 9.0
Protein Lysates	
NP40 buffer	NP40 1% (v/v) ; Tris 20 mM pH 7.4; NaCl 0.15 M; directly before use 1% (v/v) proteinase inhibitor (P2714; SIGMA) and 1% (v/v) phosphatase inhibitor (P5726; SIGMA) were added
SDS-PAGE	
5x SDS loading buffer	Tris 250 mM pH 6.8; Glycerin 50% (v/v); SDS 10% (v/v); DTT 500 mM; bromphenol blue
Separation buffer	Tris 1.5 M pH 8.8; SDS 0.4% (v/v)
Stacking buffer	Tris 0.5 M pH 6.8; SDS 0.4% (v/v)
Western Blotting	
Cathode buffer	Tris 25 mM; 6-Aminocaproic acid 40mM; Methanol 20% (v/v)
Anode buffer I	Tris 30 mM; Methanol 20% (v/v)
Anode buffer II	Tris 300 mM; Methanol 20% (v/v)
10x TBS	Tris 200 mM pH 7.6; NaCl 1.37M
TTBS	1x TBS; Tween®20 0.1% (v/v)
Blocking buffer	TTBS, nonfat dry milk powder (NFDM, Bio-Rad) 5% (w/v)
Stripping buffer	SDS 2%; Tris 62.5 mM pH 6.8

Tab. 16: Self-arranged buffers
Abbreviations are explained in the appendix.

Densitometric Quantification of Western Blot Signals

Photographic films with detected western blot signals were digitalized and quantified using the Image Studio Lite software (LI-COR Bioscience), which quantitatively measures the optical density. Upon background subtraction values were normalized to a housekeeping gene and the relative and absolute foldchange was calculated compared to an internal reference (Rel. Signal = $S_{target}/S_{housekeeper}$; Rel. Foldchange = $rel.S_{Target}/ rel.S_{Ref}$).

2.10 Statistical Analyses

Unpaired, two-tailed Student's t-tests were performed to compare two data sets having Gaussian distribution and homogeneous variances. If the conditions were not given, the non-parametric Mann-Whitney test was performed instead.
One-way ANOVAs (one variable) or Two-way ANOVAs (multiple variables) were performed if more than two data sets were compared. ANOVAs calculate if there exists a significant difference between the means of the tested groups. Bonferroni post-hoc tests were performed afterwards to analyze, which of these group differences were significant.
If One-way ANOVA could not be performed due to heterogeneous variances, the non-parametric Kruskal-Wallis test was applied instead. Dunn´s combined testing served as post-hoc test.
Survival curves were generated and analyzed after Kaplan- Meier.
All statistical analyses were performed with the GraphPad Prism 5 Software. The probabilities are indicated as follows: $^{ns}p > 0.05$ (not significant); *$p < 0.05$; **$p < 0.01$; ***$p < 0.001$; ****$p < 0.0001$.

2.11 Tissue Panels

Commercially available multiple tissue cDNA panels (Clontech) were used for expression analyses by RT-qPCR (0).

Product Name	Catalog Number
Human MTC™ Panel I	#636742
Human MTC™ Panel II	#636743
Human Digestive System MTC™ Panel	#636746
Human Immune System MTC™ Panel	#636748
Mouse MTC™ Panel I	#636745
Mouse MTC™ Panel III	#636757

Tab. 17: Tissue cDNA panels obtained from Clontech

2.12 Software

Method	Device	Software for Data Analyses	Company
Analyses of flow cytometric data	BD FACSCalibur™	BD CellQuest Pro™ Software	BD bioscience
		Flowing Software 2.5.1	Perttu Terho, University of Turku, FI; Turku Bioimaging
Statistical Analyses		GraphPad Prism 5	GraphPad Software
Light microscopy	Axio Imager.Z1	AxioVision Rel.4.8	Zeiss
Chemiluminescence detection	ChemiDoc™ XRS Q	Quantity One	BIO-RAD
Western blot quantification	Odysee XLS	Image Studio Lite software	LI-COR Bioscience
Real Time quantitative PCR	7900HT Fast Real Time PCR System	SDSv2.4	Applied Biosystems

Tab. 18: Software used for data analyses and presentation

3 RESULTS

3.1 NLRC5 – EXPRESSION AND INDUCTION

An initial step in the characterization of a protein is to evaluate its distribution within the organism. Cell type- or tissue-specific expression patterns can give clues on probable protein functions. Furthermore, factors that influence protein levels can indicate by which signaling pathways the investigated protein is regulated. Here the expression and induction of NLRC5 was evaluated on mRNA and protein levels.

3.1.1 *NLRC5* RNA IS HIGHLY EXPRESSED IN HUMAN AND MURINE IMMUNE TISSUES

TaqMan assays were performed on human and murine tissue cDNAs in order to answer the questions how *NLRC5* is expressed throughout the body, if it is ubiquitously distributed or shows a tissue-specific expression pattern and if it is abundant or rather rare (tissue panels, Clontech; Tab. 17). Furthermore, species-specific differences in the general expression and distribution of *NLRC5* were evaluated (Fig. 3-1 a, b).

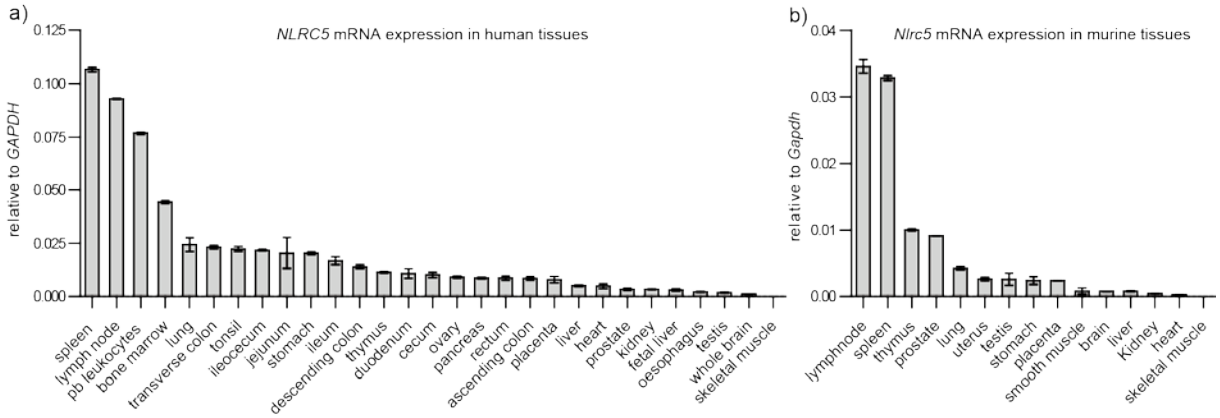

Fig. 3-1: ***NLRC5* expression in human and murine tissues**
NLRC5 TaqMan assays were performed on commercially available human and murine tissue cDNAs (Clontech, Tab. 17). Columns represent the average of technical duplicates. The standard error of the mean (SEM) is indicated by the bars. The expression of *NLRC5* was normalized to the housekeeper *GAPDH* ($\Delta Ct = 2^{-Ct\ Target} / 2^{-Ct\ Housekeeper}$). *NLRC5* mRNA expression was highest in lymphoid tissues, especially secondary lymphoid organs.

NLRC5 was expressed in all tested human and mouse tissues except skeletal muscle. Although it was ubiquitously expressed, *NLRC5* mRNA levels varied between different tissues. The highest mRNA expression was found in human and murine secondary lymphoid organs e.g. spleen and lymph nodes as well as peripheral blood (pb) leukocytes. A high expression was detected in human bone marrow and murine thymus, which are both primary lymphoid organs. Moderate *NLRC5* expression was detected e.g. in the lung and in various parts of the intestine. A marginal *NLRC5* expression was found in e.g. muscle tissues, brain, kidney and liver. The expression patterns were comparable between humans and mice. An exception presented the prostate that showed high *Nlrc5* expression in mouse, but only marginal expression in human tissue.
NLRC5 mRNA was expressed in virtually all tested human and mouse tissues. The abundance was diverse between the tissues and the expression was strikingly elevated in immune-associated tissues what could indicate an immune relevant function.

3.1.2 NLRC5 PROTEIN WAS DETECTED IN VARIOUS CELL LINES AND IS UPREGULATED BY IFNγ

In order to evaluate if NLRC5 is expressed by different cell types or if it can predominantly be found in immune cells, which constitute the lymphoid organs its expression was analyzed in human cell lines (Tab. 6) using western blotting. Therefore, cells were cultured under standard conditions. Total protein was isolated and analyzed for NLRC5 and β-ACTIN.
It was also of interest if NLRC5 can be induced or reduced by certain stimuli. Accordingly, cells were stimulated with either IFNγ or TNFα for 6 or 10 h and changes in NLRC5 protein content were quantified on the developed film after immunobloting.

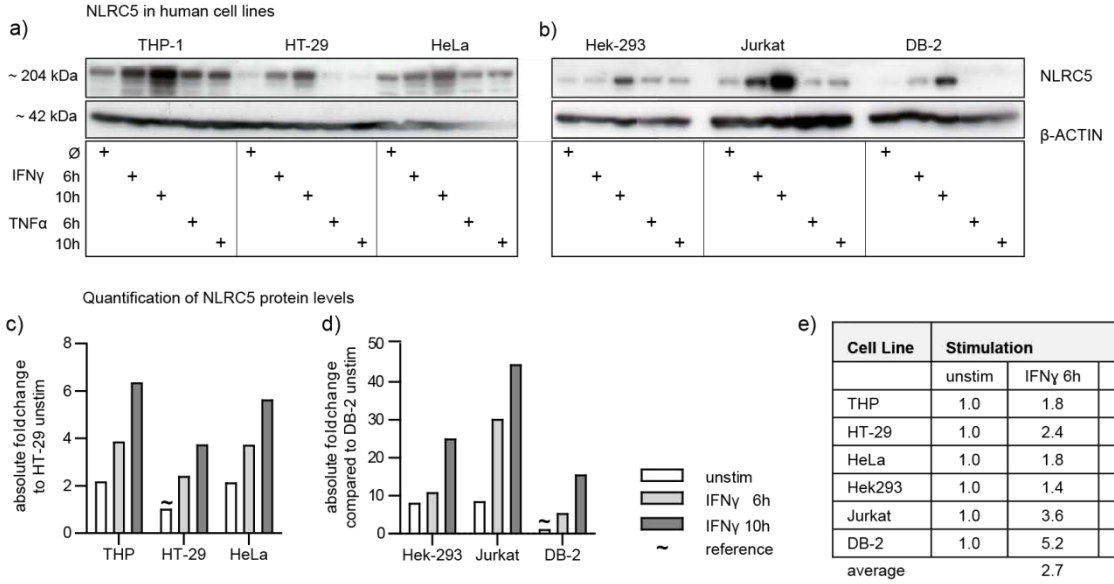

Cell Line	Stimulation		
	unstim	IFNγ 6h	IFNγ 10h
THP	1.0	1.8	2.9
HT-29	1.0	2.4	3.7
HeLa	1.0	1.8	2.7
Hek293	1.0	1.4	3.2
Jurkat	1.0	3.6	5.3
DB-2	1.0	5.2	15.4
average		2.7	5.5

Fig. 3-2: **NLRC5 protein levels and its induction in human cell lines**
Human cell lines were cultured in 6-well plates o/n under standard conditions and were either left untreated or stimulated with IFNγ (25 ng/ml; hr IFNγ; Biosource) or TNFα (20 ng/ml; hr TNFα; R&D systems®) for 6 or 10 h. Cells were lysed and western blot was performed. The membrane was probed with either anti hu NLRC5 rat IgG or anti hu β-ACTIN mouse IgG. Chemiluminescent signals were detected on hyperfilm (GE healthcare; **a+b**) and quantified using the Image Studio Lite software from LI-COR Bioscience (**c-e**). The immunoblots (**a, b**) show NLRC5 protein expression in different human cell lines (upper lane). β-ACTIN served as protein loading control (lower lane). The crosses below indicate the type and duration of cell treatment. After background subtraction values were normalized to β-ACTIN and the absolute NLRC5 increment was calculated (**e**) in comparison to a blot internal reference (**~**; **c**: unstimulated HT-29 cells; **d**: unstimulated DB-2 cells).
NLRC5 was expressed by different cell lines, predominantly leukocytes. The protein was strongly induced upon IFNγ stimulation.

NLRC5 was detected in all tested immortal human cell lines (Fig. 3-2). The protein was expressed in the leukocytic cell lines derived from human blood (THP-1 monocytes, Jurkat T cells, DB-2 B cells) as well as in the epithelial cell lines (HT-29, HeLa; HEK-293) derived from other human tissues (colon, cervix, embryonic kidney) (Tab. 6).
Basal NLRC5 levels showed differences between various cell lines. THP-1 and HeLa cells had high basal NLRC5 content, while only little of the protein could be detected in HT-29 cells (Fig. 3-2a, c). Jurkat and HEK-293 cells also showed higher basal levels compared to DB-2 (Fig. 3-2 d).
Stimulation with IFNγ led to a potent induction of NLRC5 in all cell lines (Fig. 3-2a–e). The NLRC5 protein level was induced on average 2.7–fold after 6 h and 5.5-fold after 10 h of stimulation (e). The most potent induction was seen in DB-2 B lymphocytes (5.2 fold after 6 h; 15.4 fold after 10 h) and Jurkat T lymphocytes (3.6 fold after 6 h; 5.3 fold after 10 h; e). TNFα stimulation slightly induced NLRC5 in THP-1 as well as in HEK-293 cells, but did not have an effect on other tested cell lines.

The highest basal NLRC5 levels as well as the most potent increases in NLRC5 expression were observed in human leukocytic cell lines, which convey relevant immune processes. The induction of NLRC5 by IFNγ and the consequential mRNA tissue expression pattern support the hypothesis that NLRC5 might be involved in immunological processes.

3.2 Analysis of Secondary Immune Organs in *Nlrc5* ko Mice

Secondary lymphoid organs (spleen & lymph nodes) showed the highest NLRC5 mRNA expression in humans as well as in mice (Fig. 3-1). This raised the question if NLRC5 has a special function within these organs or in the cells that are mostly domiciled there. In human cell lines it was shown that NLRC5 is highly expressed in THP-1 monocytes and Jurkat T lymphocytes and that the protein is potently induced in leukocytes upon IFNɣ stimulation (Fig. 3-2).
NLRC5 was further characterized by using *Nlrc5*-deficient mice. Especially murine spleens and mesenteric lymph nodes were further analyzed to evaluate if the deletion of *Nlrc5* has any phenotypical effects within these organs.

3.2.1 No changes in spleen weight

Alterations in spleen size and weight are indicators for inflammatory processes like an infection or an unbalanced inflammatory immune response within the body. For instance splenomegaly (lat. enlarged spleen) can be caused by diseases of the blood or lymph system, infections, cancer or liver disease (MedlinePlus).
If Nlrc5 is indispensable for proper immune function its deletion might affect spleen size. Therefore, spleens from *Nlrc5* ko and wt mice were weighted and compared (Fig. 3-3).

Fig. 3-3: **Spleen weight in *Nlrc5* ko mice**
Mice were sacrificed, spleens removed and weighted (animals: n=7–11 per group; age: 8–16 weeks). Each individual mouse is represented by a dot. The median is indicated by the bars and given below. One-way ANOVA with Bonferroni post-hoc tests was performed.
The spleen weight was not influenced by the *Nlrc5* knockout.

There were no obvious differences in spleen size, weight or color in the *Nlrc5* ko compared to wt mice. Female animals had a higher median spleen weight (~10 mg) if compared to their male counterparts in both genotypes.
The *Nlrc5* deletion did not influence the spleen weight and therefore a normal spleen function is assumed under SPF caging conditions. Normal spleen architecture and function was further evaluated using histological techniques.

3.2.2 No structural alterations in secondary lymphoid organs

There were no obvious macroscopic changes in secondary lymphoid organs of *Nlrc5* ko mice if compared to their wt counterparts. Murine spleen and mesenteric lymph nodes were further

histologically examined to compare immune organ structure. Therefore paraffin sections were stained with hematoxilin and eosin and microscopically analyzed.

Wt and *Nlrc5* ko mice showed similar lymph node architecture (Fig. 3-4a, b). The cortex (c), which is the B cell zone, was equally interspersed with lymph follicles in wt and ko mice. The homogeneous dark primary follicles (pN) and the secondary follicles (sN) with their lighter germinal centers (gc) were distinguishable. Also the paracortex (pc), which is the T cell zone, and the medullary zone with its medullary cords and sinuses showed normal architecture in *Nlrc5* ko mice.

Wt and *Nlrc5* ko mice also had similar spleen architecture (Fig. 3-4 c, d). White and red pulp could easily be distinguished. The B cell follicles of the white pulp with their germinal centers showed comparable size and structure. Also the red pulp did not show any differences.

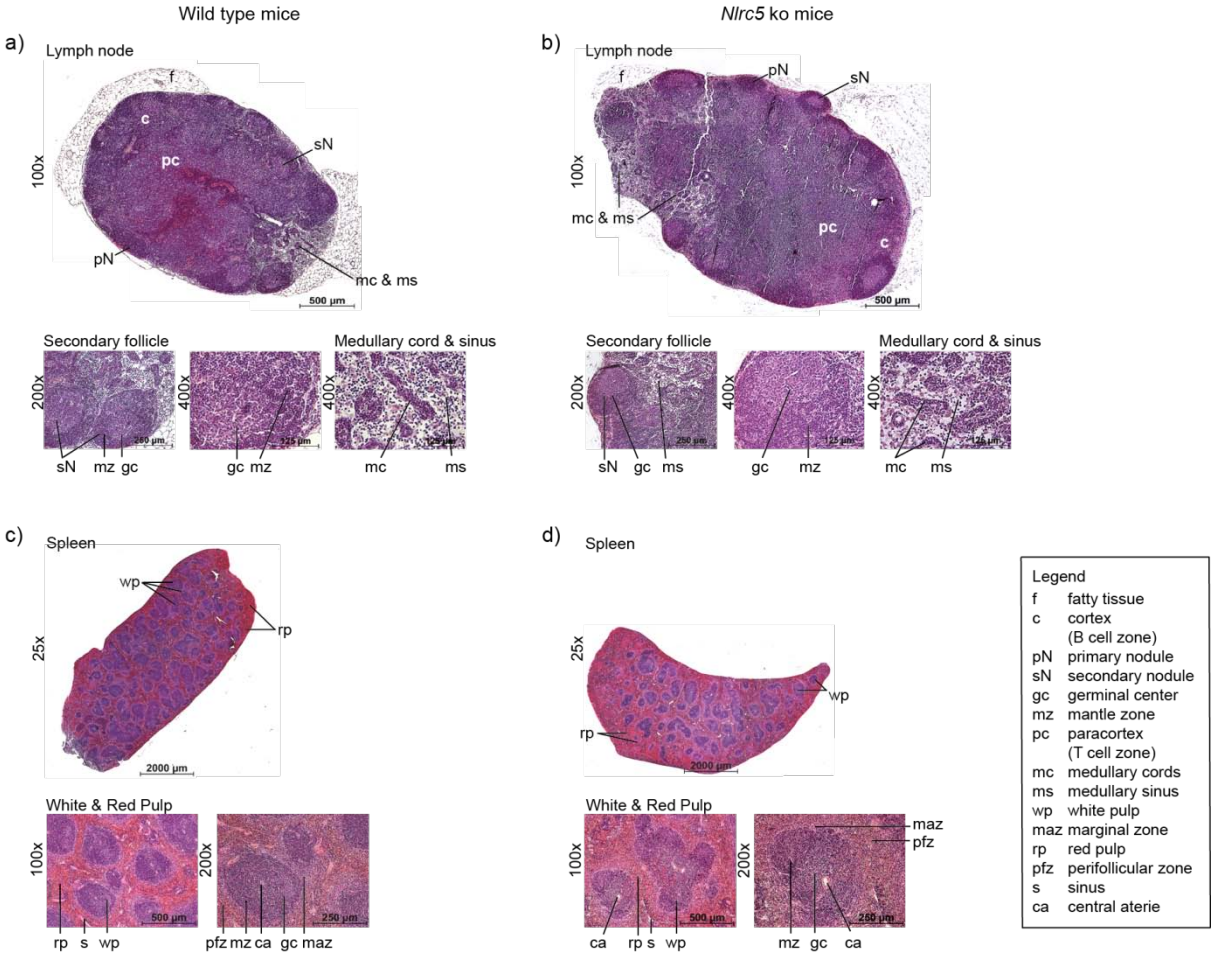

Fig. 3-4: **Structure of secondary lymphoid organs in *Nlrc5* ko mice**

Mice were sacrificed (n=2 per group). Spleens and mesenteric lymph nodes were removed. Formalin-fixed and paraffin-embedded tissues were dissected and stained with HE. Light microscopy was carried out with the Axio Imager.Z1 at indicated magnifications. Abbreviations are used for clarity and explained in the legend.

The architecture of the secondary lymphoid organs did not differ in *NLRC5* ko mice under basal conditions if compared to the wt.

Although NLRC5 is highly expressed in immune tissues as lymph nodes and spleen the histological comparison of these secondary lymphoid organs did not show any obvious changes under basal conditions that could be attributed to the *Nlrc5* deficiency.

3.2.3 ALTERED IMMUNE CELL POPULATIONS IN THE SPLEEN

NLRC5 is highly expressed in leukocytes as well as immune tissues (Fig. 3-1, Fig. 3-2) that are comprised of these cells. This suggests that the protein function might be closely related to certain immune cells.

In order to assess if *Nlrc5* ko mice had normal immune cell populations or if there were differences due to impaired generation or differentiation of certain leukocytic cell types, murine splenocytes were analyzed for various immune cell populations by flow cytometry.

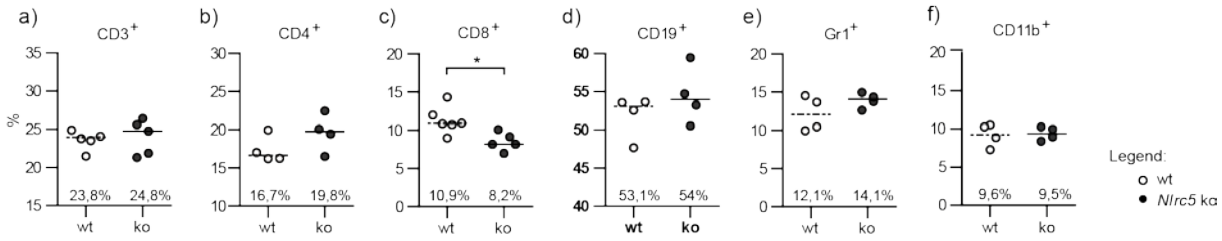

Fig. 3-5: **Immune cell populations in the spleen of *Nlrc5*-deficient mice**
Mice were sacrificed. Spleens were removed, homogenized and mixed splenocyte cultures were prepared. Cells were stained with fluorophore labeled antibodies (anti ms CD3ε FITC anti ms CD4 PE, anti ms CD8 FITC, anti ms CD19 PE, anti ms Gr-1 FITC, anti ms CD11b FITC; Immunotools) and analyzed by flow cytometry. The mapped percentage refers to the gated vivid leukocyte population. Each individual is indicated by a separate dot. Animals: n = 4–6; sex: mixed; age: 8–16 weeks. The median is indicated by the bars and written below. Student's t test was performed. *p = 0.0149
Nlrc5 ko mice showed a significant decrease in the $CD8^+$ population.

NLRC5 deficiency had an impact on certain immune cell populations: While the general CD3 expression on the T lymphocyte population was not altered (a), the $CD8^+$ cytotoxic T lymphocyte (CTL) population was significantly diminished in ko mice (c). In contrast, $CD4^+$ T helper (Th) cells as well as neutrophils ($Gr1^+$) were slightly elevated in the knockout (b, e). $CD19^+$ B cell and $CD11b^+$ monocyte/Mϕ numbers were not affected in the ko (d, f).

3.3 THE EXPRESSION OF MHC MOLECULES ON *NLRC5*-DEFICIENT CELLS

CD8 and CD4 are important co-receptors of the TCR and involved in the recognition of antigens presented by MHC molecules. MHC class I and its bound peptide are recognized by the TCR in combination with CD8 leading to the activation of the $CD8^+$ co-expressing cytotoxic T cells, while CD4 is a co-receptors for loaded MHC class II molecules leading to the activation of the $CD4^+$ co-expressing helper T cells.

Nlrc5 was shown to have a significant impact on the $CD8^+$ CTL and a minor impact on the $CD4^+$ Th lymphocyte population in mice (Fig. 3-5). Therefore, also the counterparts of CD8 and CD4, the MHC class I and II receptors, were analyzed to assess a possible impact of Nlrc5 on the surface expression of these molecules.

3.3.1 DIMINISHED MHC CLASS I EXPRESSION ON *NLRC5*-DEFICIENT LEUKOCYTES

The expression of MHC class I was analyzed by flow cytometry in different primary leukocyte cultures prepared from *Nlrc5* ko mice.

The Surface Expression of MHC Class I is Diminished on Nlrc5-deficient Murine Macrophages

The MHC class I expression was analyzed on murine Mϕs. Bone marrow was isolated from wt and *Nlrc5* ko mice. Bone marrow-derived Mϕs (BMDMs) were generated and analyzed by flow cytometry

for their surface expression of the MHC I isotype H-2Kb (Fig. 3-6). Wt and *Nlrc5* ko mice express H-2Kb. Two distinct H-2Kb positive populations were distinguishable for both genotypes (**a**). *Nlrc5*-deficient BMDMs showed a general reduction of H-2Kb expression on the cell surface (**a**). This is also reflected by the geometric mean fluorescence intensity (geometric mean), which was significantly diminished in the ko (**b**).

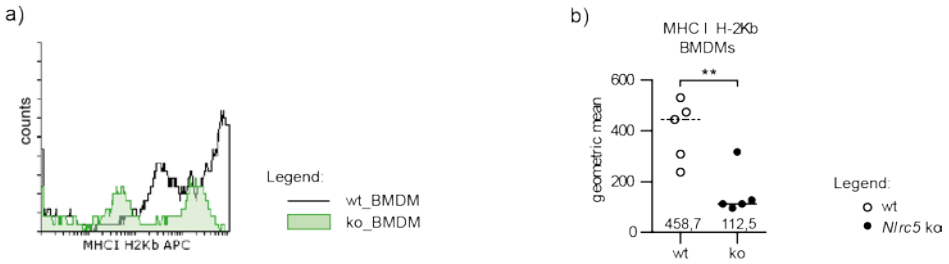

Fig. 3-6: **MHC class I expression on murine *Nlrc5*-deficient macrophages**
Mice were sacrificed, bone marrow was isolated and BMDMs were generated *in vitro*. BMDMs were stained with fluorophore labeled antibodies (anti ms H-2Kb APC, ms IgG2a K Isotype Control APC from eBioscience) and analyzed by flow cytometry.
Animals: n = 6 wt, n = 5 ko; sex: mixed; age: 16 weeks.
a The histogram compares exemplary the MHC class I surface expression on cells of one wt (black line) to the expression on cells of one ko animal (green curve). **b** Geometric mean fluorescence intensities for all tested animals are depicted. Each individual is indicated by a separate dot. The median is represented by the bars and written below. Student's t test was performed. **p = 0.0070.
Shown is the expression of MHC class I H-2Kb on the surface of BMDMs generated from wt and *Nlrc5* ko mice. *Nlrc5*-deficient bone marrow derived Mϕs (BMDMs) had a greatly reduced MHC class I H-2Kb surface expression.

The Surface Expression of MHC Class I is Diminished on Nlrc5-deficient Murine Lymphocytes

The expression of the H-2Kb and the H-2Db MHC class I isotypes was further evaluated on murine splenocytes by flow cytometry (Fig. 3-7).

Nlrc5 ko mice had a reduced MHC class I surface expression for both analyzed MHC class I isotypes (Fig. 3-7b, c, f, g). The geometrical mean fluorescence intensity was significantly diminished in ko lymphocytes (d+h).

In contrast to the murine BMDMs only one single MHC I population for each isotype was observed on wt lymphocytes. However, *Nlrc5*-deficient macrophages had two separate H-2Kb expressing populations (Fig. 3-7 b, c). Also for H-2Db, a second population with slightly reduced surface expression existed.

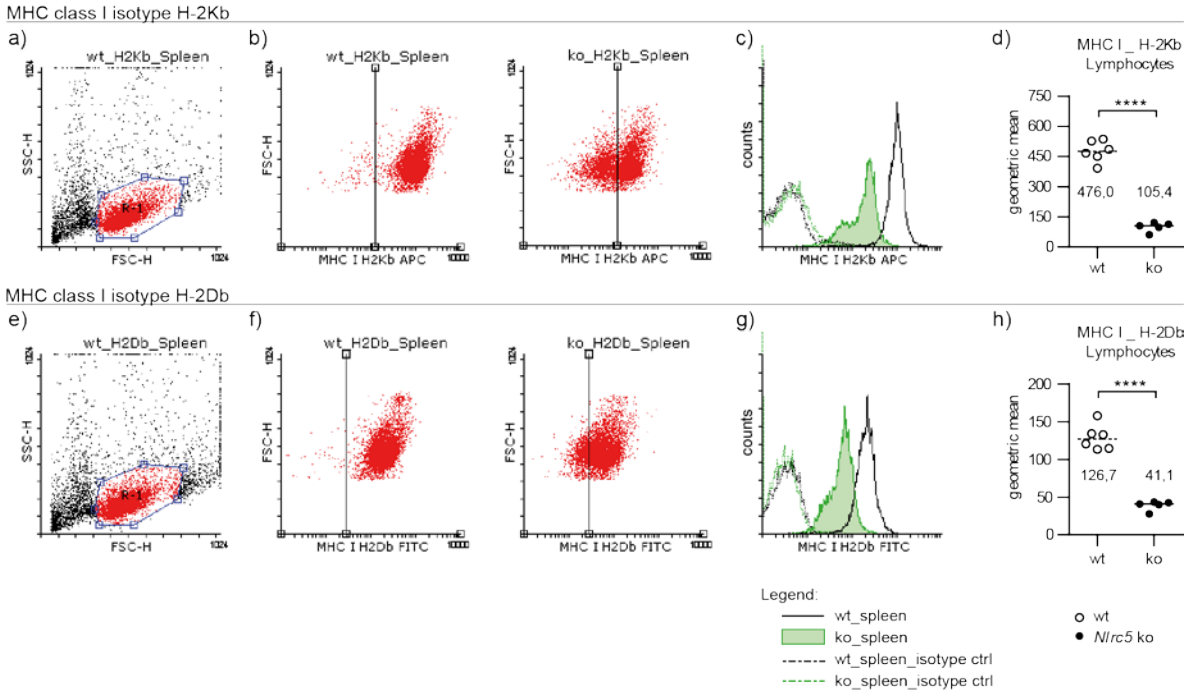

Fig. 3-7: **MHC class I expression on murine *Nlrc5*-deficient lymphocytes**
Mixed splenocyte cultures were prepared, stained with fluorophore labeled antibodies and analyzed by flow cytometry (anti ms H-2Kb APC, anti ms H-2Db FITC, ms IgG2a K Isotype Control APC from eBioscience; ms IgG2a Isotype control FITC from Immunotools). Animals: n=6 wt, 5 ko; sex: mixed; age: 16 weeks. **a+e** Lymphocytes were gated (R-1; red) from the total spleen population (black). **b+f** The MHC I fluorescence intensity is displayed for the entire lymphocyte population in comparison to the cell size indicated by the FSC. The quadrant line is drawn for orientation.
c+g The histograms display the fluorescence intensity versus the cell number and compare exemplary the MHC class I expression in one wt animal (black line) to the expression in one ko animal (green curve). Isotype controls are indicated by dashed lines (black = wt, green = ko).
d+h Geometric means of the fluorescence intensity of all tested animals are compared in the scatter plots. Each individual is shown as a separate dot. Bars indicate the median and are given as numbers. Student's t test was performed. ****p = < 0.0001.
Shown is the expression of two different MHC class I isotypes (**a–d** H-2Kb, **e–h** H-2Db) on the surface of lymphocytes from wt and *Nlrc5* ko mice. Murine lymphocytes showed a significantly and inhomogenously reduced MHC I surface expression for both isotypes.

3.3.2 Two MHC class I expressing leukocytes populations exist

Nlrc5 ko mice did not only show a reduced MHC class I surface expression, they also displayed a second MHC class I expressing population within the analyzed lymphocyte population (Fig. 3-7 b, c, g). Especially for the H-2Kb isotype these populations were clearly distinguishable. However, a second MHC class I expressing population was absent in wt lymphocytes. In order to evaluate population size and, which lymphocyte subclasses they are composed of, further flow cytometric analyses were performed using murine splenocytes (Fig. 3-8).
On average 99% of all wt lymphocytes and 98% of all *Nlrc5*-deficient lymphocytes expressed H-2Kb on their surface (d). Wt lymphocytes showed repeatedly one major H-2Kb-expressing population that included 98% of all lymphocytes, while the remaining 2% had only low (1%) or no (1%) H-2Kb on their surface (Fig. 3-8 b, d).
Lymphocytes from *Nlrc5* ko mice showed two different H-2Kb-expressing populations. On average 69% of all lymphocytes expressed moderate to high H-2Kb levels (region name "high") and 29% expressed only very low amounts of the MHC I isotype (Fig. 3-8 c, d). Also within the "high" region *Nlrc5*-deficient lymphocytes showed a strongly reduced H-2Kb expression when compared to the wt as indicated by the geometric mean fluorescence of that region (Fig. 3-8 b, c).

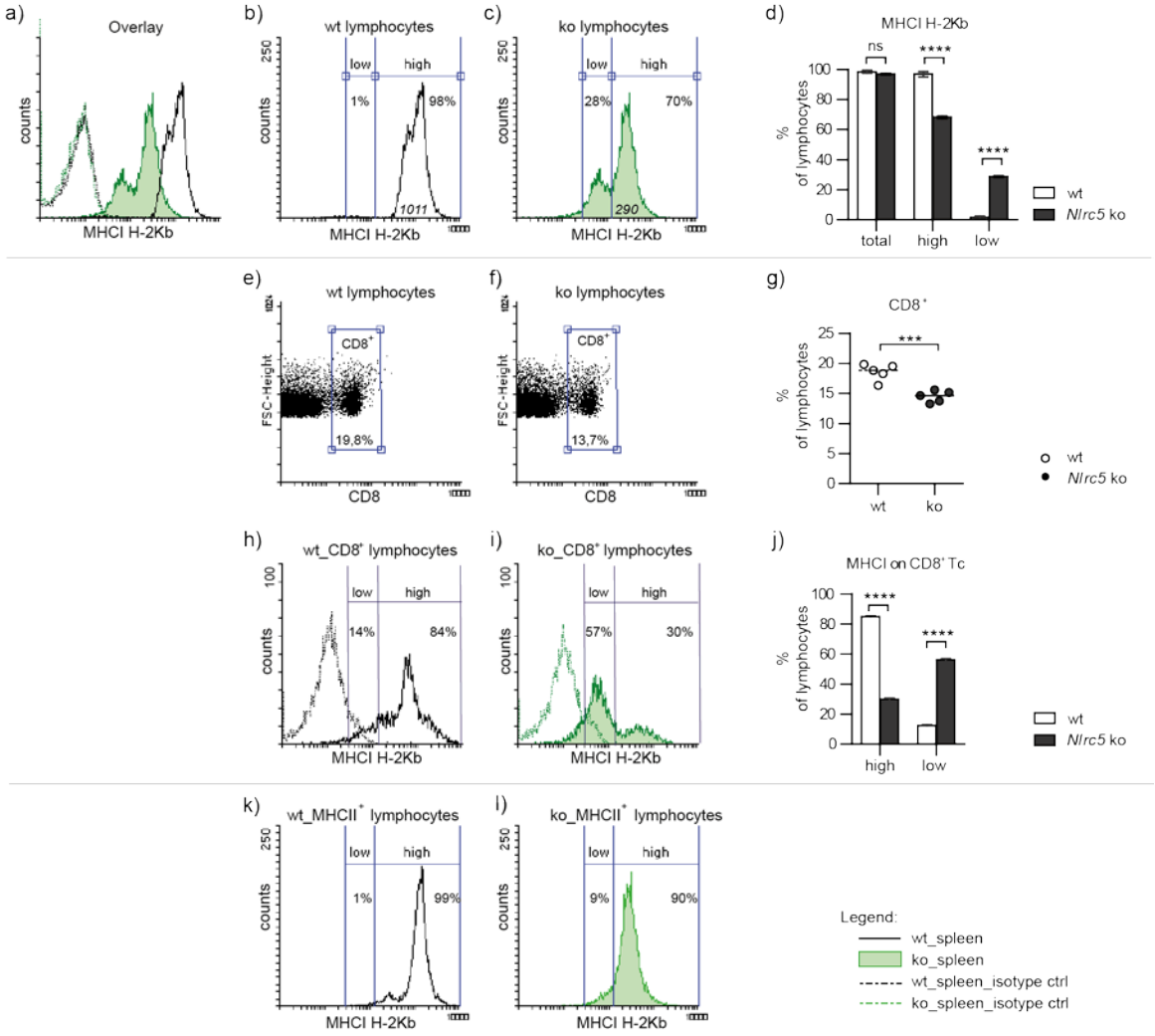

Fig. 3-8: **Identification and analysis of MHC class I (H-2Kb) expressing lymphocyte subpopulations**
Mixed splenocyte cultures were prepared and triple stained with fluorophore labeled antibodies for MHC I H-2Kb, CD8 and MHC II 1-A or their corresponding isotype controls (anti ms H-2Kb APC, anti ms MHC II (I-A) PE, ms IgG2a κ Isotype APC, rat IgG_{2b}, κ Isotype PE, eBioscience, anti ms CD8 FITC, Immunotools; rat IgG2a, κ Isotype FITC, BioLegend). Cells were analyzed by flow cytometry. Data refer to the gated vivid lymphocyte population. Animals: n = 5 wt, n = 5 ko; sex: female; age: 8–9 weeks.
a–c The surface expression of MHC I H-2Kb on wt (black lines) and ko (green curves) lymphocytes is displayed. **a** Isotype controls were used to check for nonspecific staining (dashed lines; black = wt, green = ko) and to define regions (low, high) for further population analyses. **b+c** Population sizes for the regions are given in percent. The geometric mean is indicated in italics and refers only to the high MHC I expressing population. **d** H-2Kb populations for all tested animals were compared. Given is the mean with SEM. Statistical analysis was performed with Two-way ANOVA followed by Bonferroni post-hoc tests. **** $p < 0.0001$
e–g Shown is the analysis of the $CD8^+$ lymphocyte population. The size of the gated $CD8^+$ population is given in % and the comparison of all animals is shown in **g**. Bars indicate the median. Student's t test was performed. ***$p = 0.0006$
h–j $CD8^+$ lymphocytes were gated and analyzed for their MHC I H-2Kb surface expression. The histograms compare exemplary the population size for the low and high region for one wt and one ko animal (**h+i**). **j** Shown is the comparison of the MHC I expression on the $CD8^+$ population giving the mean with SEM. Statistical analysis was performed with Two-way ANOVA followed by Bonferroni post-hoc tests. **** $p < 0.0001$
k+l MHC II $1\text{-}A^+$ lymphocytes were gated and analyzed for their MHC I H-2Kb surface expression. The histograms depict exemplary population sizes for the low and high region in one wt and one ko animal.
Nlrc5-deficient lymphocytes show an additional H-2Kb population that comprises about 30% of all ko lymphocytes. About 60% of ko $CD8^+$ CTLs, but only 10% of MHC class II^+ APCs belong to this H-2Kb low expressing lymphocyte subpopulation. 90% of MHC II^+ cells showed a high MHC I expression on *Nlrc5*-deficient lymphocytes.

The gated vivid lymphocyte population was further analyzed for CD8 expression (Fig. 3-8 e–g). On average 19% of wt lymphocytes expressed CD8 and were therefore cytotoxic T lymphocytes, while only 14% of the *Nlrc5*-deficient lymphocytes were co-expressed CD8 (see also Fig. 3-5 c). $CD8^+$ lymphocytes were subsequently analyzed for their H-2Kb expression pattern (Fig. 3-8 h–j). In the wt the majority of all $CD8^+$ CTLs expressed high H-2Kb levels (84%). In contrast, only 30% of *Nlrc5*-

deficient $CD8^+$ lymphocytes showed a high H-2Kb expression: The majority (57%) had a greatly diminished H-2Kb expression. $CD8^+$ T lymphocytes were therefore one of the lymphocyte subpopulations that account for the $H\text{-}2Kb^{low}$ expressing population among ko lymphocytes.
In contrast, the great majority of MHC class II^+ lymphocytes (99% in wt and 90% in the ko) expressed high H-2Kb levels (Fig. 3-8 k, l). Therefore, MHC II^+ cells did account for the cellular subpopulation that remained a high MHC I H-2Kb expression among *Nlrc5*-deficient lymphocytes.

3.3.3 Enlarged population of MHC class II^+ cells in the spleen

The deletion of *Nlrc5* significantly reduced the expression of MHC class I and diminished the $CD8^+$ cell population. Furthermore, $CD4^+$ cell numbers were slightly elevated. Therefore, the surface expression of MHC class II was analyzed on splenocytes as well.
MHC class II was expressed on *Nlrc5*-deficient as well as on wt leukocytes (Fig. 3-9). The amount of MHC II per cell did not strikingly differ between both genotypes (a), but the MHC II expressing cell population was enlarged in the ko. *Nlrc5*-deficient leukocytes had on average 9% more MHC II^+ leukocytes in the spleen when compared to wt cells (b).

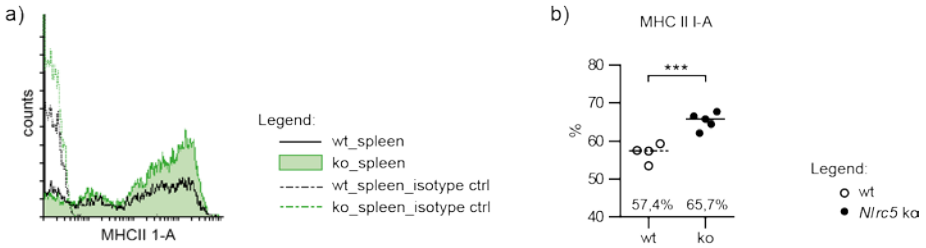

Fig. 3-9: **MHC class II expression on *Nlrc5*-deficient leukocytes**
For experimental procedure see legend to Fig. 3-8. Data refer to the gated vivid leukocyte population.
a Each curve represents the MHC class II expression of one exemplary animal (continuous lines, black = wt, green = ko). Isotype controls are used to check for nonspecific immunoglobulin binding (dashed lines; black = wt, green = ko).
b MHC class II isotype I-A positive cell populations were compared between *Nlrc5* ko and wt leukocytes. Each individual is displayed by a separate dot. The median is indicated by the bar and written below. Student's t test was performed for statistical analyses. ***p = 0.0009
Nlrc5-deficient leukocytes expressed significantly more MHC class II on the plasma membrane.

3.3.4 MHC Class I is still inducible in *Nlrc5*-deficient lymphocytes

A strong reduction of MHC class I molecules was found on *Nlrc5*-deficient immune cells. In order to evaluate if MHC class I could still be induced in *Nlrc5*-deficient cells, mixed splenocytes were stimulated with Phytohemagglutinin (PHA) and IL-2 and MHC I surface expression was monitored by flow cytometry. PHA is a natural lectin from the kidney bean (*Phaseolus vulgaris*), which agglutinates leukocyte surface receptors including the TCR. Thereby it leads to a nonspecific cell activation and proliferation of T lymphocytes as well as the release of cytokines via several pathways. Interleukin 2 (IL-2) stimulates the proliferation and differentiation of activated lymphocytes (Morgan et al., 1976) and was used to stimulate lymphocyte proliferation.
PHA significantly upregulated the MHC class I expression on the surface of wt and ko lymphocytes (Fig. 3-10 a, b, c). This was further increased if IL-2 was added.
MHC I was more potently induced in *Nlrc5*-deficient than wt cells (Fig. 3-10 c). However, although MHC I could be induced by PHA and IL-2, the total surface MHC I expression was still significantly decreased in ko lymphocytes if compared to the wt.
Nlrc5-deficient lymphocytes furthermore showed a significant increase in the number of MHC I^+ cells after the stimulation with PHA and IL-2. Without stimulation 96.6% of all wt lymphocytes carried MHC I on their surface, while in the ko this population was slightly diminished with 95.6% of all

lymphocytes being MHC I$^+$ (Fig. 3-10 d). PHA and more potently PHA/ IL-2 induced a slight increased in the number of MHC I$^+$ cells, which was significant in *Nlrc5* ko lymphocytes. After PHA/ IL-2 stimulation the MHC I$^+$ populations were similar for both genotypes, with 97.5% MHC I$^+$ wt and 97.6% MHC I$^+$ ko lymphocytes.

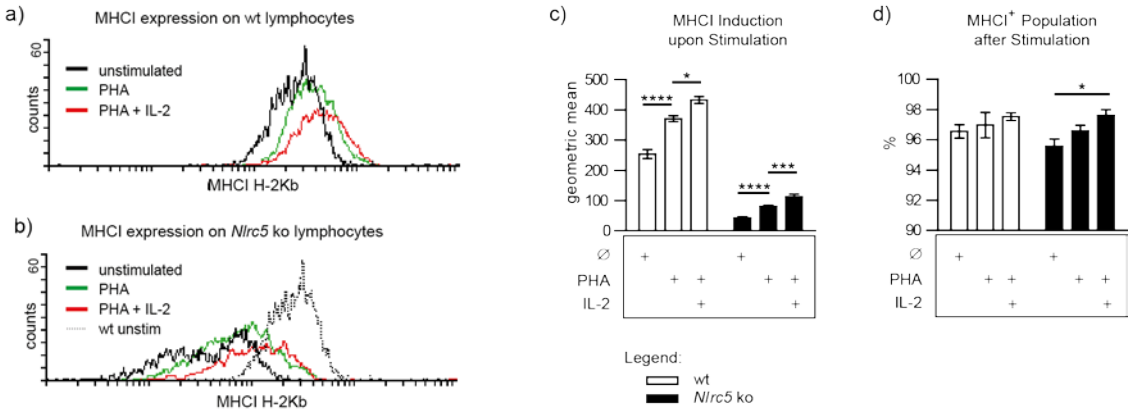

Fig. 3-10: **Surfacial MHC class I expression on murine lymphocytes upon stimulation**
Mixed splenocyte cultures were prepared (96-well format, 2 x 10^5cells/well) and stimulated with PHA (0.5 µg/ml) and IL-2 (25 ng/ml; Immunotools) for 20 h. Cells were harvested, stained with fluorophore labeled antibodies (anti ms H-2Kb APC; eBioscience) and analyzed by flow cytometry. Data refer to the gated vivid lymphocyte population. Animals: n=6 wt, 5 ko; sex: mixed; age: 16 weeks.
a+b Histograms show MHC I fluorescence intensities in unstimulated (black), PHA (green) or PHA/IL-2 (red) stimulated lymphocytes of an exemplary wt (**a**) and ko animal (**b**). The dashed line (**b**) indicates the unstimulated wt and is shown for comparison. The induction of MHC I molecules on the surface of lymphocytes is indicated by the geometric mean fluorescence and compared for all animals in **c**. Furthermore, the MHC I H-2Kb positive population was analyzed in a dot plot (MHC I versus FCS; not shown) and changes in population size upon stimulation are displayed in **d**. One-way ANOVAs with Bonferroni post-hoc tests were performed. *p < 0.05; ***p < 0.001; ****p < 0.0001
MHC class I can be induced in *Nlrc5* ko lymphocytes, as the MHC I surface expression was elevated and the total MHC I$^+$ population expanded upon cell activation.

The overall expression of MHC I was strongly upregulated upon stimulation with PHA and IL-2 in wt and ko animals. This was mainly mediated through an elevated expression of MHC I (Fig. 3-10 c) on the cell surface and only slightly influenced by an increase in the general MHC I$^+$ cell population (Fig. 3-10 d).
MHC class I can still be potently induced upon stimulation in the *Nlrc5*-deficient cells, although the MHC class I expression remained strongly alleviated in *Nlrc5*-deficient cells.

3.4 Altered Cytokine Expression in *Nlrc5*-Deficient Cells

The *Nlrc5* knockout was shown to influence certain immune populations and the surface expression of MHC class I and II molecules. In order to assess how NLRC5 influences these parameters various signaling pathways were activated in primary leukocyte cultures and the induction of typical cytokines was analyzed to evaluate if NLRC5 might be involved in immune signaling pathways. An altered immune signaling can influence the MHC expression or the generation, differentiation or survival of certain immune cell populations.

3.4.1 Impaired Induction of Type I and II IFNs

Interferons are important mediators within the immune system, especially in antiviral responses (Malmgaard, 2004) and link the innate to the adaptive immune system (Le Bon and Tough, 2002). NLRC5 was repeatedly reported to be involved in IFN signaling, but observations remained contradictory (Benko et al., 2010; Cui et al., 2010; Kuenzel et al., 2010; Neerincx et al., 2010).

Therefore, the induction of type I and type II IFNs was evaluated in *Nlrc5*-deficient cells by stimulating murine splenocytes and BMDMs *in vitro*.

Type I Interferon: IFNβ

Murine BMDMs were generated and stimulated with poly(I:C) or single stranded (ss) RNA, which both mimic viral infection (Fig. 3-11). A pretreatment with LPS was performed for poly(I:C)-induced *Ifnb* expression. The mRNA induction was analyzed using RT-qPCR.

There was no *Ifnb* mRNA detectable in unstimulated BMDMs, but it was induced upon stimulation with either LPS, LPS/ poly(I:C) or ssRNA in both genotypes. LPS pretreatment led to an equal induction of *Ifnb* (abs. foldchange $_{LPS}$: wt = 70.9 vs. ko = 70.4) in wt and ko BMDMs. Additional stimulation with the synthetic double stranded RNA analogue poly(I:C) potently induced *Ifnb* mRNA in the wt. *Ifnb* was also induced in ko BMDMs, but to a lesser extent (abs. foldchange $_{LPS/poly(I:C)}$: wt = 261.8 vs. ko = 103.5). BMDM treatment with ssRNA also induced *Ifnb* gene expression. The induction tends to be stronger in wt compared to ko BMDMs (abs. foldchange $_{ssRNA}$: wt = 282.7 vs. ko = 92.6).

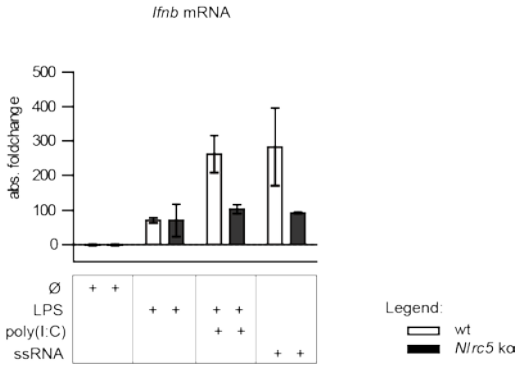

Fig. 3-11: **Induction of *Ifnb* in stimulated *Nlrc5*-deficient primary cell cultures**
Murine BMDMs were cultured in 6-well cell culture plates (0.5 x 10^6 cells/well). Cells were either prestimulated for 4 h with LPS (100 ng/ml, RC Borstel) before poly(I:C) (10 µg/ml; Calbiochem) was added o/n or they were stimulated only with ssRNA (1 µg/ml; InvivoGen) for 6 h. RNA was prepared for *Ifnb* TaqMan assay. *Ifnb* expression was normalized to *β-Actin* and the absolute foldchange was calculated in comparison to unstimulated samples. Animals: n = 2 wt, 2 ko; sex: female, age: 9 weeks. Technical duplicates were performed and averaged. Depicted is the mean of biological replicates with the SEM. TaqMan assay was obtained from Life Technologies™ (Tab. 13).
Nlrc5-deficient cells fail to induce *Ifnb* upon viral stimulation with either poly(I:C) or ssRNA.

Lymphocyte Activation

Primary murine splenocyte cultures were prestimulated with a mixture of Phorbol 12-myristate 13-acetate and Ionomycin (PMA/ Iono) or PHA. While PHA agglutinates cell-surface receptors to activate leukocytes, the combination of PMA/ Iono raises intracellular Ca^{2+} levels. Free Ca^{2+} in the cytoplasm binds calmodulin that in turn activates the calmodulin-activated phosphatase calreticulin. Calreticulin dephosphorylates members of the transcription factor family nuclear factor of activated T cells (NFAT), which can enter the nucleus and induce cell-specific gene transcription (Hogan et al., 2003). Both stimulations were used to activate resting lymphocytes to produce and release their specific cytokines.

Lymphocyte activation was monitored by the surface expression of CD25, to exclude that differences in cytokine expression are due to an altered activation status between wt and *Nlrc5* ko lymphocytes. CD25 is the alpha chain of the IL-2 receptor and was used as lymphocyte activation marker.

The expression of CD25 was elevated upon either PMA/ Iono or PHA treatment at comparable levels on wt and ko splenocytes, thus cells showed an equal activation status (Fig. 3-12 a). Cells were

activated equally upon PHA or PMA/ Iono treatment. No influence of LPS on cell activation was detected.

Type II Interferon: IFNγ

Cytokine production was further induced by subsequent LPS treatment (Fig. 3-12 b, c). The induction of *Ifng* mRNA was analyzed by RT-qPCR (TaqMan assay) and the secreted amounts of IFNɣ were measured by enzyme-linked immunosorbent assay (ELISA) in culture supernatants (0; 2.5).

There was no *Ifng* mRNA detectable in unstimulated wt and ko cells (Fig. 3-12 b). Upon stimulation with LPS, PMA/ Iono or PMA/ Iono/ LPS *Ifng* was slightly induced in both genotypes with a higher absolute foldchange in the wt (average abs. foldchange $_{PMA/\ Iono/\ LPS}$: wt = 11.8 vs. ko = 3.6). *Ifng* was potently induced after PHA stimulation and further raised if LPS was administered additionally. Overall, the expression of *Ifng* was higher in wt than in *Nlrc5*-deficient cells (average abs. foldchange $_{PHA/LPS}$: wt = 124.3 vs. ko = 37.6).

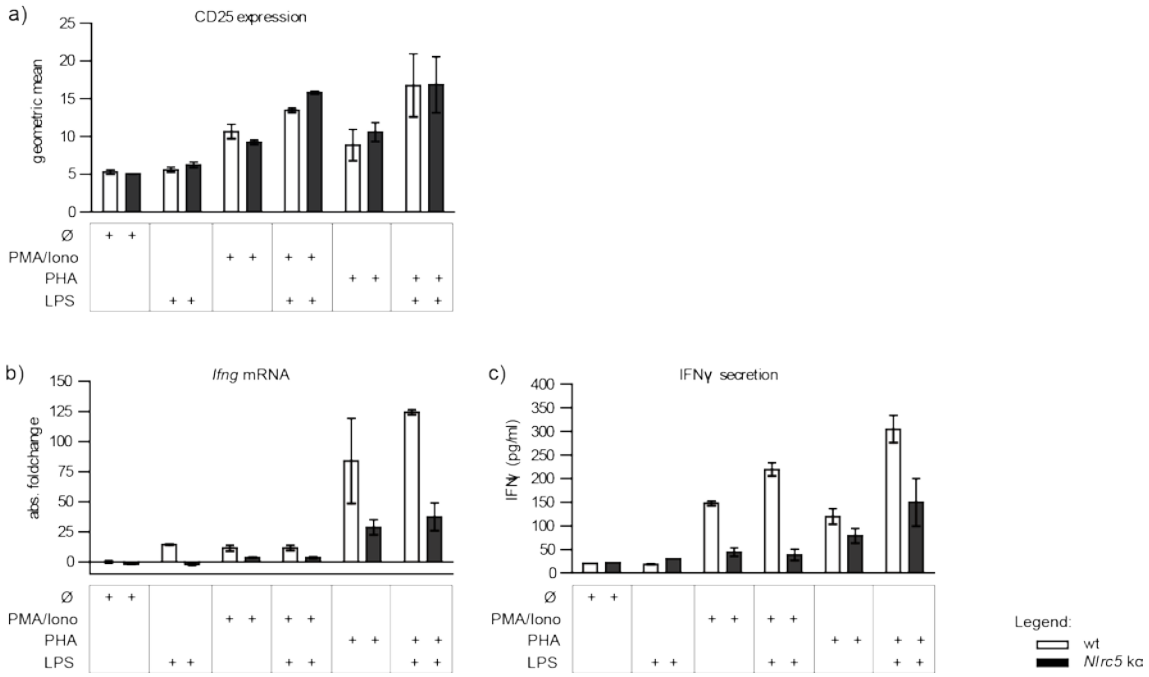

Fig. 3-12: **Activation of *Nlrc5*-deficient splenocytes & induction of IFNγ by LPS**

Mixed murine splenocytes were cultured in 12-well cell culture plates ($4x10^6$ cells/well) and prestimulated o/n with PMA/Iono (PMA: 10 ng/ml; Iono: 1 µg/ml Sigma-Aldrich) or PHA (0.5 µg/ml). Afterwards they were additionally stimulated with LPS (100 ng/ml, RC Borstel) for 24 h before supernatant was taken off for ELISA analysis (**c**) and cells were analyzed by flow cytometry (**a**) or TaqMan analyses (**b**).

a Cells were labeled with anti ms CD25 FITC (Immunotools). Results refer to gated vivid splenocytes. **b** *Ifng* TaqMan assay was performed, expression normalized to *β-Actin* and absolute foldchange calculated in comparison to unstimulated samples (Life Technologies™; Tab. 13). **c** IFNγ ELISA was performed as instructed by the manufacturer (CMC4033, Invitrogen).

Animals: n = 2 wt, 2 ko; sex: female; age: 10 weeks. Technical duplicates were performed and averaged. Depicted are the means of biological replicates with the SEM.

Wt and ko splenocytes were equally activated by PMA/ Iono or PHA, while the activation-induced expression of IFNγ was diminished in *Nlrc5* ko splenocytes.

Secreted IFNɣ levels were low in both genotypes in untreated and LPS stimulated cells (Fig. 3-12 c; average IFNγ concentration $_{unstim}$: wt = 20.8 pg/ml vs. ko = 22.0 pg/ml). An increase in IFNɣ secretion was observed in the wt upon stimulation with PMA/ Iono (147.8 pg/ml), which was further elevated by co-administering LPS (219.5 pg/ml). PHA also induced the secretion of IFNɣ (120.0 pg/ml) in wt cells, which was further increased by additional LPS treatment (305.0 pg/ml). *Nlrc5*-deficient

splenocytes produced IFNɣ to a much lesser extent. The secretion of IFNɣ was only slightly induced by PMA/ Iono (44.2 pg/ml) and not further augmented by an additive LPS treatment. Also PHA treatment induced IFNɣ in *Nlrc5*-deficient cells (78.7 pg/ml), which was further elevated by the addition of LPS (150.1 pg/ml). However, the secreted IFNɣ levels were diminished in ko compared to wt cells.
IFNɣ could be induced and secreted by *Nlrc5*-deficient splenocytes, but mRNA as well as protein levels of the type I IFN were reduced if compared to equally treated wt splenocytes.

Taken together, type I and II IFN responses were impaired in *Nlrc5*-deficient primary cultures upon *in vitro* stimulations compared to wt cells.

3.4.2 IMPAIRED INDUCTION OF IL-1β

The cytokine IL-1β is an important mediator in inflammatory cellular immunity, especially in response to lipopolysaccharides. IL-1β is mainly produced in cells of the monocytic lineage. It was observed *in vitro* that NLRC5 might be involved in IL-1β signaling (Davis et al., 2010).
IL-1β induction and secretion were analyzed in *Nlrc5*-deficient BMDMs and bone marrow-derived dendritic cells (BMDCs) to evaluate a potential role of this NLR member in IL-1β signaling processes.
Primary BMDM and BMDC cultures were stimulated with LPS to induce the expression of the IL-1β propeptide and subsequently treated with ATP to activate caspase-1, which cleaves the pro-IL-1β into its active form. RNA was isolated for TaqMan analyses.
Il1b mRNA was induced by LPS in wt and ko BMDMs (Fig. 3-13 a; abs. foldchange $_{LPS}$: wt = 16.5 vs. ko = 3.0). Interestingly, mRNA levels were further raised upon ATP treatment (abs. foldchange $_{LPS/ATP}$: wt = 63.0 vs. ko = 22.6), but the *Il1b* expression was significantly diminished in *Nlrc5*-deficient BMDMs when compared to wt cells.
The amount of secreted IL-1β was determined by performing an IL-1β ELISA using culture supernatants. The cytokine was barely detectable in wt and ko supernatants of unstimulated and LPS-treated culture wells ($wt_{unstim,\ LPS}$ = 10,7 pg/ml; ko_{unstim} = 7,5 pg/ml; ko_{LPS} = 5,7 pg/ml). IL-1β secretion was induced in both genotypes by additional stimulation with ATP upon LPS treatment (Fig. 3-13 b), but the amount of secreted IL-1β was alleviated in the ko ($wt_{LPS/ATP}$ = 40.7 pg/ml; $ko_{LPS/ATP}$ = 12.1 pg/ml).
Furthermore, IL-1β production was monitored by staining of intracellular IL-1β and its flow cytometric analysis in murine dendritic cells (Fig. 3-13 c). Again cells were stimulated with LPS alone or in combination with ATP.
Already basal intracellular IL-1β concentrations were significantly diminished in the *Nlrc5*-deficient BMDCs when compared to the wt. This tendency was observed for all stimulations. Neither the treatment with LPS nor LPS/ATP potently raised intracellular IL-1β concentrations in wt and ko BMDCs.

Fig. 3-13: **Induction and secretion of IL-1β in stimulated *Nlrc5*-deficient primary cells**
Primary BMDMs and BMDCs were generated from fresh murine bone marrow. **a & b** . Animals: n = 2 wt, 2 ko; sex: female, age: 9 weeks. BMDMs were cultured in 6-well cell culture plates (0.5 x 10^6 cells/ well). Cells were prestimulated with LPS (1 µg/ml, RC Borstel) for 4 h followed by ATP (10 µM; Sigma-Aldrich) stimulation for 20 h. ELISA was performed with supernatants, while RNA was isolated for TaqMan analysis **a** *Il1b* TaqMan assay was performed (Life Technologies™; Tab. 13), expression normalized to *β-Actin* and the absolute foldchange calculated in comparison to unstimulated samples. **b** IL-1β ELISA was performed as instructed by the manufacturer (CMC0813, Invitrogen).
c Animals: n = 6 wt, 5 ko; sex: mixed; age: 9 weeks. BMDCs were cultured in 6-well cell culture plates (1 x 10^6 cells/well) and prestimulated with LPS (100 ng/ml, RC Borstel) for 24 h before ATP (10 µM, Sigma-Aldrich) was added. Simultaneously Brefeldin A (4 µg/ml, Sigma-Aldrich) was added to all wells to inhibit protein secretion. After 6 h cells were fixed, permeabilized (BD Cytofix/Cytoperm™, BD Bioscience), stained for intracellular IL-1β as recommended by the manufacturer (ms IL-1beta mAB PE, R&D Systems®) and analyzed by flow cytometry.
Technical duplicates were performed and averaged. Depicted are the means of biological replicates with the SEM.
The induction of IL-1β was impaired in *Nlrc5*-deficient primary cultures upon stimulation.

Altogether, upon stimulation IL-1β levels were reduced in *Nlrc5*-deficient cells when compared to the wt *in vitro*.

3.4.3 ALTERED EXPRESSION OF PRO-INFLAMMATORY CYTOKINES

Various mediators play a pivotal role in immune processes. For instance TNFα, which is a very early induced mediator directing innate inflammatory processes. TNFα activates e.g. NF-κB signaling and thereby induces other signaling molecules like IL-1β, IL-6 and CXCL1 (KC, human homologue: IL-8). These mediate further steps in the course of inflammation. NLRC5 was reported to inhibit NF-κB signaling *in vitro* (Benko et al., 2010; Cui et al., 2010). To evaluate this, the expression of *Tnfa*, *Il6* and *Cxcl1* were analyzed *ex vivo* in murine BMDMs.
Murine BMDMs were stimulated with LPS (Fig. 3-14 a, b). The induction of pro-inflammatory cytokines was investigated on the mRNA level using TaqMan assays. TNFα secretion was further measured by performing ELISA assays.
Tnfa, *Il6* and *Cxcl1* were induced upon LPS stimulation to a different extent in both genotypes.
While the mRNA expression of *Tnfa* was elevated in *Nlrc5*-deficient BMDMs (Fig. 3-14 a; abs. foldchange $_{LPS}$: wt = 7.4 vs. ko = 15.0), the secretion of TNFα was higher in wt BMDMs (Fig. 3-14 b; wt $_{LPS}$ = 808.1 pg/ml; ko $_{LPS}$ = 308.5 pg/ml). Furthermore, *Cxcl1* mRNA levels were elevated in *Nlrc5*-deficient BMDMs (Fig. 3-14 d; abs. foldchange $_{LPS}$: wt = 40.9 vs. ko = 82.4) and *Il6* mRNA was induced to a similar extent upon LPS stimulation in wt and ko cultures (Fig. 3-14 c).

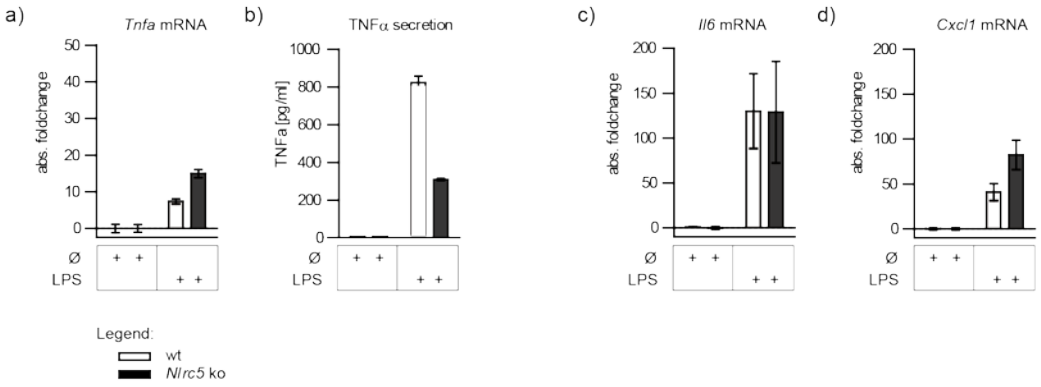

Fig. 3-14: **Induction of pro-inflammatory mediators in stimulated *Nlrc5*-deficient BMDMs**
a-d Primary BMDM cultures were generated from murine bone marrow and cultured in 6-well cell culture plates (0.5 x 10^6 cells/ well). Cells were prestimulated with LPS (1 µg/ml, RC Borstel) for 24 h. TaqMan assays were carried out on isolated mRNAs (**a, c, d;** Life Technologies™) and the ELISA on cell culture supernatants (**b**; CMC3013; Invitrogen). All assays were performed as instructed by the manufacturer. Animals: n=2 wt, 2 ko; sex: female, age: 9 weeks.
Technical duplicates were performed and averaged. Depicted are the means of biological replicates with SEM.
The induction of *Tnfa* was elevated in *Nlrc5*-deficient cells when compared to the wt; in contrast secreted TNFα concentrations were strongly alleviated in the ko. *Cxcl1* mRNA levels were elevated in *Nlrc5*-deficient BMDMs and *Il6* was induced at comparable amounts in both genotypes.

Taken together, TNFα and CXCL1 are differentially regulated in *Nlrc5*-deficient BMDMs if compared to wt cells.

3.5 The Impact of NLRC5 on Experimental Murine Colitis

An immunological phenotype was observed in *Nlrc5* ko mice. This phenotype was not only restricted to innate responses manifesting through an altered cytokine profile, but it had also an impact on adaptive mechanisms as there were striking differences in the expression of MHC molecules as well as the CD8 co-expressing T lymphocyte population if *Nlrc5* was deleted (3.2, 3.3, 3.4).
These *ex vivo* results were further evaluated *in vivo* in murine DSS-induced experimental colitis models, which induce strong inflammation in the murine colon and therefore mimic human IBD. An acute and a chronic colitis phenotype were induced, which involve innate as well as adaptive immune processes (Hall et al., 2011).
To answer if NLRC5 has an impact on the inflammatory processes disease onset, progression and severity were monitored by analyzing clinical parameters. Furthermore, NLRC5-specific parameters were examined.

3.5.1 Increased severity of acute colitis in *Nlrc5* ko mice

DSS is reported to be toxic to the colon epithelium. It destructs the epithelial barrier allowing luminal microorganisms and antigens to enter the colon tissue, which subsequently leads to the development of an experimental colitis (Hans et al., 2000a; Tlaskalová-Hogenová et al., 2005). The development of an acute DSS colitis is described to be independent of adaptive immune processes (Dieleman et al., 1994). Therefore, it is a useful model to study the impact of the NLRC5 protein on innate inflammatory processes.
Acute colitis was induced in *Nlrc5* ko and wt mice by applying 3% DSS orally for five days, followed by three days of water only (Fig. 3-15).
All acute colitis read outs described below are based on the experimental setup described in Fig. 3-15

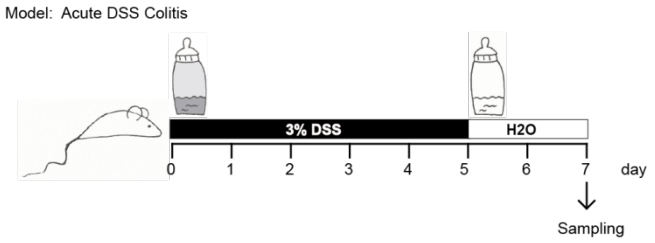

Fig. 3-15: **Treatment of experimental animals to induce acute DSS colitis**
Shown is the model of DSS treatment that was used to induce an acute colitis. Drinking water was autoclaved and contained 3% DSS at the indicated time points. The control group solely got autoclaved water at all times.
Animals treatment groups: n = 10 wt, 10 ko. Animals control groups: n = 4 wt, n = 4 ko; sex: male; age: 10–11 weeks.

3.5.1.1 Decreased survival during acute DSS treatment

Already at two to three days after DSS treatment mice started to show severe gastrointestinal symptoms such as massive diarrhea and bloody feces, which was accompanied by heavy weight loss starting at day five (Fig. 3-17). Due to the severity of disease, mice were monitored daily for weight loss and overall health state. In accordance with animal welfare guidelines mice were immediately taken out of the experiment and sacrificed if body weight loss exceeded 20% of the initially measured body weight. The survival rate is therefore an indicator of disease severity. All water-treated control animals (wt & ko) as well as all DSS-treated wild type mice survived the entire experiment (100% survival), while only 80% of *Nlrc5* knockout mice survived until the end of the experiment at day seven (Fig. 3-16).

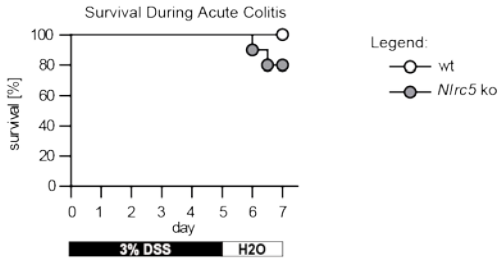

Fig. 3-16: **Survival during the course of acute DSS colitis**
The survival curves show the percentage of vivid animals during the course of the experiment. Mice that did not match the animal welfare guidelines in the course of the experiment were not further treated and prematurely sacrificed for analyses. None of the control animals had to be taken out early (survival 100%, wt and ko; not shown).
Wt mice had a higher survival rate than *Nlrc5* ko mice during the DSS-induced acute colitis.

3.5.1.2 Elevated disease activity index

During colitis gastrointestinal passage is accelerated and water resorption is diminished within the colon to clean the gut from invaded pathogens or toxins (Lippert, 2003). Typical clinical signs are diarrhea, body weight loss and intestinal bleeding due to a severe inflammation. These clinical signs can also be observed in murine colitis models and they are used to evaluate disease severity (Fig. 3-17).

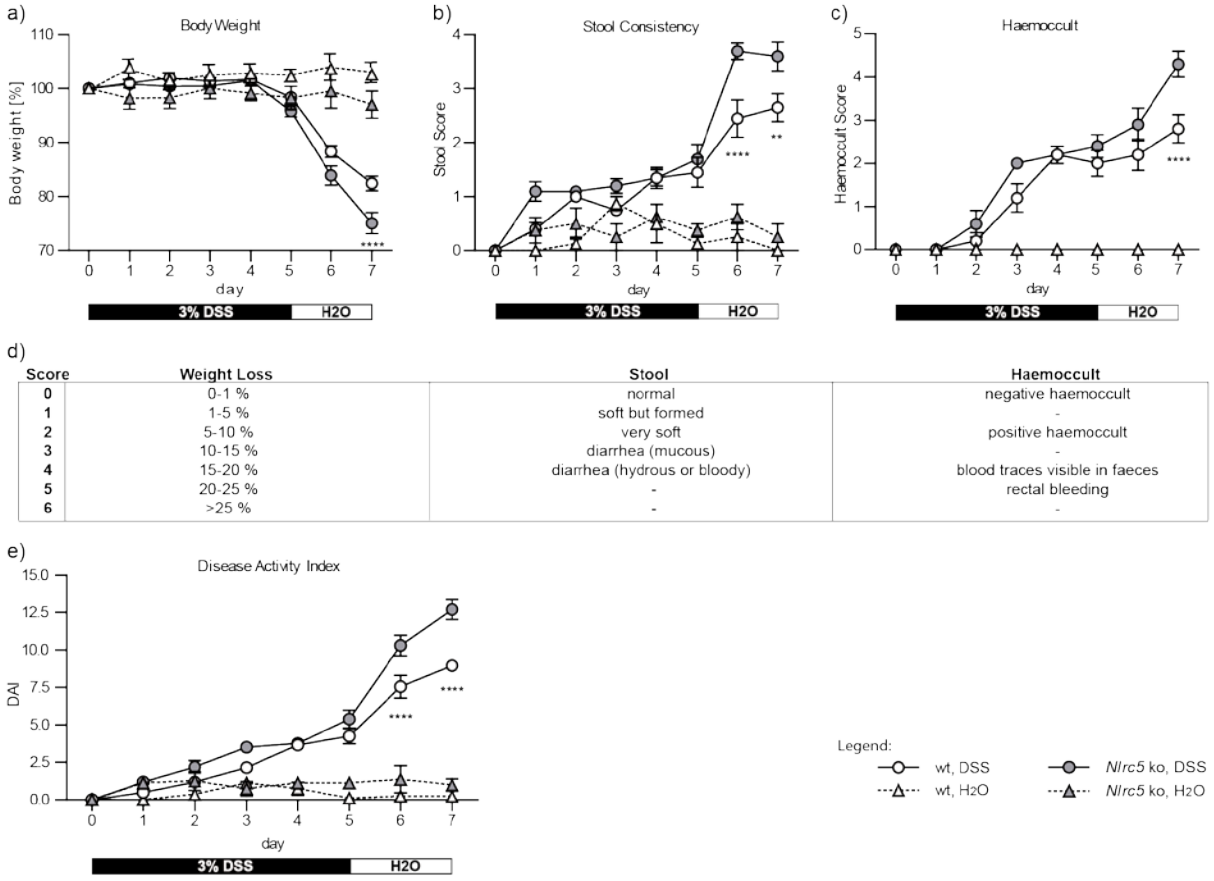

Score	Weight Loss	Stool	Haemoccult
0	0-1 %	normal	negative haemoccult
1	1-5 %	soft but formed	-
2	5-10 %	very soft	positive haemoccult
3	10-15 %	diarrhea (mucous)	-
4	15-20 %	diarrhea (hydrous or bloody)	blood traces visible in faeces
5	20-25 %	-	rectal bleeding
6	>25 %	-	-

Fig. 3-17: **DAI – A combined score of body weight, stool consistency and fecal occult blood**
To monitor disease progression mice were weighted (**a**) and stool samples were judged for consistency (**b**) and occult blood (**c**) daily. All three parameters were scored over time as indicated (**d**) and summarized to the disease activity index (DAI), which is generally used to evaluate colitis severity (**e**). Mean values of each experimental group are indicated by single dots with SEM. Two-way ANOVA and Bonferroni post-tests were performed. Stars indicate the level of significance between DSS-treated wt and ko groups at the indicated days. Please note that significances of DSS-treated groups compared to their control groups are not indicated in the figure for clarity, but mentioned in the text. **p < 0.01; ****p < 0.0001
Nlrc5 ko mice showed a more severe weight loss, diarrhea and rectal bleeding during the course of the acute DSS colitis when compared to equally treated wt counterparts, hence ko animals had a higher DAI.

DSS potently induced an acute colitis in all treated animals. A very strong indicator of disease progression and murine health status was the loss of body weight, which started slowly on the fifth day of DSS treatment, but proceeded rapidly in the course of the remaining two days until the experimental endpoint at day seven (Fig. 3-17 a). Starting from day six, DSS-treated wt and ko animals had a significantly reduced mean body weight when compared to their water-treated control groups.
Stool consistency started to soften as early as two days after DSS treatment and differences became significant between the two treatment groups (H_2O, DSS) at day six (Fig. 3-17 b). *Nlrc5* ko mice showed significantly more severe diarrhea when compared to the wt, including very watery or bloody secretions during the last two days of the experiment.
Intestinal bleeding was assessed by testing for occult blood, which was detectable in feces of DSS-treated mice already on the second day of DSS treatment (Fig. 3-17 c). The severity of bleeding worsened during the course of the experiment, so that blood was also visible on feces or in the perianal region of some animals starting on day four. Towards the end of the acute colitis experiment *Nlrc5* knockout mice developed significantly elevated intestinal bleedings if compared to wild type mice.
Body weight, stool consistency and rectal bleeding were scored (Fig. 3-17 d) and summarized in the Disease Activity Index (DAI; Fig. 3-17 e). The DAI was significantly elevated for DSS-treated ko

mice when compared to the water-treated ko control group already on the third day. Wt animals developed a significant colitis phenotype after four days of DSS treatment. Furthermore, the DAI showed significant differences among the DSS-treated groups. *Nlrc5* ko mice reached a higher score than wt animals, indicating a more severe acute colitis phenotype.
Overall clinical signs worsened most notably after DSS had been displaced by pure drinking water.
Water-treated control groups showed only minor fluctuation of body weight (around 100%) as well as a stool consistency between hard to soft, but shaped, which was considered healthy. There was no occult blood detectable in any stool sample of the water-treated controls.

3.5.1.3 COMPARABLE COLON SHORTENING

Alterations in colon length are typical for certain colitis subtypes e.g. ulcerative colitis (muscular shortening) and Crohn´s disease (fibrous shortening) and it is also characteristic for DSS-induced experimental colitis models (Okayasu et al., 1990). Therefore, colon length was assessed and compared between the treatment groups to evaluate disease severity. Colon length was also compared between the genotypes to analyze for an *Nlrc5*-specific phenotype.
After colon removal from the sacrificed mice, its length was measured before the large intestine was flushed with PBS for further analyses.

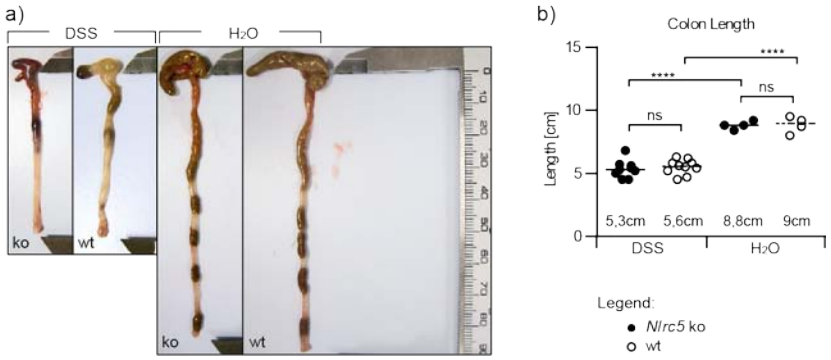

Fig. 3-18: **Colon shortening during acute colitis**
Mice were anesthetized by intraperitoneal ketamine/ xylazine injection and sacrificed by cardiac puncture. To evaluate colitis severity colons were removed and length was measured immediately (**a**). The length for each individual mouse is represented by a separate dot. The median is indicated by the bar and written out below. One-way ANOVA and Bonferroni post-tests were performed. ****p < 0.0001
Nlrc5 and wt mice had comparable colon shortening during acute DSS-induced colitis.

Water-treated control animals had an equal colon length independent of their genotype. Colons were partially filled with formed feces. The cecum appeared normal and was entirely filled with digestive remains.
In contrast, a 40% reduced colon length was observed in both DSS-treated groups when compared to the water-treated animals (Fig. 3-18 a, b). Additionally, colons were bloated up and only few hardly formed feces were found in the large intestine. The cecum was strikingly reduced in size and barely filled with digestive remains (Fig. 3-18 a). Although *Nlrc5* knockout mice showed a more severe disease phenotype with increased lethality and a higher disease activity index, both genotypes had comparable colon shortening, colon bloating, cecum size as well as amounts and shape of feces after DSS treatment.

3.5.1.4 ALTERED COLONIC INFLAMMATION AND EPITHELIAL DAMAGE

The severity of colon inflammation was determined histologically by evaluating the extension of inflammatory cell influx into the colon and the degree of epithelial alterations and damages. Feces were flushed out of the colons with PBS before colons were rolled up, formalin-fixed and paraffin-embedded for histological analyses. Slices of the rolled up colons were HE stained and the severity of inflammation as well as epithelial alterations were evaluated from the rectum up to the beginning of the transverse folds in the middle colon (Fig. 3-19). Scoring was performed according to the literature (Wirtz et al. 2007; Welz et al. 2011) with phenotype-specific adaptions (Fig. 3-19 d).

DSS-treated mice showed severe alterations and damage in the colon epithelium (Fig. 3-19 c, d). Crypts were shortened or even absent in parts of the colon. Ulcerations with total crypt loss appeared mainly in the distal and middle colon parts, while proximal parts were not affected by the acute DSS treatment.

Wt mice had a severe epithelial damage with an average total crypt loss of 29% within the analyzed colonic parts. *Nlrc5* ko mice showed an even more severe damage with significantly elevated ulcerations. On average 82% of the entire colon length showed a total loss of crypts in *Nlrc5* ko animals.

Characteristic for the inflammation within the colon is also the influx of inflammatory cells, especially neutrophil granulocytes. In both wt and ko mice inflammatory cells were observed within in colon tissue after DSS treatment. The inflammation was scored taking into account the expansion of inflammatory cells within the colon. *Nlrc5*-deficient cells showed a confluence of inflammatory cells in the lamina propria with only few points of spreading of inflammatory cells into the submucosal layer. In contrast, colons of wt animals showed more severe colonic inflammation with an extensive expansion of inflammatory cells throughout the submucosa. In both genotypes edematous alterations appeared in the submucosal layer.

Water-treated mice did not show any epithelial alterations (Fig. 3-19 a, b). Irregularities or abnormalities in the pictures for water-treated animals below are artifacts caused by sample processing, as there are no signs of inflammation visible in the colon.

Epithelial damage in the colon was more severe in *Nlrc5* ko mice, whereas in wt animals a more prominent invasion of immune cells was observed. Epithelial damage as well as immune cell influx were scored in a blinded fashion and scores were summarized into a combined histological colon score (Fig. 3-19 g). This score reflects the significantly increased severity of acute colitis in *Nlrc5* ko mice if compared to wt animals. This difference is caused by high scores for crypt loss in ko animals, which are slightly balanced by the lower inflammatory score in the ko due to a diminished influx of inflammatory cells (Fig. 3-19 e, f).

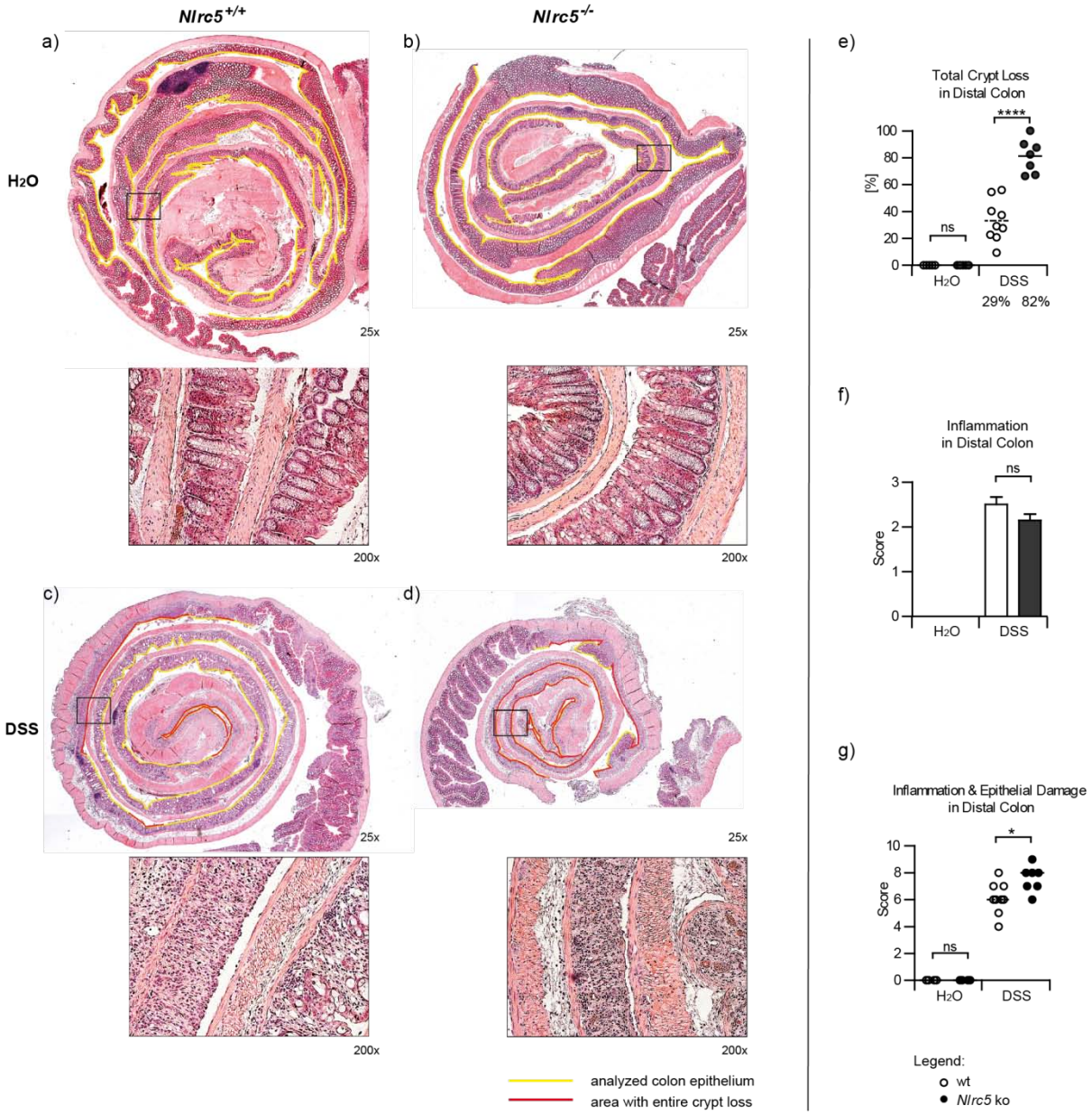

h)

Score	Inflammation	Crypt Loss
0	No or just occasional inflammatory cells in lamina propria	Intact epithelium
1	Inflammatory cells in lamina propria	Crypt shortening, altered structures like crypt abcesses Punctual crypt loss > 5% of distal colon length
2	Confluence of inflammatory cells in lamina propria extending into the submucosa (1-2 spots)	Total crypt loss 5-15% of distal colon length
3	Inflammatory cells throughout the submucosa (several spots)	15-30%
4	Transmural extention of the inflammatory infiltrate	30-50%
5	-	50-75%
6	-	75-100%

Fig. 3-19: **Infiltration of inflammatory cells and epithelial damage in the colon during acute colitis**
a–d Murine colons were flushed with PBS and rolled up for formalin fixation and paraffin embedding. Sections were stained with HE. The area of total crypt loss was measured in microscopic pictures (red line) and set into ratio (**e**) with the entire distal and middle colon length (yellow line). Magnifications are indicated.
e The percentage of colon length with a total crypt loss was compared between wt and ko. Medians are given below.
f+g The epithelial damage as well as the influx of inflammatory cells were scored as indicated in **d.** The inflammation score is displayed in **f** and the combined inflammation and epithelial damage score is given in **g**.
Each individual mouse is represented by a separate dot. Bars indicate the median. In **f** the mean scores of all animals within a group are represented with SEM as bars for clarity. One-way ANOVA and Bonferroni post-hoc tests were performed. *p < 0.05; ****p < 0.0001
During the acute colitis *Nlrc5* ko mice had more severe epithelial damage, but a reduced influx of inflammatory cells into the colon if compared to wt mice.

3.5.1.5 INCREASED GOBLET CELL HYPOPLASIA IN THE COLON

Mucins produced by goblet cells build a mucus layer within the intestine, which is of great importance for the protection of the underlying epithelium from luminal influences. Goblet cell hypoplasia is a typical histological feature in human ulcerative colitis and Crohn´s disease and it is also found in DSS-induced rodent colitis models (Gersemann et al., 2009; Shinoda et al., 2010).
Murine colons of DSS-treated and water-treated wt and ko mice were stained by Periodic Acid-Schiff reaction (PAS; 2.2.2) and the distribution of goblet cells was evaluated from the rectum up to the beginning of the transverse folds within the colon (Fig. 3-20).

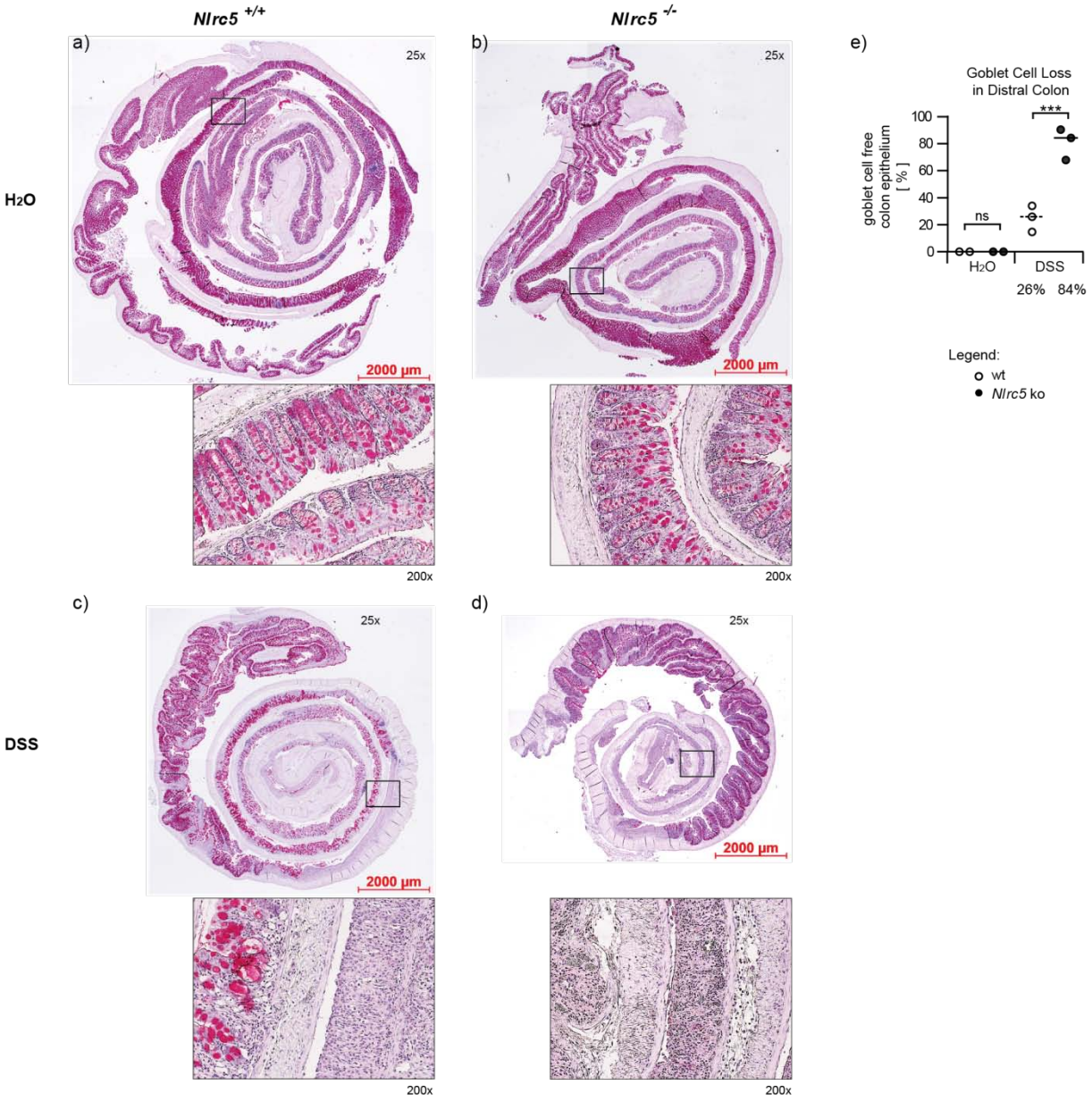

Fig. 3-20: **Depletion of mucin-containing goblet cells in murine colon during acute colitis**
a–d Murine colons were flushed with PBS and rolled up for formalin fixation and paraffin embedding. Sections were stained by PAS reaction to visualize mucin filled goblet cells. The distal and middle colon area with goblet cell-positive crypts was measured and set into ratio with the entire length of that colon part (analog to Fig. 3-20). Magnifications are indicated.
e The occurrence of goblet cells in the colon was evaluated (transverse folds were not incorporated) and the total distance with virtually no goblet cell occurrence was set into ratio to the total measured colon length. Each data point represents a measured mouse colon. The median is indicated by the bars and written out below. One-way ANOVA and Bonferroni post-hoc tests were performed. ***$p < 0.001$
Nlrc5 ko mice had a significantly elevated loss of goblet cells in the middle and distal colon during acute colitis if compared to the wt.

Water-treated mice showed intact colon epithelium (Fig. 3-20 a, b; compare also Fig. 3-19) with longer crypts at the proximal and shorter crypts within the distal colon. The density of goblet cells was especially high in the transverse folds evident by a continuous deep purple PAS staining of mucins in that area; while in more distal parts goblet cells were rather interspersed in the crypts in between other epithelial cell types. DSS-treated mice showed a significant crypt shortening and crypt loss as well as a striking goblet cell loss. Goblet cell destruction mainly occurred in the distal colon, but was also observed in other parts including the transverse folds. No goblet cells were detectable in 28% of the total distal colon length of wt mice. *Nlrc5* ko mice showed a significantly more severe goblet cell hypoplasia with 84% of the total distal colon completely lacking mucin producing cells. Crypts in the transverse folds were still interspersed with goblet cells in both genotypes, but with reduced density of mucus producing cells within the individual crypts when compared to the control groups.

3.5.1.6 ELEVATED EXPRESSION OF DISTINCT CYTOKINES

The DSS-induced breaks in the colonic epithelial barrier lead to a strong inflammatory reaction within the colon, initially characterized by the induction of pro-inflammatory cytokines. With increasing severity the inflammation becomes systemic and inflammatory mediators are detectable within blood serum.

Induction of Cytokines in Colon Tissue

DSS-treated mice developed colonic inflammation characterized by pro-inflammatory cytokine expression. RT-qPCR was performed with isolated colon RNA to analyze the induction of these cytokines during the acute colitis (Fig. 3-21).

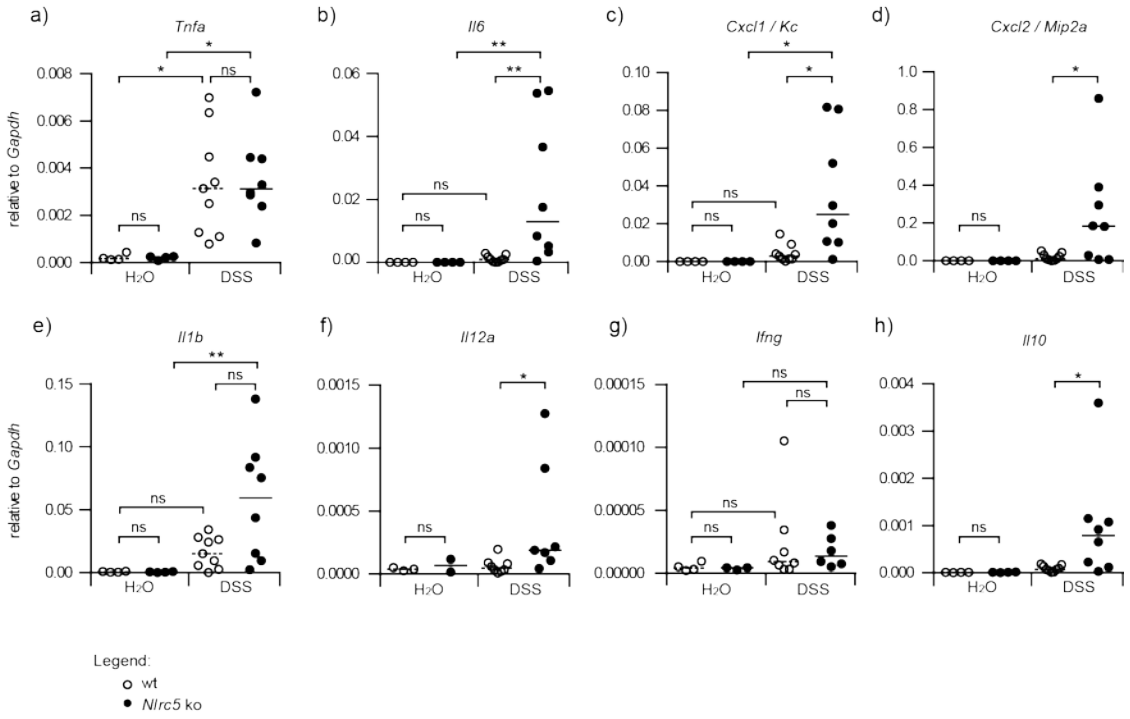

Fig. 3-21: **Cytokine expression in murine colon during acute colitis**

A longitudinal piece of colon tissue (proximal to distal) was homogenized in RNA lyses buffer using the Tissue Lyser II (QIAGEN). RNA was isolated and transcribed into cDNA for TaqMan analysis. The relative expression of various cytokines compared to *Gapdh* is displayed **a–h**. Each data point represents the average of a technical duplicate. Bars indicate the median. Due to high variances the non-parametric Mann-Whitney Test was performed for statistical analysis of the DSS-treated groups. Significances between water and DSS-treated groups are not indicated. *p < 0.05; **p < 0.01

The induction of several cytokines in the colon tissue was significantly elevated in *Nlrc5* ko mice if compared to the wt during acute colitis.

Nlrc5 ko mice showed a significantly stronger induction of pro-inflammatory cytokines like *Il6*, *Cxcl1*, *Cxcl2* and *Il12a* compared to the wt (Fig. 3-21 b-f). Also mRNA levels of the anti-inflammatory cytokine *Il10* were upregulated in ko colons during acute colitis (Fig. 3-21 h). Upon DSS treatment only in *Nlrc5*-deficient cells *Il1b* was significantly induced in the colon.
Furthermore, *Tnfa* was potently induced upon DSS treatment, but to a comparable degree in wt and ko animals (Fig. 3-21 a). There was only a minor induction of *Ifng* in both experimental groups during acute colitis. *Ifng* mRNA levels were also comparable (Fig. 3-12).

Cytokine Levels in Murine Serum
The production of cytokines was further evaluated in serum samples obtained by cardiac puncture at the end of the experiment. Several mediators could be measured within the same sample by bead-based multiplex technique (see 2.6).
In wt mice none of the analyzed cytokines (TNFα, IL-6, KC, MIP2a, IL-1β, IL-12, IFNγ, IL-10) was significantly elevated in the serum upon DSS treatment compared to their controls (Fig. 3-22 a h). In contrast, DSS-treated *Nlrc5*-deficient animals showed significantly upregulated serum concentrations of the pro-inflammatory mediators IL-6, KC and IL-1β as well as the anti-inflammatory IL-10 (Fig. 3-22 b, c, e, h).

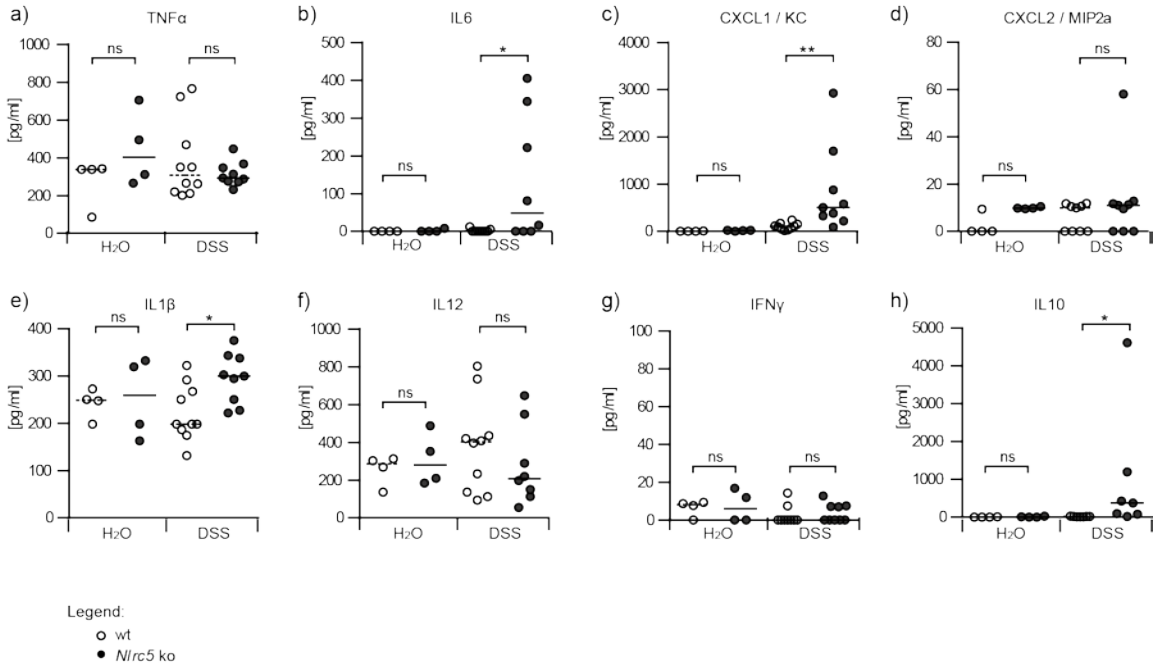

Fig. 3-22: **Serum cytokine levels during acute colitis**
At day seven of the acute DSS experiment mice were anesthetized by intraperitoneal ketamine/ xylazine injection and blood was taken by cardiac puncture. Blood was centrifuged using lithium heparin-gel blood collection tubes (Sarstedt) to obtain serum for further analyses. Cytokines were detected using multiplex assay (Bio-Rad). The measured serum concentrations of several mediators are displayed in **a–h**. Data points represent individual mice. Bars indicate the median. Due to high variances the non-parametric Mann-Whitney Test was performed for statistical analysis. Significances between water and DSS-treated groups are not indicated. *$p < 0.05$; **$p < 0.01$
Several serum cytokines were significantly elevated in *Nlrc5* ko mice if compared to the wt during acute colitis.

Overall, no altered inflammatory mediator concentrations were observed in the serum of DSS-treated wt mice, while *Nlrc5* ko animals developed a systemic upregulation of various cytokines.

3.5.1.7 ALTERED SPLEEN WEIGHT IN *NLRC5* KO AND WT MICE

Systemic inflammation is not only characterized by pro-inflammatory cytokine expression in the serum, but it can also lead to an increased spleen weight (Siegmund et al., 2001a).
At the end of the experiment mice were sacrificed and spleens weighted. The control groups had a median spleen weight of 73 mg in wt and 75 mg in ko mice (Fig. 3-23 a). Upon DSS treatment wt mice showed a 25% increased spleen weight (median 91 mg), while ko spleen weights were not changed when compared to the control groups. Alterations in the spleen weight were independent of the body weight loss during colitis (Fig. 3-23 b).

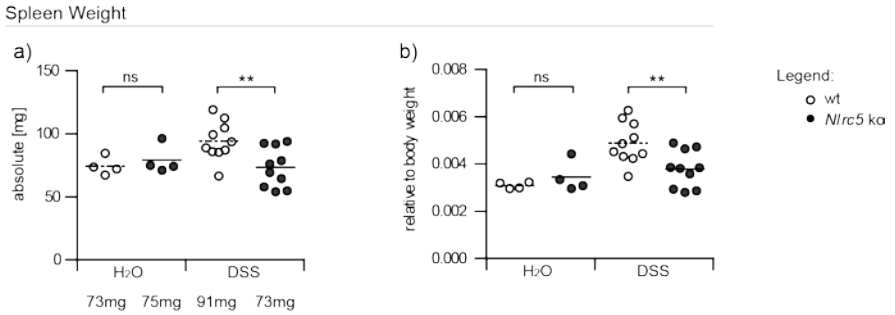

Fig. 3-23: **Murine spleen weight during acute colitis.**
Spleens were removed and weighted. **a** The absolute spleen weight is depicted. Medians are written below. **b** The spleen weight in relation to the body weight is depicted. **a+b** Each data point represents an individual mouse. Medians are indicated by the bars. One-way ANOVA with Bonferroni post-tests was performed. **p < 0.01
The absolute and relative spleen weight was significantly higher in wt compared to *Nlrc5* ko mice during acute colitis, while under steady state conditions spleen weights were comparable between the genotypes.

3.5.1.8 ELEVATED MYELOPEROXIDASE EXPRESSION

The enzyme myeloperoxidase (MPO) is mainly expressed in neutrophil granulocytes and its induction or activity is directly associated with the presence of neutrophils in the examined tissue. To evaluate *Mpo* expression RNA was isolated from spleen tissue and analyzed using RT-qPCR.
Mpo was induced in wt and ko spleens during the acute colitis. The expression of *Mpo* was significantly higher in *Nlrc5*-deficient spleens compared to the wt, indicating that there was a greater neutrophil influx in spleens of *Nlrc5* ko mice.

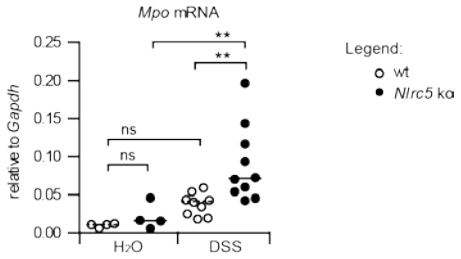

Fig. 3-24: **Expression of myeloperoxidase during acute colitis**
The induction of myeloperoxidase (MPO) is significantly elevated in *Nlrc5* ko, but not in wt mice during acute colitis. Murine spleens were homogenized in RNA lyses buffer using the Tissue Lyser II (QIAGEN). RNA was isolated and transcribed into cDNA for TaqMan analysis. The relative expression of *Mpo* compared to *Gapdh* is displayed. Each data point represents the average of a technical duplicate. Bars indicate the median. One-way ANOVA with Bonferroni post-tests was performed. **p < 0.01

3.5.1.9 Reduced *Cd8* expression in murine spleen

The development of acute colitis is reported to be independent of the presence of T or B lymphocytes (Dieleman et al., 1994), but adaptive responses develop as the inflammation proceeds (Hall et al., 2011).
Nlrc5 knockout mice were shown to have significantly diminished $CD8^+$ cytotoxic T cells and slightly upregulated $CD4^+$ T helper cell numbers in the spleen (Fig. 3-5). The development of both T cell subpopulations and its dependence on NLRC5 expression was analyzed in the experimental acute colitis.
Cd8 as well as *Cd4* were expressed in murine splenocytes (Fig. 3-25).
Water-treated *Nlrc5* ko mice showed a diminished, although not significant, *Cd8* expression when compared to the wt as described before (Fig. 3-25 a, Fig. 3-5, Fig. 3-8). During acute colitis *CD8* levels were strikingly reduced in both genotypes. There were significantly lower *CD8* RNA levels detectable in *Nlrc5*-deficient splenocytes compared to the wt.
The expression of *CD4* was also significantly reduced during the acute colitis when compared to the healthy controls. However, the expression of *Cd4* in murine splenocytes was comparable between the genotypes under healthy conditions as well as during acute colitis and therefore not affected by the *Nlrc5* ko (Fig. 3-25 b).

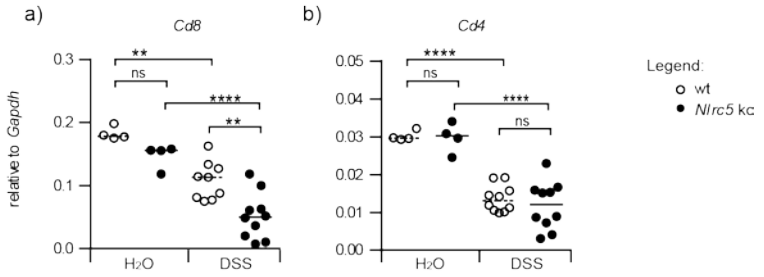

Fig. 3-25: **Expression of *Cd8* and *Cd4* in murine spleens during acute colitis**
Murine spleens were homogenized using the Tissue Lyser II (QIAGEN), RNA was isolated and TaqMan analysis was performed. Displayed is the relative expression of *Cd8* as well as *Cd4* compared to *Gapdh*. Each data point represents the average of a technical duplicate. Bars indicate the median. One-way ANOVAs with Bonferroni post-tests were performed. **$p < 0.01$; ****$p < 0.0001$
Cd8 and *Cd4* mRNA level are strikingly reduced upon DSS treatment. The expression of *CD8* is significantly diminished in *Nlrc5* ko mice compared to the wt (**a**), while *CD4* level are comparable between both genotypes (**b**).

Taken together, the mRNA expression of the CD4 and CD8 T cell co-receptors was significantly diminished in spleens of wt and *Nlrc5* ko animals with acute DSS-induced colitis. While *CD4* RNA levels were similar in both genotypes, *CD8* was significantly lower in *Nlrc5* ko mice during colitis if compared to the wt.

3.5.2 Increased Severity of Chronic Colitis in *Nlrc5* ko Mice

While innate immune cell populations like neutrophil granulocytes start expanding after only one day of DSS treatment, adaptive T and B lymphocyte populations begin to expand within the murine colon only at the transition to chronification (Hall et al., 2011). Chronic colitis was induced in mice to evaluate if NLRC5 affects disease severity by influencing adaptive immune mechanisms.

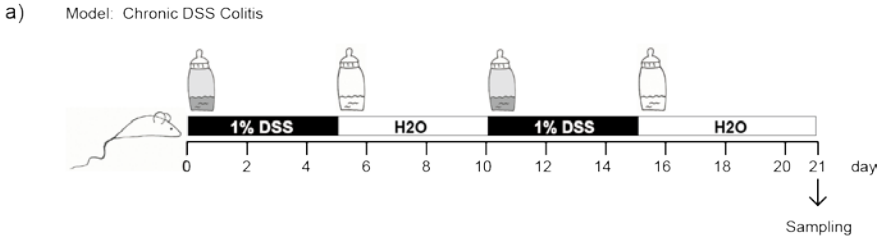

Fig. 3-26: **Treatment of experimental animals to induce chronic DSS colitis**
Shown is the model of DSS treatment to induce chronic colitis. Mice were kept under SPF conditions. Drinking water was autoclaved and contained 1% DSS at the indicated days. The control groups solely got autoclaved water at all times. Animal treatment groups: n = 9 wt, 10 ko; age: 10–11 weeks; sex: male; Animal control groups: n = 3 wt, n = 3 ko; age: 8–12 weeks; sex: male.

Chronic intestinal inflammation was induced in mice by repeatedly applying 1% DSS dissolved in drinking water alternating with applying water only. One treatment cycle consisted of 5 days DSS followed by 5 days of water (Fig. 3-26). The experiment was planned to last four DSS cycles, but had to be aborted after the second cycle, due to disease severity in *Nlrc5* ko mice.
All chronic colitis read outs described below are based on the experimental setup described in Fig. 3-26.

3.5.2.1 Decreased survival during chronic DSS treatment

During DSS treatment mice were monitored every 1–2 days for body weight changes, diarrhea and their overall state of health. Mice were excluded from further treatments and sacrificed if their body weight loss exceeded 20% as animals in this state of disease were expected to die within the next 24 h due to disease progression accompanied by further weight loss.
None of the water-treated control animals (wt, ko) had to be sacrificed early due to weight loss. Upon DSS treatment 90% of wild type mice survived until the end of the experiment (Fig. 3-27). *Nlrc5* ko mice had a strikingly elevated mortality. Only 60% of DSS-treated ko mice survived until day 21 so that it was decided to end the experiment at that time point. Early deceased ko mice (n=4) were separately evaluated as ko_{abort} after preparation and sampling, as they had more severe disease progression compared to the remaining ko_{d21} animals.

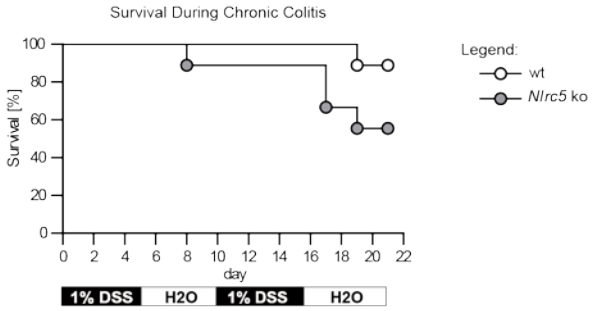

Fig. 3-27: **Survival during the course of chronic DSS colitis**
The Kaplan-Meier survival plot gives the percentage of living animals during the course of the experiment. Mice that did not match the animal welfare guidelines due to DSS treatment had to be taken out of the experiment and were sacrificed for analyses. None of the wt or ko control animals had to be taken out early (survival 100%; not shown).
Wt mice had a higher survival rate during chronic DSS colitis when compared to *Nlrc5*-deficient mice.

3.5.2.2 Progression of body weight loss and diarrhea during chronic colitis

Over the course of the repeated DSS treatment body weight changes and stool consistency were monitored every second day (Fig. 3-28). All DSS-treated mice developed a colitis phenotype.

Control animals continuously gained weight until the end of the experiment (day 19–20), which reflects their general health state and appropriate housing conditions in the animal facility. DSS-treated mice gained weight during the initial DSS period, before a slight decline became detectable toward the end of the DSS treatment, which continued even after DSS deprivation (on average 1% on day 6). The body weight recovered completely in wt and ko mice until the middle of the following DSS cycle before it dropped again and reached its minimum during the second DSS break (~90% of the initial weight on day 18). This body weight loss was significant in wt and ko DSS-treated mice compared to their control groups. The weight started to recover again approximately one week after DSS deprivation (around day 19).

Mean body weight changes were comparable between *Nlrc5* ko and wt mice during the development of chronic colitis, but ko mice showed very high variances within the treatment group. Four out of ten ko animals had to be sacrificed until day 19 due to massive weight loss (> 20%), while the rest had only moderate weight loss (around 10%), which was comparable to wt animals.

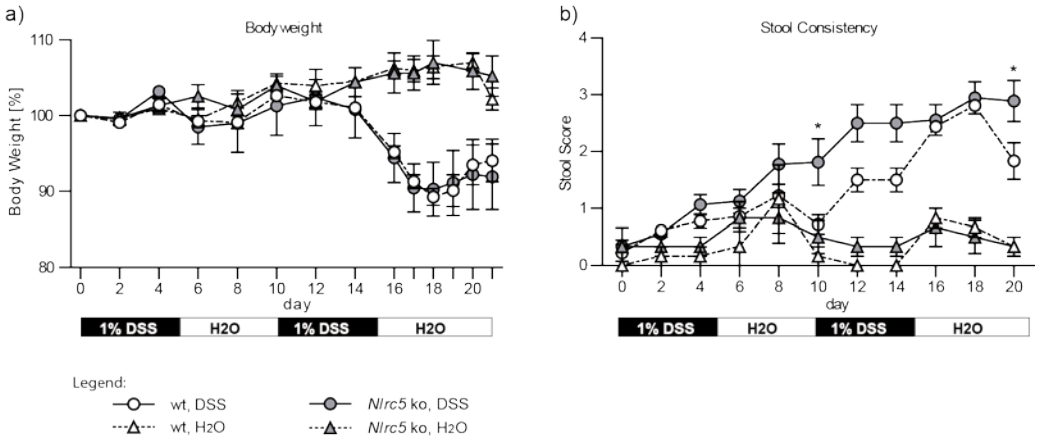

Fig. 3-28: **Body weight changes and diarrhea score**

To monitor disease progression mice were weighted (**a**) and stool samples were judged (**b**) every 1–2 days. The graphs show the development of body weight as well as diarrhea over the course of time. For further experimental information see also Fig. 3-26. The Stool score is explained in Fig. 3-17. All individuals within one group are indicated by a single dot with SEM. Two-way ANOVA and Bonferroni post-tests were performed for statistical analyses. *$p < 0.05$

Body weight loss during chronic colitis is comparable between DSS-treated *Nlrc5*-deficient and wt mice, but ko mice develop a more severe diarrhea, which is progressive even during DSS breaks.

Drinking water supplemented with 1% DSS also led to altered stool consistency. Stool started to soften after four days of DSS treatment. In the wt stool consistency normalized again upon DSS deprivation and worsened during the subsequent DSS treatment to a mucous diarrhea. During the water period the severe diarrhea improved again back to unshaped soft feces. In contrast, ko animals showed progressive stool softening over the entire time course with no improvements during DSS breaks. A mucous diarrhea developed towards the second DSS cycle.

Overall it was observed that body weight loss and stool consistency worsened most notably after the DSS treatment was already terminated and mice were given only drinking water. *Nlrc5* ko mice suffered severe diarrhea even towards the end of these DSS breaks, while wt animals always recovered during that phase.

During the cyclic DSS treatment mice, especially the ko, showed a high biological diversity with strong data variances independent of caging, so that it was decided to divide the *Nlrc5* ko treatment group into the ko_{d21} subgroup sacrificed at day 21 and the ko_{abort} group.

3.5.2.3 SEVERE COLON SHORTENING IN *NLRC5* KO MICE

After terminating the experiment colon shortening was determined to evaluate disease severity. Therefore, colons were removed from the mice and their length was measured (Fig. 3-29). Subsequently, colons were flushed with PBS to be further analyzed.

Nlrc5 ko animals had slightly elevated median colon lengths in the control a well as in the treatment groups (wt vs. ko_{d21}). During chronic colitis a minor colon shortening of 6% was observed in DSS-treated wt and 8% in ko_{d21} mice compared to the control groups. In contrast, colons of early aborted ko animals (ko_{abort}) showed a median colon shortening of 32% upon DSS treatment if compared to the control. Colon shortening was significantly increased in the ko_{abort} than in the ko_{d21} subgroup of *Nlrc5*-deficient mice.

Furthermore, colons were bloated upon DSS treatment. They were still filled with feces, but these were poorly formed and held more water compared to the control groups. In contrast to the acute DSS model, the cecum had normal size and was filled with digestive remains (not shown).

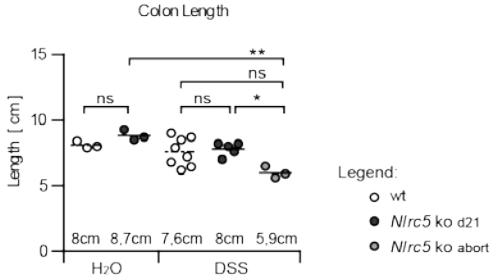

Fig. 3-29: **Colon shortening during chronic colitis**

Mice were anesthetized by an intraperitoneal ketamine/ xylazine injection and sacrificed by cardiac puncture. To evaluate colitis severity colons were taken out and length was measured. Due to altered disease severity *Nlrc5* ko animals that had to be taken out early were evaluated separately and are termed ko_{abort}. The length of each individual colon is assigned by a separate dot. The median is indicated by the bar and written out below. One-way ANOVA and Bonferroni post-tests were performed. *$p < 0.05$; **$p < 0.01$

Colons are significantly shortened in the severely affected *Nlrc5* ko subgroup ko_{abort}.

3.5.2.4 ELEVATED CRYPT LOSS IN AN *NLRC5* KO SUBGROUP

Colonic inflammation was determined histologically in the chronic colitis model. Murine colons were removed and flushed with PBS before they were rolled up, formalin-fixed and paraffin-embedded for histological analyses. After HE staining colons were scored for epithelial alterations and the influx of inflammatory cells. The middle colon (distal from the transverse folds) and the terminal colon (including the rectum) were histologically analyzed.

Both control groups (wt and ko) did not show any epithelial alterations (Fig. 3-30 a, b). Crypts were intact and there were no signs of inflammation. Histological irregularities in the pictures of water-treated animals were artifacts caused by sample processing, as there were no signs of inflammation visible in the colon of these control mice.

DSS treatment groups (wt, ko) showed alterations in the architecture of the colon wall, e.g. submucosal edema was observed in almost all DSS-treated animals. Areas in which crypts were shortened or lost entirely were scattered throughout the colon, but were more abundant in distal regions. Also crypt abscesses were observed in approximately half of all DSS-treated mice. Furthermore, there were ulcerations and a strong influx of inflammatory cells into the mucosal and submucosal layer. It is noteworthy that there were strong interindividual differences in the degree of epithelial damage among wt as well as ko animals.

Distances with complete crypt loss were measured within the colons as described in Fig. 3-19. Wt mice had an epithelial damage with a total loss of crypts on 7% of the analyzed colon epithelium

(Fig. 3-30 f). *Nlrc5* ko_{d21} animals showed a complete crypt loss on 13% of the measured colon length, while the ko_{abort} group showed a severe destruction of the colonic epithelium with a loss of crypts on 50-100% of the colon epithelium. This reflects the severity of disease in this ko subgroup.
DSS treatment led to a severe influx of inflammatory cells into the colon wall. This inflammation was comparable among DSS-treated wt and ko animals. Inflammatory cells were dispersed all throughout the mucosal layer and spread into the submucosa. In the majority of animals inflammatory cells even crossed the *Muscularis externus*, leading to a transmural inflammation.
The epithelial damage and the influx of inflammatory cells into the colon were scored as indicated in Fig. 3-19 and scores were summarized (Fig. 3-30 f g). The inflammatory score was equal for wt and ko animals of both subgroups (median = 3.5) and is not separately shown in Fig. 3-30. DSS-treated wt and ko_{d21} animals had a more severe colitis phenotype when compared to control animals. Colitis severity was further significantly elevated in the ko_{abort} subgroup compared to wt animals.

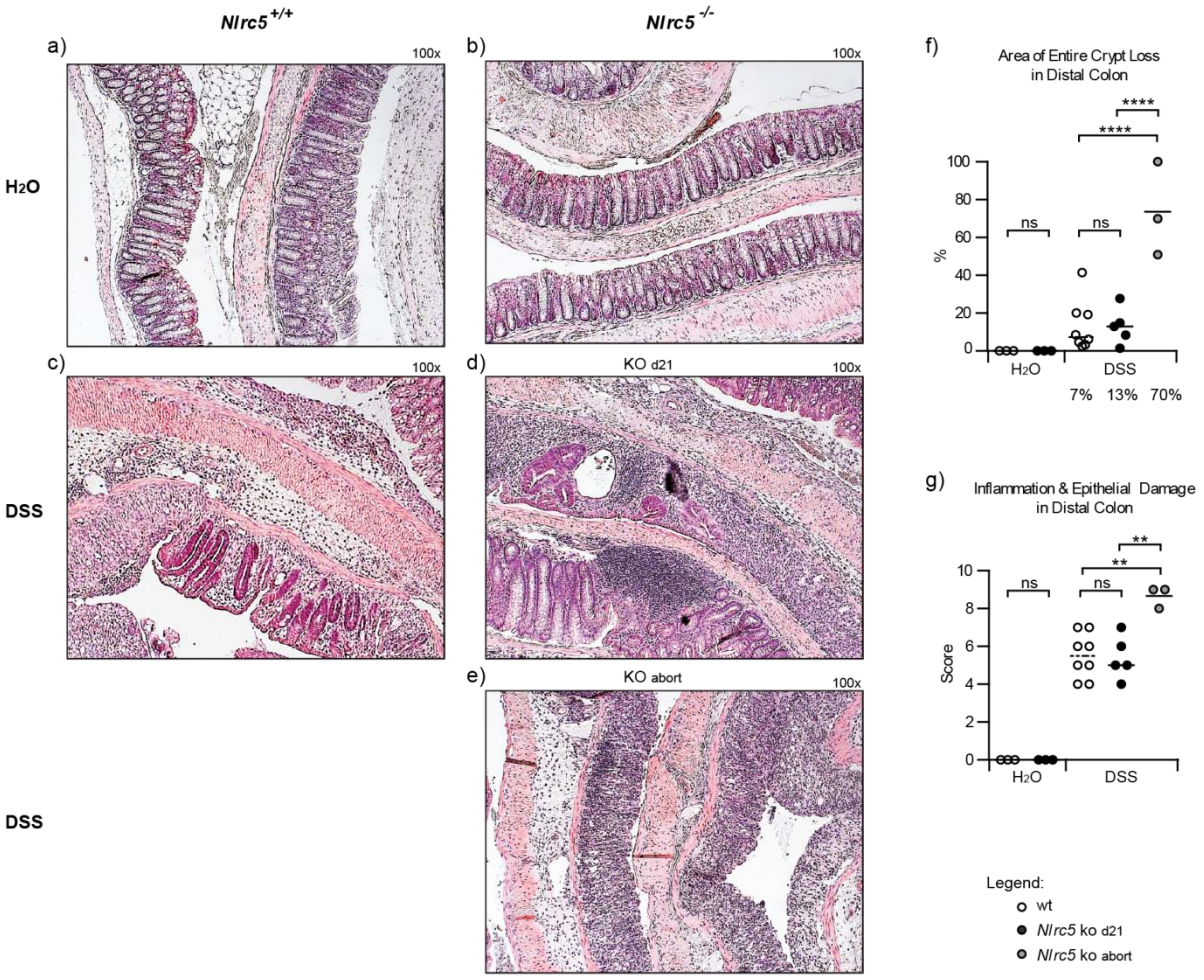

Fig. 3-30: **Infiltration of inflammatory cells and epithelial damage in the colon during chronic colitis**
a–e Murine colons were flushed with PBS and rolled up before formalin-fixation and paraffin-embedding. Sections were stained with HE. The total length of crypt loss was measured and set into ratio with the entire colon length from the rectum to the beginning of the transverse folds at the proximal colon (**f)** as described in Fig. 3-19. Magnifications are indicated. **f** The median distance of crypt loss is written below the diagram. **g** The influx of inflammatory cells into the colon tissue and the epithelial damage were scored as indicated in Fig. 3-19 h and summarized. **f+g** Each individual mouse is represented by a separate dot. Bars show the median. One-way ANOVA and Bonferroni post-tests were performed. **p < 0.01; ****p < 0.0001
During chronic colitis the *Nlrc5* ko_{abort} subgroup had a significantly more severe epithelial damage in the colon compared to wt and ko_{d21} mice. However, the influx and distribution of inflammatory cells within the colon was not altered when compared to the wt.

The widespread occurrence of lymphoid follicles in the colons of *Nlrc5*-deficient as well as wt animals upon repeated DSS treatment was noticeable. These lymphoid follicles reached from the *Muscularis*

externus through the submucosal layer. The occurrence of colonic lymph nodes during chronic colitis was increased in DSS-treated mice when compared to control groups, but it was also increased when compared to animals that suffered an acute DSS-induced colitis (Fig. 3-31).

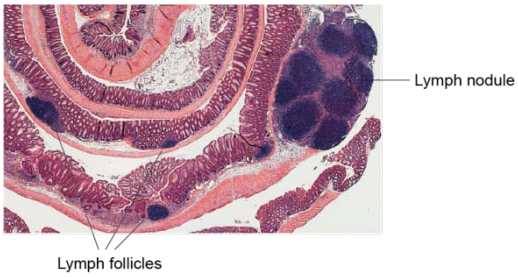

Fig. 3-31: **Lymphatic tissue in murine colons upon repeated DSS treatment**
The occurrence of lymphoid follicles was increased in murine colons upon DSS treatment. Shown is the colon of an *Nlrc5*-deficient mouse. For technical procedure see Fig. 3-30.

3.5.2.5 Elevated expression of distinct cytokines

Induction of Cytokines in Colon Tissue

The severity of the DSS-induced inflammation was further characterized by analyzing the local production of inflammatory cytokines. RNA was extracted from murine colons after repeated DSS treatments and RT-qPCR was performed to analyze cytokine induction in colon tissue during the experimental chronic colitis (see 2.8).

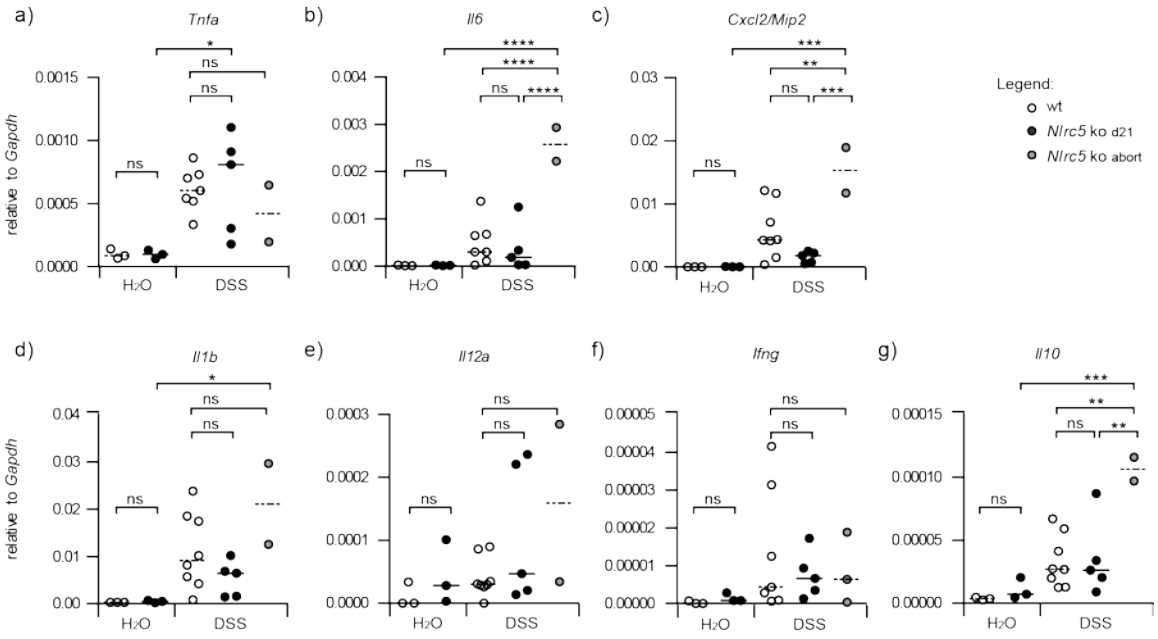

Fig. 3-32: **Cytokine expression in murine colon during chronic colitis**
A longitudinal piece of colon tissue (proximal to distal) was homogenized using the Tissue Lyser II (QIAGEN), RNA was isolated and TaqMan performed. **a–g** The relative expression of various cytokines in the colon compared to *Gapdh* is displayed. Each data point represents the average of a technical duplicate. Bars indicate the median. One-way ANOVA and Bonferroni post-tests were performed.
*p < 0.05; **p < 0.01; ***p < 0.001; ****p < 0.0001
Distinct cytokines were upregulated during chronic DSS colitis. RNA levels of the pro-inflammatory *Il6* and *Cxcl2/Mip2*, but also the anti-inflammatory *Il10* were significantly elevated in the severely affected *Nlrc5* ko_{abort} subgroup when compared to DSS-treated wt animals.

The pro-inflammatory cytokines *Tnfa*, *Il6*, *Cxcl2* and *Il1b* were induced upon DSS treatment in murine colons (Fig. 3-32 a–f). The level of induction was comparable between wt and ko_{d21} mice, but the DSS

effect showed a strong interindividual variability. Also mRNA levels for the anti-inflammatory *Il10* were increased (Fig. 3-32 g). The *Nlrc5* ko_{abort} animals showed significant upregulation of *Il6*, *Cxcl2*, *Il1b* and *Il10* compared to the controls or the ko_{d21} animals. The induction of *Ifng*, *Il12a* and *Il10* was only weak. *Ifng* and *Il12a* mRNA levels did not show significant differences between water and DSS-treated animals.

Distinct cytokines were upregulated in colon tissue during chronic DSS colitis, but their induction was not as potent as observed during the DSS-induced acute inflammation (Fig. 3-21).

Cytokine Levels in Murine Serum

Systemic inflammation was further analyzed by determining cytokines levels in murine serum using multiplex assay (see 2.6), but no significant differences were found in the systemic induction of cytokines neither between the treatment groups nor between the genotypes during chronic colitis (Fig. 3-33). *Il12a* mRNA levels tended to be elevated in DSS-treated wt and ko_{d21} animals when compared to their control groups. In contrast, *Il12a* was not upregulated in the ko_{abort} group after DSS treatment.

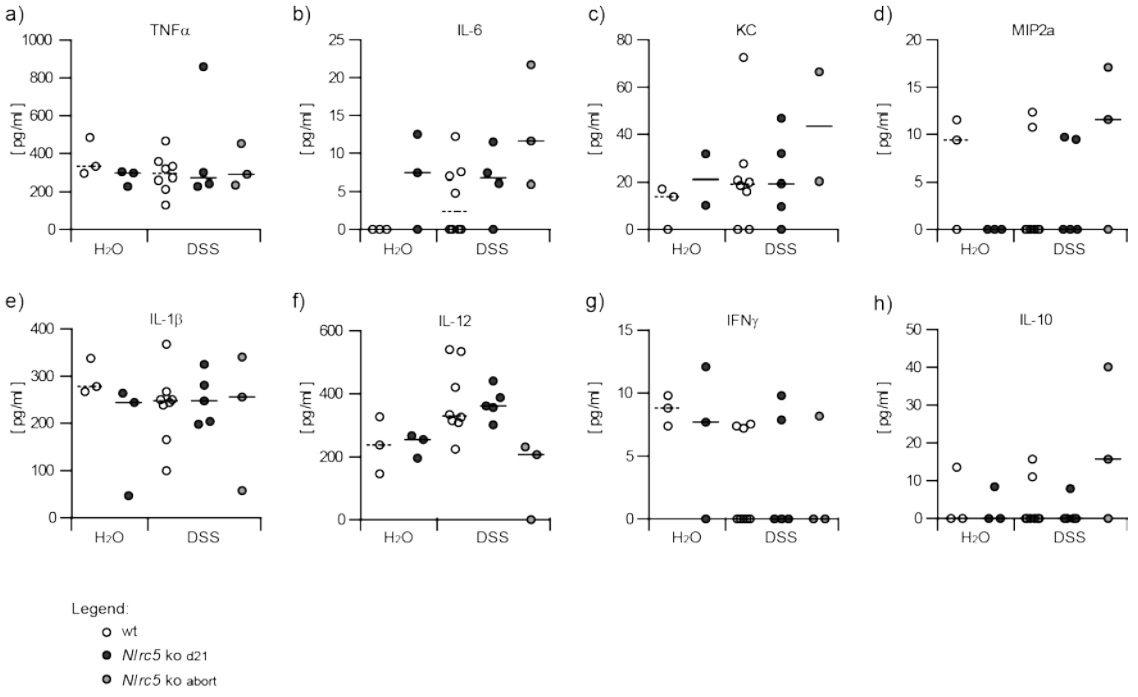

Fig. 3-33: **Serum cytokine levels during chronic colitis**

Mice were anesthetized by intraperitoneal ketamine/ xylazine injection and blood was taken by cardiac puncture. Blood was centrifuged using lithium heparin-gel blood collection tubes (Sarstedt) to obtain serum for further analyses. Cytokines were detected using multiplex assay (Bio-Rad). Measured serum concentrations are displayed in **a–h**. Data points represent individual mice. Bars indicate the median. Due to high variances the non-parametric Mann-Whitney Test was performed for statistical analysis.

None of the analyzed pro- or anti-inflammatory cytokines showed a significantly altered serum concentration during chronic colitis. There were also no significant differences between wt and *Nlrc5* ko mice.

3.5.2.6 Altered spleen weight in *Nlrc5* ko and wt mice

After the induction of the chronic DSS colitis, murine spleens were removed and weighted (Fig. 3-34 a). There were already slight differences between the genotypes comparing spleen weights of water-treated animals. Spleens of *Nlrc5*-deficient mice weighted approximately 35% more than their wt counterparts, although mice had comparable maturity.

Repeated DSS treatment resulted in 36% elevated spleen weight in wt animals, while no effect could be seen in the majority of ko_{d21} mice.
In the ko_{abort} subgroup a significant influence of DSS treatment was observed as spleen weight was reduced by 65% when compared to water-treated controls. Changes in spleen weight were independent of the DSS-induced body weight loss (Fig. 3-34 b).

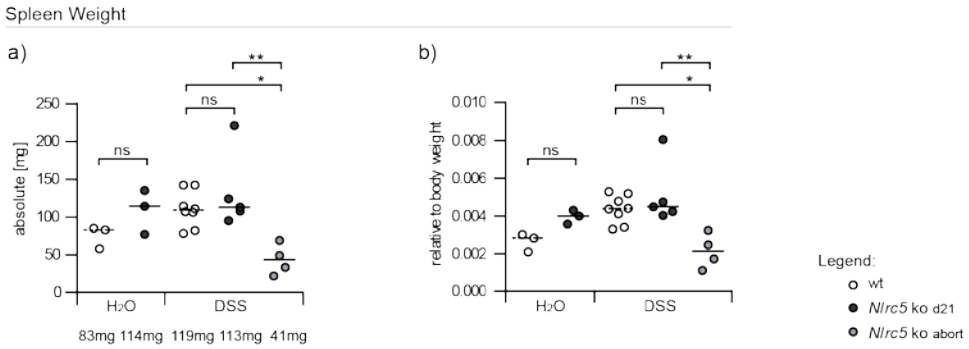

Fig. 3-34: **Murine spleen weight during chronic colitis**
Spleens were removed and weighted. **a** The absolute spleen weight is depicted. Medians are written below. **b** Shown is the spleen weight in relation to the body weight. **a+b** Each data point represents an individual mouse. Medians are indicated by the bars. One-way ANOVA with Bonferroni post-tests was performed. *p < 0.05; **p < 0.01
A significantly reduced absolute and relative spleen weight was measured in the *Nlrc5* ko_{abort} subgroup during chronic DSS-induced colitis when compared to either DSS-treated wt or DSS-treated ko_{d21} animals.

3.5.2.7 Elevated myeloperoxidase expression

The expression of Myeloperoxidase in murine spleen tissue was analyzed by RT-qPCR after RNA processing (Fig. 3-35). *Mpo* mRNA was induced upon DSS treatment in wt as well as in ko animals. Both genotypes showed high variances in *Mpo* expression, but in contrast to the wt, ko animals with very low *Mpo* expression had one further common characteristic: they all had a very severe colitis phenotype with major weight loss (> 20%) and colon epithelial damage (> 50%) and had to be taken out of the experiment early. Hence, ko mice suffering from chronic colitis having low *Mpo* expression represented exactly the ko_{abort} group.

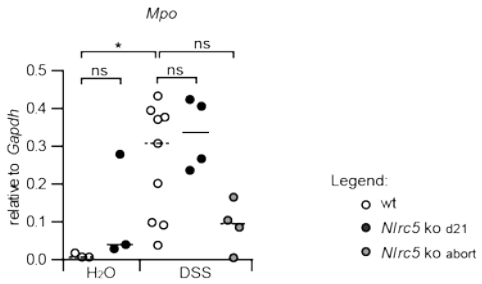

Fig. 3-35: **Expression of myeloperoxidase during chronic colitis**
Spleens were homogenized using the Tissue Lyser II (QIAGEN), RNA was isolated and TaqMan analysis performed. Displayed is the relative *Mpo* mRNA expression in comparison to *Gapdh*. Each data point represents the average of a technical duplicate. Bars indicate the median. One-way ANOVA with Bonferroni post-tests was performed. *p < 0.05
Mpo mRNA was significantly induced during chronic colitis in wt mice, while in the severely affected *Nlrc5* ko_{abort} only minor *Mpo* levels were detectable.

3.5.2.8 Expression of *Cd4* and *Cd8* in murine spleen and colon tissue

Adaptive immune responses arise in the late acute phase of colitis and persist during chronic colitis. They lead to an accumulation of lymphocytes within the colon (Hall et al., 2011).

Here, the expression of the T cell co-receptors *Cd8* and *Cd4* was analyzed in spleen and colon tissue from mice with DSS-induced chronic colitis using RT-qPCR (see 2.8). Both receptors were expressed in murine spleens and to a much lesser extend also in the colons (Fig. 3-36).
In the control groups, *Cd8* mRNA levels were slightly lower in spleens of *Nlrc5*-deficient mice when compared to the wt. During DSS-induced chronic colitis the *Cd8* expression decreased significantly within the splenocytes and the differences between wt and ko persisted.
The splenic *Cd4* expression was slightly diminished in the spleens of control animals as well. During the DSS-induced inflammation *Cd4* RNA levels in spleen tissue were potently reduced to similar levels in wt and *Nlrc5* ko mice.
The expression of *Cd8* and *Cd4* in the spleen was comparable to data obtained during acute colitis.

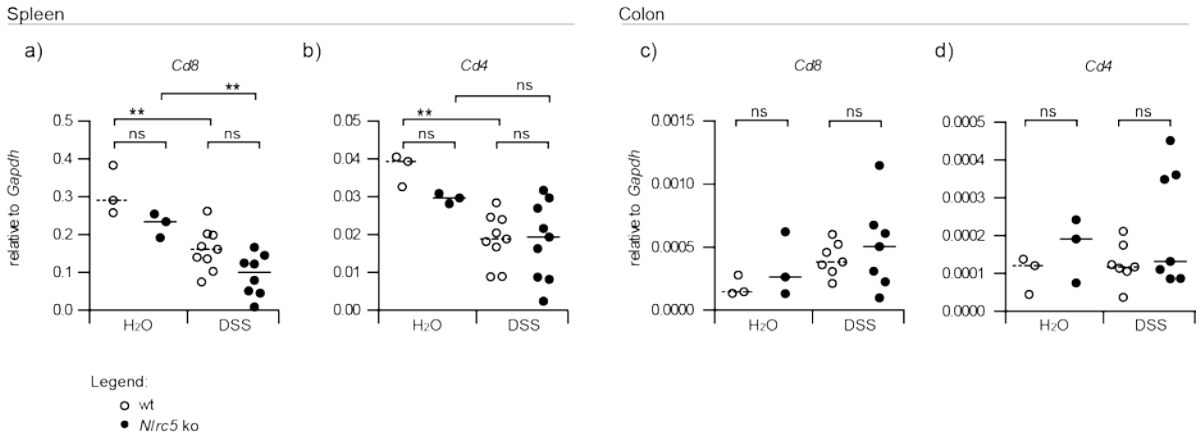

Fig. 3-36: **Expression of *Cd8* and *Cd4* in murine spleen and colon during chronic colitis**
Murine spleens and colon tissues were homogenized using the Tissue Lyser II (QIAGEN). RNA was isolated and TaqMan analysis was performed. Displayed is the relative expression of *Cd8* (**a, c**) as well as *Cd4* (**b, d**) compared to *Gapdh*. Each data point represents the average of a technical duplicate. Bars indicate the median. One-way ANOVAs with Bonferroni post-tests were performed. **$p < 0.01$
The expression of *Cd8* and *Cd4* on murine splenocytes was reduced during chronic colitis. *Cd8* level were diminished in *Nlrc5* ko, while *Cd4* levels were comparable to the wt.

The colon harbors only minor lymphocyte populations under healthy conditions, but during the proceeding inflammation lymphocytes invade the colon tissue.
Under healthy conditions ko mice tended to have a slightly higher median *Cd8* and *Cd4* expression in the colon if compared to the wt.
Upon DSS treatment *Cd8* was upregulated in both genotypes, but a higher median expression was observed in ko mice. The expression of *Cd4* was not altered in wt mice during the DSS-induced inflammation, while *Cd4* was potently induced in half of the DSS-treated ko group.
Overall there were very strong interindividual differences in mRNA expression, but the expression of *Cd4* and *Cd8* was not dependent on the abort day, therefore all ko animals were analyzed together without distinguishing between ko_{d21} and ko_{abort}.

4 DISCUSSION

Publications on the biological function of NLRC5 were strikingly inconsistent regarding e.g. protein expression, subcellular localization and protein function. Still, all of them implicated NLRC5 to participate in immune-relevant mechanisms. This functional discordance gave motivation to further study this NLR member and to clarify its functional relevance. We hypothesized that NLRC5 is involved in immunity.
An *Nlrc5* knockout mouse model was generated and the basal phenotype investigated. The *Nlrc5* ko mouse was supposed to clarify if NLRC5 participates in the initiation or regulation of innate immune defense mechanisms, accordingly if NLRC5 plays a pro- or anti-inflammatory role.
Further, I was interested to see if NLRC5 also participates in adaptive immune mechanisms. Although NLR-induced innate responses are known to be important for the subsequent initiation of adaptive effector mechanisms, only the NLR member CIITA had been shown to be directly involved in the generation of adaptive responses by then. With the identification of the co-transcriptional activity NLRC5 exerts on MHC class I encoding *HLA* genes (Meissner et al., 2010), a particular function of NLRC5 in the development of adaptive cytotoxic T cell responses can be suggested.

NLRC5 was neither essential for normal development, survival nor reproduction as *Nlrc5* ko mice were inconspicuous under SPF conditions. The ko was not lethal. Mice were born at normal mendelian ratio and they had an average life expectancy. Moreover, ko mice displayed a median body weight as well as normal macroscopic and microscopic organ structure (data shown for secondary immune organs, Fig. 3-4).

4.1 NLRC5 EXPRESSION – IMPLICATIONS FOR POTENTIAL FUNCTIONS

Several observations underlined an immune relevance of NLRC5. The protein was found to be ubiquitously expressed in humans and mice with predominant expression in immune tissues in both species. Levels were especially high in secondary and primary lymphoid organs as well as in organs bearing mucosal linings (Fig. 3-1). This is in agreement with Neerincx and Staehli (Neerincx et al., 2010; Staehli et al., 2012). Others rather suggested the highest NLRC5 expression in primary lymphoid organs (Benko et al., 2010; Cui et al., 2010; Davis et al., 2010). The expression of NLRC5 in immune organs is therefore indisputable and seems to rely on leukocytes, which are the predominant cell type in these tissues. Mucosa-lined organs as the lung with its bronchus-associated lymphoid tissue (BALT) and diverse sections of the bowel with the gut-associated lymphoid tissue (GALT) had the highest NLRC5 expression among non-immune organs (Fig. 3-1). This is also supported by others (Davis et al., 2010; Kuenzel et al., 2010).
From this expression pattern several hypothetical functions can be presumed for NLRC5. Firstly, it can be hypothesized that NLRC5 is involved in the differentiation of naïve lymphocytes from hematopoietic precursors in the thymus or bone marrow. Secondly, the protein could be of structural relevance in immune tissues. And thirdly, NLRC5 might participate in the proliferation and differentiation of naïve lymphocytes to generate adaptive effector cells in secondary lymphoid tissues.

Lymphocytes differentiate and proliferate in primary lymphoid organs, while they encounter antigens, clonally expand and mature to effector cells in the secondary lymphoid organs. NLRC5 does not seem to play an indispensable role for the generation of T and B lymphocytes as B cell and T cell areas were histologically distinguishable in lymphoid tissues in *Nlrc5*-deficient mice (Fig. 3-4, Fig. 3-31).

Moreover, normal $CD3^+$ T cell and $CD19^+$ B cell populations were encountered in the spleen (Fig. 3-5).
The group around D. Philpott reported a low NLRC5 expression in $CD4^+ CD8^+$ and $CD4^- CD8^-$ thymocytes, which are generated from hematopoietic precursors in the thymus and represent the direct precursors of naïve $CD4^+$ or $CD8^+$ T lymphocytes. Hence, they presumed a potential role for NLRC5 during T cell development (Benko et al., 2010). However, these $CD4^+ CD8^+$ and $CD4^- CD8^-$ thymocyte populations were observed to be normally sized in *Nlrc5* ko mice, which does not support a specific role of the NLR member in lymphocyte generation (Yao et al., 2012).
Beyond, the ubiquitous expression of NLRC5 in immune tissues makes it rather unlikely that the protein is functionally restricted to lymphocyte development in primary lymphoid tissues.

Histological studies revealed that NLRC5 had no structural function in secondary lymphoid organs as *Nlrc5* ko mice showed a normal spleen and lymph node architecture (Fig. 3-4). NLRC5 was dispensable for the proliferation of T and B lymphocytes in these organs as T and B cell areas existed in spleen, lymph nodes and lymph follicles in *Nlrc5* ko mice (Fig. 3-4, Fig. 3-31). These areas showed a tissue-typical distribution and architecture. Secondary nodules, which represent ongoing B cell proliferation, were observed in lymph nodes. In addition, the general occurrence of $CD3^+$ T lymphocytes and $CD19^+$ B lymphocytes in murine spleens was not altered in the absence of NLRC5 (Fig. 3-5). NLRC5 did not have an obvious effect on the development of lymphoid tissue as the formation and enlargement of lymph follicles in the colon of *Nlrc5* ko mice was not altered to the wt during an inflammation induced immune response as the chronic colitis (Fig. 3-31).
Additionally, *Nlrc5*-deficient mice displayed a normal spleen weight under baseline conditions, indicating a normal organ function (Fig. 3-3). Splenic dysfunctions like inadequate lymphocyte proliferation are usually reflected by changes of the organ weight or the overall architecture.

B and T lymphocytes occur throughout the body, but highest lymphocyte concentrations are found in secondary and primary lymphoid organs as well as in mucosa-associated lymphoid tissues. This correlates with the observed *Nlrc5* mRNA expression pattern found in human as well as murine tissues (Fig. 3-1). Accordingly, it was assumed that NLRC5 is primarily expressed by immune cells, especially lymphocytes.
Experiments on immortal cell lines did not support this hypothesis as NLRC5 was only moderately expressed under baseline conditions and levels were comparable between immune and non-immune cell lines (Fig. 3-2). Additionally, others found an equal *NLRC5* mRNA expression in Jurkat, THP-1 and HeLa cell lines (Neerincx et al., 2010), hence immune and non-immune cells. Some even observed severely diminished *NLRC5* mRNA levels in Jurkat T lymphocytes and various tested B cell lines (Benko et al., 2010).

IFNɣ treatment led to the induction of NLRC5 in all tested cell lines. The most potent increase was detected in immortalized T and B lymphocytes (Fig. 3-2).
IFNɣ is potently induced during infections with intracellular microorganisms as bacteria or viruses. It subsequently induces ISGs that convey immune relevant functions to defeat the encountered pathogens (Malmgaard, 2004; Müller et al., 1994).
An induction of NLRC5 in diverse cell types by IFNɣ could indicate that NLRC5 is involved in those immune defense mechanisms. IFNɣ signals via the JAK/STAT pathway and activates STAT1 for nuclear import and transcriptional activity (Schroder et al., 2004). NLRC5 might itself be an ISG as two STAT1 binding sites were described within its promoter region (Kuenzel et al., 2010).

NLRC5 seems to exert its function in various cell types, but the rapid and potent induction in lymphoid tissue-derived cell lines by IFNɣ might further indicate a function that is particularly characteristic for lymphocytes.
TNFα treatment did not affect NLRC5 protein levels (Fig. 3-2). TNFα signals via the NF-κB or the MAPK pathway and subsequently leads to the expression of distinct target genes. Here no evidence was found that *NLRC5* is regulated by these particular signaling pathways.

While NLRC5 was only moderately expressed in various immortalized cells and not particularly elevated in immune-derived lineages under baseline conditions (Fig. 3-2), some groups observed significantly altered levels among primary immune cells isolated from lymphoid organs. *NLRC5* mRNA was highly expressed in T helper cells, B cells, CTLs, natural killer (NK) and natural killer T (NKT) cells as well as MΦs and DCs (Benko et al., 2010; Neerincx et al., 2010; Staehli et al., 2012). These data support our findings that NLRC5 is mainly expressed in immune and immune-associated tissues, which are mainly comprised of these immune cells (Fig. 3-1). The data further reflect the elevated NLRC5 protein levels we detected in immune cell lines when compared to non-immune cells upon IFNɣ treatment, while levels were comparable under baseline conditions (Fig. 3-2).
The group around Staehli further analyzed the expression of NLRC5 in various different human and murine T and B cell lines in comparison to the expression pattern in primary total spleen, isolated B or T lymphocytes (Staehli et al., 2012). Interestingly, all of the murine and most of the human immortal lymphoid lineages showed a decreased NLRC5 protein level when compared to primary lymphoid cells. Accordingly, this suggests a probable function for NLRC5 in the defense against mutated cells. The potent down regulation of NLRC5 in lymphoid tumors was a common pattern even between species and can indicate that a down regulation enables cancerous cells to escape immune surveillance.

4.2 THE EXPRESSION OF MHC MOLECULES IS ALTERED ON *NLRC5* DEFICIENT CELLS

4.2.1 NLRC5-DEPENDENT MHC CLASS I EXPRESSION ON IMMUNE CELLS

The surface expression of MHC class I receptors was significantly diminished in *Nlrc5*-deficient mice (Fig. 3-6, Fig. 3-7, Fig. 3-8, Fig. 3-10). This reduction was more pronounced on lymphocytes when compared to Mϕs and it correlated with the NLRC5 expression pattern (Fig. 3-2). The impaired MHC class I expression was not limited to one specific MHC I isotype (Fig. 3-7).
NLRC5 could have an impact on the surface expression of MHC class I by different means. Firstly, NLRC5 might influence MHC class I peptide loading. Secondly, it could be involved in transport of assembled MHC I complexes to the plasma membrane. Thirdly, it might regulate the initial expression of genes coding for MHC class I, β2M or other involved components.

Empty MHC complexes are retained in the ER and finally degraded. Defects in proteins that are involved in MHC I loading have been associated with a reduced MHC I surface expression. For instance, *Tapasin*-deficient mice show decreased MHC class I levels in combination with a reduced cytotoxic T cell response (Garbi et al., 2000). The impaired MHC I expression in *Nlrc5* ko mice could be due to a similar mechanism if NLRC5 is involved in MHC I loading.
Defects in MHC class I loading should not affect MHC class II expression as peptide loading onto the MHC II complex requires a different machinery (1.3.5). In this study the surface MHC II expression on *Nlrc5*-deficient BMDMs was not altered, but the overall MHC II^+ cell population was elevated (Fig. 3-9).

After peptide loading, MHC I complexes need to be transported from the ER via the trans-Golgi network to the plasma membrane. A decreased MHC I surface expression in *Nlrc5*-deficient mice could also be due to a defect in intracellular transport pathways from the ER via the trans-Golgi network to the plasma membrane, which NLRC5 might be involved.
A recently published study found NLRC5 to be localized to the Golgi apparatus when infected with *Human rhinovirus* (Triantafilou et al., 2013). Viral infections also lead to an upregulation of MHC I molecules on the cell surface (Herzer et al., 2003; Yossef et al., 2012). A functional implication of NLRC5 in a rapid membrane transport of newly loaded MHC I complexes can therefore be supposed. This would explain the impaired MHC class I surface expression observed in *Nlrc5* ko mice.
However, this hypothesis is only supported by a MHC class I-specific and not by a general NLRC5-supported membrane transport as the expression of other surface markers (e.g. CD3, CD11b, Gr-1; Fig. 3-5) was not influenced by the *Nlrc5* ko.

MHC class I is ubiquitously expressed on nucleated cells and thrombocytes, but the expression levels vary between tissues and cell types. MHC I is especially elevated in immune-associated tissues as well as tissues with mucosal linings, while e.g. in the brain no protein is detectable (Human Protein Atlas, 2015). Therefore, the MHC I expression pattern reassembles that of NLRC5, which indicates that both might be linked (Fig. 3-1).
It was postulated that NLRC5 is a transcriptional regulator of MHC class I-coding *HLA* genes (Meissner et al., 2010). This has now been confirmed and mechanism of the nuclear import as well as gene transactivation have been studied in greater detail (Biswas et al., 2012; Meissner et al., 2012a, 2012b; Neerincx et al., 2012; Robbins et al., 2012).

4.2.2 NLRC5-INDEPENDENT MHC CLASS I EXPRESSION ON IMMUNE CELLS

The surface expression of MHC Class I was significantly decreased in *Nlrc5* ko mice. However, MHC class I was not equally reduced on *Nlrc5*-deficient immune cells. There existed two distinct MHC I expressing cell populations among *Nlrc5*-deficient splenocytes, while all wt cells expressed equal amounts of the surface receptor (Fig. 3-7 c, Fig. 3-8 a-c). Observing the co-expression of either CD8 or MHC class II on *Nlrc5*-deficient MHC class I^+ lymphocytes revealed that e.g. $CD8^+$ CTLs carried less MHC class I on their surface than MHC II expressing B lymphocytes (Fig. 3-8).
As already mentioned, NLRC5 has been identified as a co-transactivator of genes coding for *HLA-A-G* and genes involved in MHC class I peptide presentation. This explains the severely diminished MHC class I expression in *Nlrc5* ko mice, but neither the remaining basal MHC class I expression (Fig. 3-6, Fig. 3-7, Fig. 3-8), an altered expression among lymphocytes nor the residual ability to induce the expression of NLRC5 upon stimulation (Fig. 3-10).

The data presented here indicate that at least one additional NLRC5-independent mechanism exists that regulates the transcription of MHC class I genes. This mechanism accounts for the persisting expression of MHC class I molecules in *Nlrc5*-deficient immune cells under baseline conditions.
MHC I-inducing mechanisms seem to account differently for the MHC class I expression in distinct cell types. The expression of MHC class I in CTLs is particularly dependent on the regulation by NLRC5, which in turn leads to a potent MHC I decrease within this cell population in the absence of NLRC5. However, in MHC II^+ cells an NLRC5-independent mechanism contributes more effectively to the transcription of MHC I-coding genes, which leads to an attenuated MHC I decline on *Nlrc5*-deficient APCs, e.g. B lymphocytes (Fig. 3-8).

These findings are supported by others that also found an unequal reduction of MHC class I on the surface of different immune cell populations in *Nlrc5* ko mice. They all observed the most prominent decline on $CD4^+$, followed by $CD8^+$ T lymphocytes. An intermediate reduction was seen on B lymphocytes and only a mild MHC I decrease found on Mϕs (Robbins et al., 2012; Staehli et al., 2012; Tong et al., 2012). Some even observed no reduction of MHC class I on *Nlrc5*-deficient BMDMs as well as BMDCs (Biswas et al., 2012). These cell type-specific differences regarding the decline of MHC class I in *Nlrc5* ko mice correlate with the NLRC5 expression pattern in wt mice. NLRC5 has the highest expression in T lymphocytes, followed by B lymphocytes, while hematopoietic cells of the myeloid lineage e.g. DCs and Mϕs only show a moderate expression (Benko et al., 2010; Neerincx et al., 2010; Staehli et al., 2012).

Although the MHC class I surface expression was impaired in *Nlrc5* ko mice, MHC class I could still be induced upon stimulation with PHA (Fig. 3-10). Even others reported that an *Nlrc5* ko did not abolish the potential to induce MHC class I by stimulating cells with either IFNγ (Biswas et al., 2012; Robbins et al., 2012; Staehli et al., 2012) or LPS (Yao et al., 2012). These data support the idea of mechanisms that regulate the expression of MHC class I coding *HLA* genes in addition to NLRC5.

CIITA is primarily known as transcriptional co-activator for MHC class II genes, but it was shown *in vitro* that it can also enhance the expression of MHC class I-coding genes (Gobin et al., 1998a; Martin et al., 1997). Under baseline conditions CIITA is solely expressed in Mϕs, DCs as well as B lymphocytes, which are referred to as professional APCs. They constitutively carry peptide-loaded MHC class II complexes on their surface (Singer and Devaiah, 2013; 1.3.5.1).
An expression of CIITA and the subsequent CIITA-induced transcription of MHC class I-coding genes could account for a higher MHC I surface expression in *Nlrc5* ko lymphocytes that co-express MHC class II in contrast to $CD8^+$ co-expressing CTLs (Fig. 3-8). An alternating CIITA expression can therefore lead to the inhomogeneous MHC class I expression on distinct cell types in *Nlrc5*-deficient mice.
Ex vivo differentiated *Nlrc5*-deficient BMDMs also showed a diminished MHC class I expression with two distinguishable populations. These are probably due to different developmental stages of the primary culture (Fig. 3-6).

The remaining inducibility of MHC I on *Nlrc5*-deficient lymphocytes might be explained to an induction of CIITA by IFNγ. The stimulation of murine primary cultures with PHA led to the induction of IFNγ (Fig. 3-12). IFNγ potently induces CIITA in most other cell types besides APCs (Muhlethaler-Mottet et al., 1997; Steimle et al., 1994). CIITA can subsequently induce MHC class II in these cells. Simultaneously the expression of MHC class I-encoding genes is enhanced.
The induction of CIITA could explain the remaining inducibility of MHC class I molecules in *Nlrc5*-deficient cells upon stimulation as well as the expression of MHC class I-coding genes after a stimulation with either IFNγ or LPS as described above.
CIITA is crucial for the basal expression of MHC class II molecules and their induction upon stimulation. In contrast, I could show here that NLRC5 is neither essential for a basal MHC I expression nor for the induction of MHC class I. Both can be conveyed by an additional mechanism, probably CIITA, instead. However, the expression of MHC class I molecules is significantly impaired in the absence of NLRC5 as this mechanism cannot rescue the impaired MHC I levels to a physiological level.

Although CIITA is likely to account for the cell-specific decline in MHC class I surface expression as well as the persisting inducibility of MHC I in *Nlrc5*-deficient immune cells, it cannot explain the remaining MHC I expression on $CD8^+$ cytotoxic lymphocytes that was observed under baseline conditions (Fig. 3-8).
CTLs do not constitutively express CIITA (Glimcher and Kara, 1992) and primary cultures were not stimulated to induce this NLR member. Accordingly, there has to exist yet another transcriptional regulator for the induction of MHC class I-encoding *HLA* genes. These genes contain an ISRE within their promoter region (Girdlestone, 1996). Therefore, they are ISGs, which are presumed to be directly induced by IFNs.
MHC class I and NLRC5 are supposed to be induced by IFNɣ-mediated JAK/STAT signaling. NLRC5 can subsequently lead to the transcriptional co-activation of MHC I-encoding genes. Accordingly, the expression of MHC class I might be upregulated directly by IFNɣ signaling via the binding of STAT dimers to the ISRE and indirectly via an IFNɣ-mediated induction of NLRC5.
The direct transcriptional regulation of MHC class I-encoding-genes by IFNɣ could explain the residual basal MHC I level in *Nlrc5*-deficient cells and also an induction of MHC I upon stimulation (Fig. 3-10).
NLRC5 is potently induced already early after IFNγ treatment (Fig. 3-1). In future studies, both the temporal upregulation of MHC class I and NLRC5 upon IFNɣ stimulation could be monitored and compared to evaluate if there is a temporally shifted, but mutual induction of MHC class I by IFNɣ and NLRC5 and to what extent both mechanisms contribute to the overall MHC class I expression.
Eventually, an *Nlrc5/Ciita* double ko mouse model might reveal if IFNγ has an impact on MHC expression, if additional MHC class I regulators might exist or if the expression of MHC molecules is entirely regulated by the two NLR members NLRC5 and CIITA.

4.2.3 *NLRC5* DEFICIENCY AFFECTS THE EXPRESSION OF MHC CLASS II

The number of MHC class II^+ leukocytes was elevated in the spleens of *Nlrc5*-deficient mice by about 9% (Fig. 3-9). Within the leukocyte population monocytes, B lymphocytes and dendritic cells constitutively express MHC class II receptors. The population of B cells and macrophages/monocytes were normally developed in *Nlrc5*-deficient mice and cannot explain an enhanced MHC II^+ population (Fig. 3-5). However, genes encoding MHC II proteins can also be induced by IFNɣ in other cell types, e.g. lymphocytes, granulocytes, endothelial and epithelial cells.

The amount of MHC class II expressed on the surface of an individual cell was not altered between the genotypes (Fig. 3-9). This indicates that NLRC5 is not directly involved in the surface expression of MHC class II molecules. In contrast, CIITA is known to regulate the induction of both types of MHC molecules (Singer and Devaiah, 2013).
Other groups also found evidence *in vitro* that NLRC5 does not regulate the induction of MHC class II-encoding genes (Meissner et al., 2010, 2012a, 2012b; Neerincx et al., 2012). Moreover, studies using *Nlrc5*-deficient mice revealed a normal MHC II expression within immune tissues as well as on immune cells (Biswas et al., 2012; Yao et al., 2012). It has been published that the N-terminal NLRC5 domain conveys transcriptional activity for both, MHC class I and II-coding *HLA* genes when linked to a CIITA backbone. However, the physiological NLRC5 backbone is missing the MHC II transactivating ability (Neerincx et al., 2014).
Taken together, the MHC II expression is not directly regulated by NLRC5.

An increased MHC class II^+ cell population in the absence of NLRC5 can also be due to an altered regulation of CIITA. The impaired MHC class I expression in *Nlrc5*-deficient mice cannot be counter steered via the induction of NLRC5. To assure basal MHC class I expression and antigen presentation, CIITA might be induced in *Nlrc5*-deficient animals. CIITA could subsequently mediate the transcription of MHC class I-encoding genes. Simultaneously, MHC class II-encoding *HLA* genes are induced. CIITA can be expressed in various cell types. Hence, NLRC5 is not involved in the constitutive expression of MHC class II molecules on professional APCs. However, an impaired MHC class I expression might induce CIITA, which next to MHC I also leads to the expression of MHC II molecules in non-APCs and thereby augments the MHC class II^+ cell population upon *Nlrc5* deficiency.
This hypothesis must be further evaluated in future experiments. Data of Biswas et al. revealed a slightly elevated *Ciita* expression in *Nlrc5*-deficient splenocytes, however no upregulation of MHC II was observed (Biswas et al., 2012).

4.3 *NLRC5* DEFICIENCY LEADS TO A DIMINISHED $CD8^+$ T CELL POPULATION

During the analysis of splenic cell populations it was observed that the number of $CD8^+$ T lymphocytes was significantly reduced in *Nlrc5* ko mice, while there were no changes in any other analyzed immune cell population (Fig. 3-5, Fig. 3-8 g, Fig. 3-25, Fig. 3-36).
$CD8^+$ cells are predominantly cytotoxic T lymphocytes (CTLs). These are indispensable in adaptive responses towards intracellular pathogens as CTLs possess a tightly regulated mechanism to identify and eliminate infected cells via MHC class I-presented foreign antigens. In addition to adaptive immune responses the expression of MHC class I is further crucial for the development of single positive $CD8^+$ thymocytes and their positive selection during T cell development in the thymus. CTL-determined thymocytes only survive if they encounter and recognize a self peptide presented on a self MHC class I receptor (Janeway, 2005). An impaired MHC I expression can lead to an impaired CTL generation. Accordingly, the reduced splenic $CD8^+$ T cell population in *Nlrc5* ko mice might be due to the impaired MHC class I expression (Fig. 3-5).
It can be speculated that differences in CTL numbers are even more pronounced during $CD8^+$-mediated immune responses, because the proliferation of CTLs is initiated by MHC class I-presented antigens. CTL proliferation is expected to be impaired in the absence of NLRC5 due to a diminished MHC class I expression.
Taken together, an NLRC5 deficiency significantly impairs the surface expression of MHC I, which can consecutively influence the generation of $CD8^+$ T cells in the thymus and their expansion in secondary lymphoid organs. Interestingly, Biswas et al. observed a diminished proliferation of *Nlrc5*-deficient CTLs even if the antigen was properly presented to CTLs by B lymphocytes (Biswas et al., 2012).

The effects of an *Nlrc5* ko on MHC class I expression as well as the indirect influence on the CTL population assign the protein a function in adaptive cytotoxic T cell immunity. Therefore, it is assumed that *Nlrc5* ko mice show an impaired adaptive response against intracellular pathogens. Due to diminished $CD8^+$ T cell numbers intracellular microbes might be able to proliferate and spread more potently to neighboring cells, which subsequently leads an increased disease progression. These considerations were further supported by Yao et al., who systemically infected *Nlrc5*-deficient mice with *L. monocytogenes* and observed severely decreased $CD8^+$ T cell numbers as well as increased bacterial loads in various organs (Yao et al., 2012). This underlines a defective cytotoxic capability in the absence of NLRC5. In contrast, Tong et al. rather observed reduced virus titers and a pronounced

survival of *Nlrc5* ko mice during an infection with systemic *Vesicular stomatitis virus* (VSV) (Tong et al., 2012).

4.4 *NLRC5* DEFICIENCY DOES NOT AFFECT $CD4^+$ T CELL NUMBERS

While the decreased MHC class I expression led to a reduced $CD8^+$ T population in *Nlrc5* ko mice, elevated MHC II^+ leukocyte numbers did not significantly alter the $CD4^+$ T cell population (Fig. 3-5). Differentiation, proliferation and activation of $CD4^+$ lymphocytes depends on the recognition of MHC class II-bound antigens presented on APCs. Basal MHC II expression was not altered in *Nlrc5* ko mice; therefore the differentiation and proliferation of $CD4^+$ T cells might not be affected. However, an increased expression of MHC class II molecules on non-APCs can enhance the presentation of antigens to effector $CD4^+$ T cells and thereby favor their activation. An enhanced activation of $CD4^+$ effector cells is reflected in increased effector functions e.g. an elevated cytokine production.

4.5 NLRC5 HAS A COMPLEX INFLUENCE ON CYTOKINE RESPONSES IN PRIMARY IMMUNE CELLS

A function for NLRC5 on inflammatory signaling pathways has repeatedly been reported. Within this project the question was addressed if the protein influences the innate signaling cascade and thereby the induction of inflammatory cytokines. Several interesting observations affecting distinct pathways were made.

1. *Nlrc5*-deficient BMDMs showed a reduced *Ifnb* mRNA expression upon stimulation with viral RNA analogues when compared to the wt (Fig. 3-11). In contrast, LPS stimulation led to a comparable *Ifnb* induction in both genotypes. Accordingly, NLRC5 seems to be required for a proper IFNβ expression induced by either viral ss or dsRNA.
Throughout the literature an effect of NLRC5 on the induction of type I IFNs has been under debate, but a particular role has not been identified. Findings by T. Kufer and J. Ting et al. support our data as they report a decreased IFNβ induction upon poly(I:C) treatment or SeV infection in cells in which *Nlrc5* was knocked down or knocked out (Neerincx et al., 2010; Robbins et al., 2012). Others observed no NLRC5-specific influence on the expression of IFNβ (Kumar et al., 2011; Staehli et al., 2012; Yao et al., 2012) or even an increased IFNβ expression in *Nlrc5* ko mice infected with SeV or VSV (Robbins et al., 2012; Tong et al., 2012).
On the molecular level, NLRC5 might be involved in PRR downstream signaling pathways that lead to the transcription of *Ifnb*. LPS only induced a minor expression of IFNβ that did not differ between wt and ko. LPS is recognized by TLR4 and internalized TLR4 receptors can induce *Ifnb* via the MyD88-independent TRIF pathway as in TLR3 signaling (Tanimura et al., 2008). Hence, an NLRC5-specific effect on the TRIF pathway is not likely.
It can rather be speculated that NLRC5 has a positive effect on the IPS-1-dependent IFNβ induction via MDA5, RIG-I or NOD2. This is supported by the observation that NLRC5 interacts with TBK1. NLRC5 might regulate TBK1 activity and hence IRF3 phosphorylation (Kumar et al., 2011).
In contrast, it was reported that NLRC5 overexpression inhibited the RIG-1 induced IRF3 phosphorylation as well as ISRE activation by MDA5 and RIG-I (Benko et al., 2010; Cui et al., 2010). and that NLRC5 interacts directly with RIG-I and MDA5 to negatively regulate type I IFN signaling (Cui et al., 2010). This inhibitory effect of NLRC5 on the induction of IFNβ is neither supported by our *in vivo* data nor by those of other groups (Kumar et al., 2011; Robbins et al., 2012).

It can also not be ruled out that NLRC5 might be directly involved in the recognition of viral ss or dsRNA ligands to induce type I interferons and hence possess receptor functions as initially assumed for all NLR members.

Type I IFNs are important for antiviral protection as they induce a set of ISGs that interfere with viral replication. IFNs act in an autocrine as well as in a paracrine manner. Hence, they induce an antiviral state in the infected cell as well as in yet unaffected neighboring cells. An alleviated expression of IFNβ in *Nlrc5* ko mice might consequently lead to an impaired innate antiviral defense and to more widespread and aggravated viral infections. An impaired type I expression can subsequently lead to a diminished induction of the type II IFNɣ.

2. We found that *Nlrc5*-deficient leukocytes expressed and secreted significantly diminished amounts of IFNɣ upon cell activation, although wt and *Nlrc5*-deficient cells were activated to a comparable extend as evaluated by the expression of the activation marker CD25 (Fig. 3-12 a-c).
Our data were supported by other groups that observed an impaired production of IFNɣ in *Nlrc5* ko mice after an infection with *L. monocytogenes* (Yao et al., 2012). Interestingly, there were no alterations in the expression of IFNɣ in a microarray performed with *NLRC5* mutants (Meissner et al., 2010).
An impaired induction of type II IFNɣ in activated T lymphocytes can indicate defects in certain signaling pathways. Here, cells were stimulated with LPS to induce IFNβ. IFNβ binds the surfacial type I interferon receptor (IFNAR) and induces JAK/STAT signaling. Thereby, STAT1 becomes phosphorylated and phospho-STAT1 dimers bind the GAS element within the IFNɣ promoter and potently induce the production of IFNɣ (Rawlings et al., 2004). LPS induced the expression of IFNɣ in wt, but not in ko splenocytes. This was not due to an altered IFNβ production (Fig. 3-11), but might reflect an impaired IFNβ-mediated JAK/STAT signaling in *Nlrc5*-deficient mice. It was reported that the expression of STAT1 is not altered in *Nlrc5* ko mice (Biswas et al., 2012). However, further experiments should be performed to study the induction of type I and II IFNs in *Nlrc5* ko cells. Moreover, the components of the JAK/STAT signaling pathway and their phosphorylation status should be investigate to reveal if NLRC5 directly influences the IFN signaling.
The impaired $CD8^+$ T cell population observed in *Nlrc5* ko mice (Fig. 3-5) might also account for an impaired IFNɣ production in mixed murine splenocyte cultures, as activated CTLs are a major source of the cytokine. Interestingly, CTLs in *Nlrc5* ko mice were observed to produce normal amounts of IFNɣ upon activation, which indicates that the production of IFNɣ is not generally impaired in ko cells (Yao et al., 2012). This also supports the idea that a reduced CTL population rather than a deregulated JAK-STAT signaling pathway leads to a diminished overall IFNɣ production in a mixed immune cell culture.

IFNɣ is predominantly secreted by T lymphocytes, NK as well as NKT cells. The cytokine is necessary for a potent activation of Mϕs to phagocytose and present digested peptides. Furthermore, it induces the expression of MHC molecules for antigen presentation. A deficient IFNɣ production in *Nlrc5* ko mice can therefore impair the uptake and destruction of invading pathogens by Mϕs as well as the generation and presentation of antigens. As a consequence, innate immune responses might arise that are impaired in removing invading pathogens and that lead to a more widespread inflammation. In combination with the decreased MHC class I expression and a reduced CTL number the decreased IFNɣ levels could further favor the development of tumors in *Nlrc5* ko mice (Ikeda et al., 2002).

3. Beyond its impact on the induction of interferons NLRC5 also influenced the production of NF-κB-dependent cytokines and their maturation.

A role of NLRC5 in the production of mature IL-1β has been indicated by different publications. The data presented here indicate that NLRC5 is involved in the generation of IL-1β as *Nlrc5*-deficient cells showed reduced IL-1β levels (Fig. 3-13).
IL-1β is a pro-inflammatory cytokine. A diminished induction can lead to an impaired innate immune defense in *Nlrc5*-deficient mice as these might not be able to develop a potent inflammatory response.
The group around J. Ting found evidence that NLRC5 positively regulates IL-1β signaling as part of the NLRP3 inflammasome (Davis et al., 2010), while others even claimed that NLRC5 inhibits IL-1β signaling (Benko et al., 2010). NLRC5 could be a part of the NLRP3 inflammasome as IL-1β levels were significantly impaired upon treatment with ATP in *Nlrc5* ko cells (Fig. 3-13). However, the IL-1β production upon ATP stimulation was not entirely abrogated in the *Nlrc5*-deficient cells. This indicates that NLRC5 is either a dispensable component of the NLRP3 inflammasome or that there exists a distinct NLRC5-dependent mechanism to activate caspase-1, which can be induced by ATP.
Our data indicate that NLRC5 might rather be necessary for a potent induction of the IL-1β propeptide by NF-κB than its cleavage into the mature form due to caspase activation as *Il1b* mRNA levels were decreased in *Nlrc5*-deficient cells (Fig. 3-13 a).

Various groups did not find any NLRC5-specific effects onto the NF-κB signaling pathway performing *in vitro* experiments (Davis et al., 2010; Kuenzel et al., 2010; Meissner et al., 2010; Neerincx et al., 2010; Ranjan et al., 2014). Some again claim NLRC5 to inhibit NF-κB signaling as a reduced promoter activation and a diminished induction of NF-κB target genes were observed in *Nlrc5* overexpression studies (Benko et al., 2010; Cui et al., 2010; Kumar et al., 2011; Li et al., 2014). To further evaluate the impact of Nlrc5 on NF-κB signaling, BMDMs were stimulated with LPS and the induction of selected NF-κB target genes was measured.
From our data no general effect can be concluded as distinct NF-κB target genes were differentially influenced by the *Nlrc5*-deficiency. Upon LPS stimulation *Nlrc5*-deficient BMDMs showed different effects depending on the monitored NF-κB target gene. While *Il6* and *Cxcl1* mRNA levels were not altered in the ko (Fig. 3-14 c, d), *Tnfa* mRNA was significantly elevated in *Nlrc5* ko cells. However, the secretion of TNF-α was impaired in *Nlrc5*-deficient BMDMs (Fig. 3-14 a, b), which might rather be due to defects in TNF-α secretion than an impaired *Tnfa* induction in ko animals.
Many contradictory observations exist that try to clarify the impact of NLRC5 in NF-κB signaling (Biswas et al., 2012; Kumar et al., 2011; Staehli et al., 2012; Yao et al., 2012; Tong et al., 2012; Kumar et al., 2011). A general influence of NLRC5 on NF-κB signaling and NF-κB-induced gene expression cannot be ruled out, but more dedicated future analyses are needed.

4.6 INFLUENCE OF NLRC5 ON EXPERIMENTAL COLITIS *IN VIVO*

NLRC5 was assigned a pro-inflammatory role from the preceding *in vitro* experiments.
It was presumed that individuals with functional defects in *Nlrc5* are more susceptible to infections as distinct innate as well as adaptive immune mechanisms were observed to be impaired in *Nlrc5*-deficient mice. Inflammatory disorders were presumed to develop less aggravated.
Since, NLRC5 has not been studied in the context of intestinal inflammation, its role in the onset, progression and chronification of colitis was evaluated here. This inflammatory disorder involves innate as well as adaptive mechanisms (Geremia et al. 2014).

During the initial characterization *Nlrc5* ko mice were shown to have an impaired MHC class I surface expression, a diminished $CD8^+$ population and a reduced production of IFNs and IL-1β. All of these factors are thought to be protective in IBD (Bär et al., 2013; Bisping et al., 2001; Fais et al., 1991, 1994; Ligumsky et al., 1990; Mahida et al., 1989; Müller et al., 1998; Noguchi et al., 1995; Okazaki et al., 1993; Reinecker et al., 1993; Sasaki et al., 1992; Satsangi et al., 1987). Accordingly, *Nlrc5* ko mice were expected to develop an alleviated colitis upon DSS treatment when compared to wt animals.

4.6.1 MICE LACKING *NLRC5* ARE MORE SUSCEPTIBLE TO DSS-INDUCED COLITIS

Nlrc5-deficient mice developed colitis upon DSS treatment. The intestinal inflammation worsened after DSS withdrawal during regeneration phases in the acute as well as the chronic model. Some ko animals even had to be prematurely sacrificed as they suffered an extraordinary disease aggravation.

The temporal onset of colitis upon acute DSS-treatment was comparable between *Nlrc5*-deficient and wt mice. However, ko animals developed a more pronounced disease, which was e.g. characterized by a premature drop out of 20% of DSS treated ko animals (Fig. 3-16). Regarding the clinical phenotype, *Nlrc5* ko mice suffered from a more severe diarrhea, they showed more pronounced intestinal bleedings and had a greater body weight loss during the course of the experiment. This is collectively represented by the increased DAI (Fig. 3-17). DAI-specific clinical signs are caused by the severe epithelial destruction in the colon, which hinders a proper resorption of water from the feces and thereby leads to the disease-typical diarrhea. The impaired uptake of nutrients and electrolytes induces the severe body weight loss. The progressive inflammation further causes intestinal bleedings that were detectable as occult blood in the feces.
Moreover, colon shortening was observed in all ko and wt mice during acute disease. The degree of shortening was comparable between the genotypes, although ko animals had a more pronounced epithelial damage in the colon as well as a more pronounced clinical disease. Therefore, they were initially assumed to show an increased colon shortening (Fig. 3-18). Colon shortening is a typical feature found in IBD patients. It has also been described for rodents suffering from DSS-induced colitis (Chassaing et al., 2014). Organ shortening reflects the severe local inflammatory processes, due to which the colon loses fluid and its flexibility as epithelial lesions are repaired by inflexible scar tissue.
Histopathologically, *Nlrc5*-deficient mice showed a severely elevated epithelial destruction in the distal colon with a great loss of goblet cells and entire crypts during acute colitis (Fig. 3-19, Fig. 3-20). Inflammatory mediators like IL6 and KC were significantly elevated in colon and serum of ko mice compared to the wt (Fig. 3-21, Fig. 3-22).

During the induction of a chronic DSS-induced colitis, *Nlrc5*-deficient and wt animals initially did not show alterations in the clinical phenotype. However, 40% of ko mice suddenly developed an exaggerated disease during the repeated regeneration phases and had to be sacrificed early (Fig. 3-27). They were analyzed separately as ko_{abort} subgroup as they showed significant differences regarding their disease pathology when compared to the more moderately affected ko animals, which were designated ko_{d21}. DSS-induced chronic colitis in these ko_{d21} animals was comparable to that in wt animals with regard to all analyzed parameters.
However, Ko_{abort} mice showed a more pronounced loss of crypts within the distal colon and an upregulation of distinct inflammatory mediators as IL6 and MIP2α in the colon (Fig. 3-32). The bowel of ko_{abort} animals was significantly shortened when compared to the control group or even ko_{d21} *Nlrc5*-

deficient mice, what also reflects the more aggravated disease and the rapid pathophysiological changes that justified this experimental subgroup (Fig. 3-29).

Altogether, the loss of NLRC5 led to an increased susceptibility towards acute as well as chronic DSS-induced intestinal inflammation, an observation that was contrary to the initial hypothesis.

4.6.2 THE PRODUCTION OF INFLAMMATORY CYTOKINES WAS ELEVATED IN *NLRC5*-DEFICIENT MICE UPON DSS TREATMENT

Several inflammatory cytokines have been implicated in the onset and perpetuation of IBD (Neurath, 2014). Thus, the expression of certain cytokines was evaluated locally in the colon as well as systemically in the serum.
Under baseline conditions, the expression of cytokines was not altered in *Nlrc5* ko mice. Acute as well as chronic DSS treatment led to a potent induction of cytokines in the colon (Fig. 3-21). Detected levels varied greatly between individual animals. In the acute disease the pro-inflammatory IL-1β, IL-6, IL-12, the anti-inflammatory IL-10 as well as the chemokines CXCL1/KC and CXCL2 were significantly upregulated in the colons of *Nlrc5*-deficient animals. During chronic colitis cytokines were induced equally in the colon of wt and ko_{d21} mice, only the severely affected ko_{abort} animals showed an enhanced expression of IL-6, CXCL2, IL-10 and IL-1β in the colon.
The elevated cytokine production in ko mice upon DSS treatment correlated with the degree of injury observed in the colon epithelium and the severity of disease.

In IBD patients, an elevated expression of IL-1β in the gut has been observed. The cytokine is produced spontaneously by mononuclear cells within the lamina propria during active CD and UC, while it is not detectable in healthy controls (Ligumsky et al., 1990; Mahida et al., 1989; Reinecker et al., 1993; Satsangi et al., 1987). In murine DSS-colitis models IL-1β is also potently induced (Arai et al., 1998) and disease severity can be reduced by inhibiting the IL-1β production or signaling pathway (Kwon et al., 2005; Okada et al., 2011; Siegmund et al., 2001b). The pro-inflammatory cytokine is thought to increase the permeability of the intestinal epithelium by affecting tight junctions (Al-Sadi and Ma, 2007), which enables pathogens, commensals and food antigens to enter more easily. In addition, IL-1β increases the recruitment of granulocytes and diverse cells of the lymphoid lineage in the intestine (Coccia et al., 2012).
The production of IL-1β by *Nlrc5* ko cells was observed to be impaired in preceding *in vitro* experiments upon stimulation (Fig. 3-13). Therefore, *Nlrc5*-deficient mice were hypothesized to have a diminished IL-1β production in the gut, which was assumed to be protective in the development of the DSS-induced colitis. However, we observed an enhanced IL-1β production in the colon of ko animals compared to the wt (Fig. 3-21, Fig. 3-22). This further correlated with the development of a more severe colitis phenotype in *Nlrc5*-deficient mice (Fig. 3-17). IL-1β supports the ongoing inflammation by increasing the epithelial permeability and the recruitment of neutrophils to the site of inflammation.

A more severe course of disease was also reflected by an increased production of IL6, CXCL1 (KC, murine IL-8 homologue), CXCL2 (MIP2a) and IL-10 in *Nlrc5*-deficient mice.
CXCL1 and CXCL2 support the inflammation by activating and recruiting phagocytes from the blood to the site of injury or inflammation as they promote endothelial adhesion and diapedesis (Kobayashi, 2006). IL-6 can enhance disease severity by activating various target cells e.g. APCs and T cells to produce specific mediators. The cytokine also prevents the apoptosis of effector T cells and therefore

keeps the inflammation from ceasing (Neurath, 2014). IL-10 down-regulates the production of pro-inflammatory cytokines. It is upregulated to limit intestinal inflammation. IL-10 levels correlate with the severity of colitis Mutations impairing IL-10 production or signaling are associated with IBD in humans and mice (Engelhardt and Grimbacher, 2014; Rennick et al., 1997).

Although all *Nlrc5*-deficient mice had elevated levels of the cytokines discussed above two important inflammatory mediators were not altered between the genotypes during DSS-induced colitis. These were IFNɣ and TNFα.
An enhanced intestinal IFNɣ production has been observed during IBD, especially in CD patients (Breese et al. 1993; Sasaki et al. 1992; Fais et al. 1991; Fais et al. 1994; Bisping et al. 2001a). There was also a therapeutical benefit observed if patients suffering from Crohn's disease were treated with the humanized anti-interferon γ antibody Fontolizumab (Ghosh et al., 2006; Hommes et al., 2006). Several experimentally induced colitis models in rodents furthermore revealed a correlation of the intestinal inflammation and the IFNɣ production as colitis did not develop in the absence of IFNɣ (Ito et al., 2006; Powrie et al., 1994) or disease severity was significantly ameliorated, when the production of IFNɣ was inhibited or secreted IFNɣ was neutralized by monoclonal antibodies (Hans et al., 2000b; Obermeier et al., 1999; Okada et al., 2011). Lymphocytes in the lamina propria were found to spontaneously release IFNɣ in CD patients (Fais et al., 1991). These were identified to be CTLs, which are activated for cytokine secretion upon antigen recognition. They are a major source of IFNɣ during an adaptive response (Bisping et al., 2001).
Due to the decreased MHC class I expression and the reduced $CD8^+$ T cell numbers it was initially presumed that the activation of CTLs and thereby the release of IFNɣ was impaired in *Nlrc5*–deficient mice (Fig. 3-6, Fig. 3-7). An impaired expression of IFNɣ in *Nlrc5*-deficient splenocytes had already been observed *in vitro* upon stimulation (Fig. 3-12). IFNɣ activates endothelial cells, induces T cell proliferation and initiates the recruitment and activation of additional leukocytes into the gut (Koboziev et al., 2010; Noguchi et al., 1995). Therefore, we initially hypothesized that the impaired production of IFNɣ alleviates the DSS-induced colitis in *Nlrc5* ko animals.
However, we measured comparable IFNɣ levels in *Nlrc5*-deficient animals during DSS-induced colitis (acute: Fig. 3-21, Fig. 3-22; chronic: Fig. 3-32, Fig. 3-33). Ko mice were not protected from colitis by an impaired IFNɣ production as we presumed. In contrast, they even suffered a more aggravated disease.
IFNɣ levels did not correlate with disease severity in this study (Fig. 3-17), which might reflect the inability of *Nlrc5*-deficient mice to produce proper amounts of IFNɣ in response to intestinal inflammation. An imbalance of disease severity and IFNɣ production might reveal that IFNɣ is usually upregulated during colitis, but that disease severity is not due to the elevated IFNɣ production.
On the other hand one could also hypothesize that the aggravated disease in *Nlrc5*-deficient mice is especially due to the impaired IFNγ production. This is supported by the observation that mesenchymal stromal cells need to be activated by IFNγ to exert immunosuppressive properties. Activated mesenchymal stromal cells can thereby attenuate DSS-induced colitis in mice (Hommes et al., 2006).

TNFα was also induced at comparable amounts in the colons of wt and *Nlrc5* ko mice during DSS-colitis, although ko animals suffered a more aggravated disease. The pro-inflammatory TNFα is known to be potently upregulated in IBD patients (Braegger et al., 1992; Breese et al., 1994; Komatsu et al., 2001) as well as in experimental colitis models in rodents (Perse et al., 2012; Yan et al., 2009). Today, humanized anti-TNFα antibodies (e.g. Infliximab, Adalimumab) are one of the most effective therapeutical options to treat IBD patients.

However, in *Nlrc5*-deficient mice TNFα levels did not correlate with the severity of the DSS-induced colitis. As with IFNγ it is tempting to speculate that this reflects the inability of *Nlrc5*-deficient mice to produce proper amounts of TNFα in response to intestinal inflammation and that the upregulation of TNFα might rather be a consequence, but not an initial cause during intestinal inflammatory diseases.

In summary, the diminished production of IL-1β and IFNγ in *Nlrc5*-deficient cells *in vitro* supported a pro-inflammatory role of the NLR member and favored the hypothesis of an alleviated colitis phenotype in *Nlrc5*-deficient mice. However, cytokine levels were not reduced *in vivo* and ko animals developed a more aggravated DSS-induced colitis. The enhanced production of cytokines that was observed in the colon of ko animal could be due to an elevated influx of inflammatory cells, an enhanced activation of local immune and non-immune cells or impaired regulatory mechanisms.
The induced pro-inflammatory mediators perpetuate the inflammation. Further immune cell populations are recruited, which can subsequently account for the prominent epithelial destruction in *Nlrc5*-deficient mice.

4.6.3 THE ENHANCED EPITHELIAL DESTRUCTION IN THE COLON OF *NLRC5* KO MICE IS NOT DUE TO AN ELEVATED INFLUX OF INFLAMMATORY CELLS

Histological analyses revealed that mice suffering from DSS-induced colitis show damages in the epithelium of the large bowel (Fig. 3-19, Fig. 3-30). During acute disease, the epithelial destruction was characterized by an extensive loss of goblet cells as well as entire crypts (Fig. 3-19, Fig. 3-20). It was strikingly more severe in *Nlrc5* ko mice when compared to wt animals. In the chronic model, there was only a moderate and comparable epithelial damage in the colons of wt and ko_{d21} animals, while the ko_{abort} group showed an extensive loss of crypts (Fig. 3-30). The enhanced epithelial destruction in this subgroup correlated with the severity of disease (Fig. 3-27, Fig. 3-28, Fig. 3-29).

The primary epithelial destruction in DSS-colitis models is assumed to be mediated by cytotoxic effects DSS exerts onto intestinal cells. These impair the epithelial barrier and subsequently lead to the onset of inflammation in response towards the tissue injury and the intruding luminal antigens (Ni et al., 1996). *Nlrc5*-deficient mice developed a more severe epithelial damage in the distal colon when compared to wt animals. This could reflect an altered susceptibility towards the DSS-induced epithelial damage or the inability to efficiently cope with the induced epithelial damage.

Beyond DSS, immigrating immune cells and resident non-immune cells can mediate an epithelial destruction during colitis.
The level of IL-1β, CXCL1 and CXCL2 in the colon of DSS-treated *Nlrc5* ko animals was significantly increased when compared to wt mice (Fig. 3-21; Fig. 3-32). These cytokines promote the chemotactic invasion of phagocytes (especially neutrophils) from the blood. Therefore an increased influx of inflammatory cells was assumed in the bowel of *Nlrc5*-deficient animals. Immigrating neutrophils can be involved in the severe destruction of the intestinal epithelium (Fournier and Parkos, 2012; Fig. 3-19).
Intestinal inflammation usually originates at the intestinal epithelium were pathogens, commensals as well as food constituents can enter if the epithelial barrier is disrupted e.g. by DSS. Subsequently, antigens are presented to intraepithelial immune cells, which become activated to secrete cytokines and induce the influx of immune cells into the site of inflammation. Depending on disease severity immigrating cells penetrate the lamina propria and subsequently intersperse the submucosa or even break through the muscular layers into the abdominal cavity. During disease onset predominantly

neutrophils, monocytes and DCs migrate into the colon, while after approximately five days also T and B lymphocytes are attracted to the site of inflammation (Perse et al., 2012).
In our study an infiltration of inflammatory cells into the different layers of the colon wall was observed upon DSS treatment (Fig. 3-19, Fig. 3-30). However, the influx of immune cells into the damaged intestine was not altered between *Nlrc5* ko and wt mice (Fig. 3-19, Fig. 3-30). During acute disease colons of ko mice even tended to be less interspersed with infiltrating cells. Inflammatory cells accumulated mainly in the lamina propria, while in several colons of wt mice they also migrated into the submucosa (Fig. 3-19). During chronic disease the migration of immune cells into the bowel was more pronounced as most animals showed transmural inflammation (Fig. 3-30). Wt, ko_{d21}, and ko_{abort} animals had a comparable influx and distribution of inflammatory cells, although the ko_{abort} group showed significantly higher cytokine levels and a more severe disease phenotype.
The enhanced mediator production and the aggravated disease severity observed in *Nlrc5*-deficient mice did not correlate with the influx of inflammatory cells into the bowel, neither in the acute nor in the chronic model. This was an unexpected finding as the influx of inflammatory cells as well as their tissue distribution are usually used to evaluate disease severity in experimentally induced colitis models as they are assumed to correlate with one another (Wirtz et al., 2007).

The influx of neutrophils into the bowel is an early event during colitis. The subsequent recruitment and activation of lymphocytes severely exacerbates tissue destruction and aggravates disease. Therefore, $CD8^+$ and $CD4^+$ lymphocyte populations were monitored during colitis.
$CD8^+$ effector cells are supposed to be involved in the pathogenesis of colitis as their numbers are increased in patients suffering from IBD (Bisping et al., 2001; Müller et al., 1998). CTLs are activated by MHC class I-presented antigens and contribute to the development and progression of IBD by different mechanisms. On the one hand, CTLs isolated from colons of IBD patients produce elevated amounts of IFNɣ and thereby perpetuate the local inflammation (Bisping et al., 2001). On the other hand, higher levels of the CTL-specific granule constituents perforin and granzyme A were detected in the lamina propria of colons from IBD patients (Müller et al., 1998; Waldner et al., 2010). Perforin lyses the target cell, which is bound via the TCR, while granzymes enter the cell and induce the programmed cell death. Accordingly, an increased cytotoxicity was observed in intestinal lesions of IBD patients. It contributes to the epithelial destruction during colitis and was shown to be MHC class I restricted (Okazaki et al., 1993). A deficient perforin production was reported to attenuate colitis, which underlines the role of CTLs in the course of IBD (Waldner et al., 2010).
CTLs preferentially locate to sites within the bowel that face the intestinal lumen where they recognize MHC class I-presented antigens on IECs (Müller et al., 1998). Upon activation, CTLs induce cytolysis of the antigen-presenting IEC and thereby damage the intestinal epithelium. IECs constitutively express MHC class I. This surface expression is increased in IBD patients (Hershberg and Mayer, 2000; Mayer et al., 1991). Within the intestine, IECs separate the host's immune components from the non-self components within the gastrointestinal lumen. IECs present luminal antigens to intraepithelial lymphocytes and thereby activate intestinal $CD4^+$ and $CD8^+$ T lymphocytes (Bisping et al., 2001; Dotan et al., 2007).
Due to the impaired $CD8^+$ T cell population in *Nlrc5* ko mice it was initially assumed that there is a reduced capacity to release perforin and granzymes compared to wt animals (Fig. 3-5). In addition, it was presumed that fewer antigens are presented to $CD8^+$ T cell due to the reduced MHC class I surface expression (Fig. 3-6, Fig. 3-7). Collectively, an alleviated epithelial destruction and hence a reduced intestinal inflammation was expected in *Nlrc5*-deficient mice.
$CD8^+$ numbers in the spleen were diminished in *Nlrc5* ko mice under basal conditions as well as during colitis (Fig. 3-5, Fig. 3-8, Fig. 3-25, Fig. 3-36). However, the $CD8^+$ population in the colon was

comparable to wt animals (Fig. 3-36). The loss of crypts in the distal colon was more severe in *Nlrc5*-deficient mice and the decreased presentation of antigens due to the impaired MHC class I expression did not alleviate the epithelial destruction (Fig. 3-17, Fig. 3-19). It can be speculated that an aberrant activation of CTLs in the bowel of *Nlrc5* ko mice augments the cytotoxic death of IECs upon MHC I-antigen presentation. An overactivation can account for an aggravated epithelial destruction and consequently a more severe colitis in ko mice.
$CD4^+$ T cell numbers were not significantly altered between the genotypes neither in the spleen nor in the colon (Fig. 3-5, Fig. 3-25, Fig. 3-36). In the course of disease we observed that $CD8^+$ and $CD4^+$ lymphocyte numbers decreased in the spleens of wt and ko mice (Fig. 3-25, Fig. 3-36). This is assumed to be due to their migration to the site of inflammation. Accordingly, the number of $CD8^+$ and $CD4^+$ cells within the colon expanded (Fig. 3-36). In addition to the chemotactic invasion of T lymphocytes from the spleen, an enhanced proliferation of naïve T cells in the gut-associated lymphoid tissue might account for an extending lymphocyte population in the bowel (Fig. 3-31). Accordingly, although $CD8^+$ T cell numbers were diminished in *Nlrc5*-deficient mice, their proliferation and migration was not affected. A decreasing T cell population in the spleen and an increasing population in the colon during colitis have also been described by others (Hall et al., 2011; Perse et al., 2012).

During future experiments it should be evaluated if there is a normal activation of CTLs in *Nlrc5* ko mice during an intestinal inflammation. Therefore perforin and granzyme levels can be measured and the $CD8^+$ IFNɣ-producing CTL population in the colon can be evaluated.

4.6.4 AN ALTERED MHC EXPRESSION IN *NLRC5*-DEFICIENT MICE CAN FAVOR INTESTINAL INFLAMMATION BY DIFFERENT MEANS

Food and microbial antigens can induce inflammation and initiate adaptive responses if their MHC-presented antigens are recognized by $CD4^+$ as well as $CD8^+$ effector cells. A well established tolerance towards luminal antigens limits these immune responses and prevents from aberrant intestinal inflammation, which could easily become chronic as the sensitizing antigens do not fade.

Genetic analyses revealed that certain human MHC class II coding *HLA* alleles are associated with UC or CD and emphasize an important role for MHC class II molecules in the development of IBD (Forcione et al., 1996; Stokkers et al., 1999). Additionally, certain MHC class II isotypes were found to be upregulated in active inflammatory lesions (Fais et al., 1987; Mayer et al., 1991). Therefore, next to specific *HLA* alleles, also a high MHC class II expression is associated with IBD.
An increased MHC class II^+ cell population was found among splenocytes in *Nlrc5*-deficient mice (Fig. 3-9). An elevated MHC class II expression presumably leads to an enhanced presentation of extracellular antigens towards $CD4^+$ T lymphocytes. This can induce an enhanced proliferation and activation of $CD4^+$ T cells and favor the development of adaptive responses. The proliferation and activation of $CD4^+$ Th cells in the intestine is especially upregulated if the epithelial barrier is damaged (e.g. upon DSS treatment) and luminal components can enter the tissue. Their antigens are presented by MHC class II molecules e.g. on Mϕs, DCs or IECs (Dotan et al., 2007).
Although *Nlrc5* ko mice had an increased MHC class II population, we did not observe an altered proliferation of $CD4^+$ T cells in ko mice, neither under baseline conditions nor upon DSS treatment (Fig. 3-9, Fig. 3-5, Fig. 3-25, Fig. 3-36).

Next to an elevated MHC class II expression also the impaired expression of MHC class II molecules on non-hematopoietic cells in the gut (e.g. IECs) is implicated in the onset of colitis (Thelemann et al., 2014).

Nlrc5-deficient mice had an increased MHC II^+ cell population among immune cells. However, MHC II is not constitutively expressed in IECs, but needs to be induced by IFNγ (Fig. 3-9). *In vitro* experiments implicated that the production of IFNγ is impaired in *Nlrc5*-deficient cells (Fig. 3-12). Additionally, intestinal IFNγ levels were alleviated during chronic disease if correlated to disease severity (Fig. 3-21, Fig. 3-32). Impaired IFNγ levels can lead to a reduced MHC II expression on IECs and thereby to a decreased presentation of antigens to $CD4^+$ T cells. In future experiments it should be evaluated if *Nlrc5*-deficent mice have a reduced expression of MHC II molecules on IECs and if they subsequently suffer from an impaired immunological tolerance.

Oral tolerance is not induced centrally during lymphocyte development, but in the periphery upon antigen contact, predominantly by IECs (Westendorf et al., 2009). This peripheral tolerance is established by the differentiation of $CD4^+$ cells into inducible regulatory T cells (iTregs), Th3 or type 1 T regulatory (Tr1) cells. These regulatory cells suppress $CD4^+$ as well as $CD8^+$ T cell effector functions in a contact-dependent manner (iTreg) or via regulatory cytokines (Th3, Tr1) (Martin et al., 2004; Mempel et al., 2006). Additionally, lymphocytes can become anerg if they recognize presented antigens, but do not receive a proper inflammatory co-stimulus. Anerg lymphocytes remain inactive also if they encounter the particular antigen again at a later time point (Janeway, 2005). A proper antigen presentation by IECs is important to establish oral tolerance towards the plethora of antigens derived from food and gut microbiota that are in constant contact with the intestinal epithelium (Marguerat et al., 1999). A tolerization of $CD4^+$ cells requires MHC class II presentation of innocuous antigens in combination with regulatory or inhibitory secondary signals.

An impaired oral tolerance favors intestinal inflammation and could contribute to the aggravated severity of colitis in *Nlrc5* ko mice after DSS treatment.

A spontaneous onset of a disseminate inflammation can occur if regulatory T cells are reduced or functionally dysregulated. The gastrointestinal tract is usually affected early as it is constantly stimulated by food and microbial antigens (Zenewicz et al., 2009). The population of regulatory T cells was found to be decreased in IBD patients, which favors an aberrant activation of T effector cells (Boden and Snapper, 2008).

Beyond $CD4^+$ regulatory T cells diverse $CD8^+$ regulatory T cell populations exist. They only make up a small portion within the peripheral circulation, but are more frequent among intestinal epithelial lymphocytes (Wang and Alexander, 2009). $CD8^+$ Tregs specifically regulate the effector functions of activated antigen-driven $CD4^+$ T cells either by secreting regulatory cytokines or in a contact-dependent manner by releasing cytotoxic granules (Jiang and Chess, 2000; Wang and Alexander, 2009). Regulatory $CD8^+$ T cells are found in the lamina propria of the healthy intestine. They are absent in IBD patients (Brimnes et al., 2005). It was shown that IECs from IBD patients cannot properly expand $CD8^+$ Tregs *in vitro*. This might play an important role in mucosal tolerance and therefore in the pathogenesis of IBD (Mayer and Eisenhardt, 1990).

In *Nlrc5* ko splenocyte cultures $CD8^+$ T cell populations were significantly diminished, but their numbers were not altered in whole colon tissue (Fig. 3-5, Fig. 3-36). However, $CD8^+$ T regulatory cells in the lamina propria can still be impaired in ko mice as cell populations within the distinct sublayers of the colon tissue were not evaluated. A more detailed analysis of $CD8^+$ T reg cells on isolated lamina propria samples of murine colons could reveal if this population is reduced in *Nlrc5* ko animals. This could contribute to an enhanced susceptibility to develop intestinal inflammations.

Existing $CD8^+$ Tregs might furthermore be impaired in conveying their contact-dependent regulatory functions in *Nlrc5*-deficient mice as the expression of MHC I is severely reduced in these animals. Consequently, overshooting T cell effector functions might not be properly alleviated or inhibited and aberrant effector cells are not deleted. A normal MHC I expression especially on $CD4^+$ T cells can therefore be crucial for a normal $CD8^+$ Treg-mediated peripheral tolerance in the gut. Reduced MHC I expression as well as reduced $CD8^+$ Treg numbers might account for the severe colitis phenotype observed in DSS-treated *Nlrc5* ko mice.

In future studies it will be promising to evaluate if $CD4^+$ and $CD8^+$ regulatory T cell populations are normally developed in *Nlrc5*-deficient mice. Decreased numbers can contribute to an aggravated development of DSS-induced colitis.

4.6.5 *NLRC5* KO MICE ARE SUSCEPTIBLE TO DEVELOP AN AGGRAVATED CHRONIC COLITIS ACCOMPANIED BY HYPOSPLENISM

In this study we observed that distinct cytokines were significantly upregulated in the serum of *Nlrc5*-deficient mice during acute colitis (IL-6, IL-1β, CXCL1), while in wt animals the acute DSS-treatment had no effect on serum cytokines (Fig. 3-22). In addition, the expression of *Mpo*, a cytokine produced by activated neutrophils and Mϕs, was elevated in the spleen of *Nlrc5*-deficient mice (Fig. 3-24). While IL-6 and IL-1β promote the development of a systemic inflammatory response, CXCL1 activates and attracts phagocytes from the blood. The elevated *Mpo* expression in the spleens of ko animals therefore correlates with enhanced CXCL1 serum concentrations.

During the acute DSS colitis wt mice developed splenomegaly, while spleen weight was not altered in *Nlrc5*-deficient animals. Spleen enlargement usually reflects an exaggerated spleen function. It indicates a systemic immune activation with a vivid lymphocyte proliferation in the spleen and the development of adaptive responses (Medscape, 2014). Spleen enlargement in the course of DSS treatment has already been reported and is believed to reflect the establishment of a systemic inflammation (Chassaing et al., 2014). Moreover, altered spleen sizes have repeatedly been observed in IBD patients. Splenomegaly as well as hyposplenism was reported. Splenomegaly effects especially CD patients, while hyposplenism was rather observed in UC (Muller and Toghill, 1995; Pereira et al., 1987; Rozen et al., 1977; Ryan et al., 1978).
Elevated serum cytokine levels and the pronounced splenic MPO expression reflect systemic effects of the DSS-induced intestinal inflammation. These developed earlier in *Nlrc5* ko mice than in wt animals. This early systemic response can indicate that the local response is not efficient enough to cope with the DSS-induced injury or its subsequent effects. Furthermore, regulatory mechanisms might be impaired that can curtail an inflammation to the site of injury. Both would support an aggravated colitis phenotype as observed in ko mice. Although ko mice developed a prominent systemic innate response, they did not show spleen enlargement, which usually indicates the development of a systemic adaptive response. It can be speculated that *Nlrc5* ko mice are impaired in generating proper adaptive responses to fight pathogens that invade via the defective intestinal barrier. An excessive inflammation might be induced to combat an infection by innate mechanisms, which casually leads to the exaggerated tissue damage in ko mice.

During chronic disease, serum cytokine levels were comparable between *Nlrc5*-deficient and wt animals. The splenic *Mpo* expression was equally elevated in wt and ko_{d21} mice and the spleen weight was alike in these two experimental groups. In contrast, in ko_{abort} mice a significantly diminished

induction of *Mpo* was observed in the spleen and the spleen weight was greatly reduced compared to wt or ko_{d21} mice (Fig. 3-34; Fig. 3-35).

A decreased spleen weight can indicate a collapsed spleen function (hyposplenism). The spleen is important for adaptive responses, as effector lymphocytes are generated and proliferate here. It is also the major reservoir for monocytes, which are key players in the innate response. Hyposplenism is a common complication in severely inflamed UC patients, which either suffered persisting active disease or a pronounced relapse. Patients with hyposplenism are more prone to bacterial infections, sepsis and intravascular coagulation due to the reduced spleen functionality, which recovered upon resection of the affected colon parts (Ryan et al., 1978).

Analog it can be speculated here, that the early onset of the strong systemic innate responses in *Nlrc5*-deficient mice during DSS-induced colitis leads to the exhaustion of the spleen function. This might subsequently result in organ resignation and the reduction of spleen weight.

I hypothesize that the impaired spleen function contributes to the severe course of disease as well as the elevated mortality that was observed in ko_{abort} animals (Fig. 3-27, Fig. 3-28) as the impaired immune system is unable to properly cope with the epithelial damage and the arising inflammation within the intestine.

5 CLINICAL RELEVANCE & FUTURE PERSPECTIVES

5.1 NLRC5 IS POTENTLY INVOLVED IN INNATE AND ADAPTIVE DEFENSE AGAINST INTRACELLULAR PATHOGENS

From the initial characterization of *Nlrc5*-deficient mice it is presumed that individuals with functional defects in NLRC5 are more susceptible to infections with intracellular pathogens as their innate (decreased production of IFNs and IL-1β) as well as their adaptive (reduced MHC class I expression and $CD8^+$ population) immune mechanisms are impaired. Accordingly, NLRC5 defects could favor the development of more widespread, longer lasting and recurrent infections. NLRC5 can therefore be assigned a pro-inflammatory role.

In future studies it should be investigated if *Nlrc5*-deficient mice show alterations in immune defense mechanisms or disease susceptibility, when infected with intracellular pathogens (viruses, intracellular bacteria).
It would be of interest if *Nlrc5* ko mice develop normal IFN responses during viral infections or if the induction of IFNs and subsequently ISGs is impaired in those animals. The $CD8^+$ CTL population and its activation status should also be analyzed and it should be investigated if alterations are due to a diminished MHC class I expression. Moreover, it can be evaluated if infected *Nlrc5* ko mice develop a premature and prominent systemic inflammation possibly accompanied by hyposplenism as observed during chronic colitis.
Altogether, these studies can reveal if a loss of *Nlrc5* leads to a more widespread infection with intracellular pathogens, an impaired clearance of infected cells and a pronounced clinical picture.

5.2 NLRC5: A NEW SUSCEPTIBILITY GENE FOR IBD OR INFLAMMATORY DISEASES?

In addition to its pro-inflammatory role, NLRC5 might exert important regulatory functions. The data presented here reveal that functional NLRC5 protects from a fulminate course of colitis. This could also implicate a role of NLRC5 in the pathogenesis of IBD in humans.
Several NLR family members have been associated with intestinal inflammation. While mutations in NOD2 are known to favor the onset of CD in humans (Hampe et al., 2001; Hugot et al., 2001; Ogura et al., 2001), other NLRs were shown to be protective in murine colitis models e.g. NOD1 (Chen et al., 2008), NLRP1 (Williams et al., 2015), NLRP3 (Allen et al., 2010; Villani et al., 2009; Zaki et al., 2010), NLRC4 (Carvalho et al., 2012), NLRP6 (Elinav et al., 2011) and NLRP12 (Zaki et al., 2011).
Although *Nlrc5* deficiency worsened the intestinal inflammation in the DSS-induced murine model, genome-wide association studies did not reveal any IBD-associated *NLRC5* variants so far (Jostins et al., 2012).

NLRC5 initiates the transcription of MHC class I-coding *HLA* genes. Studying *Nlrc5* ko mice underlined the importance of proper MHC class I expression for intestinal homeostasis.
Here we hypothesize that a decreased MHC class I expression and a diminished $CD8^+$ Treg cell population in individuals bearing functionally defective *NLRC5* variants might lead to an impaired intestinal tolerance. It was reported that regulatory $CD8^+$ T cells are diminished in the lamina propria of IBD patients (Brimnes et al., 2005). Therefore, analyzing the role of MHC class I and its

transcriptional regulator NLRC5 for intestinal tolerance might advance the understanding of IBD pathogenesis.
An inefficient tolerance towards gut antigens favors an aberrant activation of T effector cells, which can lead to a recurring or chronic intestinal inflammation as triggering antigens derived from food or microbiota persist within the bowel. More dedicated studies are needed to clarify the involvement of NLRC5 in gut tolerance. It should be investigated if *Nlrc5* ko mice have an altered $CD8^+$ and $CD4^+$ regulatory cell population under baseline conditions, but also during DSS-induced colitis. Furthermore, the activation of these regulatory cells should be assed, e.g. by analyzing the secretion of regulatory or inhibitory mediators as TGF-β or IL-10.
In addition, it should be analyzed if *Nlrc5*-deficient mice have an impaired expression of MHC II molecules on IECs and if this correlates with an impaired IFNγ production. An impaired MHC II expression could further impair the establishment of intestinal tolerance mediated by $CD4^+$ T cells.

If it shows that NLRC5 is involved in immunological tolerance in the gut the protein could also have a functional relevance on other surfaces of the body (e.g. within the lung). Accordingly, functional *NLRC5* defects might favor the onset of various inflammatory disorders.

5.3 NLRC5 MIGHT BE A PROMISING TARGET TO ENHANCE TUMOR IMMUNITY

The presentation of endogenous antigens on MHC class I molecules in malignant cells and their subsequent lysis by CTLs underline the importance of NLRC5 regarding tumor immunity. Longitudinal studies on aging animals should be performed to evaluate if *Nlrc5* ko mice are more prone to develop tumors due to their impaired MHC class I expression as a down regulation of MHC class I surface expression is a common mechanism of tumors to hide and escape the body's immune surveillance (Bubeník, 2003). Understanding the mechanisms of MHC I expression and its induction by NLRC5 and other mechanisms (e.g. CIITA) can be of use for cancer research as a targeted MHC upregulation on malignant cells presumably enhances endogenous tumor immunity.

5.4 FUNCTIONAL NLRC5 DEFECTS MIGHT INDUCE A CLINICAL PICTURE COMPARABLE TO BLS I

This study revealed that a loss of *Nlrc5* is associated with a more severe intestinal inflammation in a murine DSS-induced colitis model. It can be presumed that a functional NLRC5 defect in humans might cause a more complex clinical picture that involves not only inadequate inflammation (due to missing tolerance), but also widespread infections (due to ineffective innate and adaptive defenses towards intracellular pathogens) as well as susceptibility to malignant transformations (due to an impaired expression of abnormal cellular antigens).

An impaired expression of MHC molecules in humans is known to cause severe combined immune deficiencies (SCID) that have various clinical signs. SCIDs in general are characterized by an impaired generation or activation of functional T or B lymphocytes due to various genetic mutations.
A deficient MHC class I expression as seen in *Nlrc5*-deficient mice is designated Bare Lymphocyte Syndrome I (BLS I). The reduced MHC class I expression is usually caused by a defective TAP complex, but NLRC5 defects could have a similar clinical manifestation. Patients suffer from chronic or recurring inflammation in different compartments e.g. respiratory and gastrointestinal tract as well as the skin (Gadola et al., 2000). Interestingly, no BLS I phenotype has been shown so far to be caused by mutations in the *NLRC5* gene, which might be due to a compensatory albeit reduced MHC class I

induction by NLRC5-independent mechanisms (e.g. CIITA). Accordingly, patients with defects in the *NLRC5* gene might only develop an alleviated BLS I phenotype.
MHC class II deficiency, which is referred to as BLS II is the more common SCID among the two MHC deficiencies. It is caused by mutations in genes involved in MHC II transcription e.g. CIITA, which lead to an impaired or abrogated MHC class II surface expression. As for BLS I, patients suffer from repeated severe infections e.g. within the gastro intestine, the respiratory tract and the skin.

5.5 Future perspectives & Concluding remarks

NLRC5 is an important molecular switch to influence diverse clinical conditions due to its co-transcriptional activation of MHC class I coding *HLA* genes. More detailed studies are needed to elucidate the role of NLRC5 (and thereby the importance of MHC class I molecules) in viral and bacterial infections, the establishment of immunological tolerance and inflammatory disorders as well as the development of cancer.
Further research might unravel how NLRC5 impacts the production of IL-1β. NLRC5 was shown to be involved in IL-1β maturation. Although it was postulated that it might be associated with the NLRP3 inflammasome (Davis et al., 2010; Yao et al., 2012) there is still no model available that sufficiently describes interaction partners, activating ligands or regulatory mechanism. Our data rather imply an impact on the NF-κB-mediated induction of the IL-1β propeptide, but the mechanism needs to be elucidated.
The impact of NLRC5 on the production of IFNs was not unraveled so far. The NLR member might have an important innate immune function in initiating antiviral responses as our data indicate that NLRC5 is involved in the induction of IFNs. Diminished IFNγ levels in the gut can impair local tolerance. IFNγ is necessary for the activation of mesenchymal stromal cells to exert their immunosuppressive functions. The cytokine further induces MHC class II molecules, which are needed to activate $CD4^+$ T cells and prime regulatory lymphocytes. IFNɣ also inhibits the expression of IL-23, a cytokine implicated in the development of inflammatory disorders (Sheikh et al., 2010). It should be evaluated if the induction of IL-23 is altered in *Nlrc5* ko mice and if this correlates with a decrease in IFNɣ. In future experiments it can be analyzed if the reconstitution of a normal IFNγ-level in *Nlrc5*-deficient mice attenuates the DSS-induced colitis and how it impacts IL-23 and the MHC II expression in the intestine.

The presented results support a pro-inflammatory as well as a regulatory role for NLRC5 depending on the depicted mechanism the protein is involved. Furthermore, this study reveals the significance of a proper *Nlrc5*-mediated MHC class I expression to prevent severe intestinal inflammation.
If we understand how NLRC5 is regulated this might be a powerful target to manipulate the expression of MHC class I molecules and thereby gain treatment options for distinct medical conditions. A selective upregulation of MHC class I can favor the clearance of infectious diseases and enhance endogenous tumor immunity, while a down regulation could be beneficial during chronic inflammation as well as for organ transplantations. NLRC5 could be the gateway.

Before, CIITA was the only known NLR member with implications in adaptive immune regulations. With the identification of NLRC5 as the major co-transcriptional activator for MHC class I-coding *HLA* genes and its subsequent importance for adaptive immune responses, the significance of the NLR family beyond innate pathogen recognition becomes even more obvious.

6 SUMMARY

The complex mammalian immune system comprises diverse synergizing mechanisms to protect organisms from constant potentially deleterious environmental effects, but also to establish tolerance towards innocuous influences. To understand disease pathogenesis and develop treatment strategies it is inevitable to elucidate and investigate the plethora of immune mechanisms.

Here, the NOD-like receptor (NLR) NLRC5 was studied. NLRs are predominantly understood as cytoplasmic pathogen recognition receptors (PRRs), which initiate innate responses towards foreign pathogen-associated or endogenous danger-associated molecular patterns. No ligand is known for NLRC5 so far, but the protein is assumed to possess immune function. NLRC5 was initially reported to influence the expression of IFNs and NF-κB target genes as well as the production of IL-1β. However, its impact is controversially discussed. NLRC5 was identified to share several similarities with CIITA, an NLR member that functions as the major co-transcriptional activator for MHC class II-encoding *HLA* genes and is therefore essential for adaptive immune processes. In analogy, NLRC5 was reported to initiate the transcription of MHC class I-encoding *HLA* genes.

This study aimed to define the contribution of NLRC5 to innate signaling pathways as well as to adaptive immune mechanisms. Therefore, *Nlrc5*-deficient (ko) mice were generated. They were viable and fertile and had no obvious immune defects under specific pathogen-free housing conditions.

NLRC5 was predominantly expressed in immune tissues and potently induced by IFNγ. In accordance with its role as transcriptional regulator, *Nlrc5* ko mice had a severely decreased MHC class I surface expression. However, a residual, cell type-dependent MHC class I expression remained. Furthermore, MHC class I was still inducible in *Nlrc5*-deficient cells. This points to the existence of other MHC I regulating mechanisms. It is assumed that one of these mechanisms is the transcriptional activation of MHC class I-coding genes by CIITA.

The decreased MHC class I levels led to an impaired generation of $CD8^+$ T lymphocytes in *Nlrc5*-deficient mice. In contrast, the MHC class II^+ cell population was increased, but did not affect the number of $CD4^+$ T lymphocytes. Next to these adaptive immune functions, NLRC5 was involved in innate immune signaling pathways. The protein was crucial for a proper induction of type I and II IFNs as well as IL-1β.

The diminished $CD8^+$ T cell population as well as the impaired production of IFNγ and IL-1β found during the characterization was presumed to render *Nlrc5* ko mice less susceptible to an intestinal inflammation. In contrast this work revealed that ko mice develop an aggravated DSS-induced colitis. The pronounced phenotype correlated with an enhanced epithelial destruction and an upregulated production of inflammatory cytokines. However, there was no increased influx of inflammatory cells into the colon.

Various mechanisms are discussed here that try to unravel the unexpected severity of DSS-colitis in *Nlrc5*-deficient mice. The severe epithelial damage in the intestine of ko animals is assumed to be due to an aberrant activation of local effector T lymphocytes. The diminished expression of MHC I molecules and an impaired $CD8^+$ Treg population as well as decreased IFNγ level might hinder the establishment of proper intestinal tolerance and thereby favors an aberrant activation of mucosal lymphocytes and subsequently intestinal inflammation.

Taken together, NLRC5 was found to be involved in pro-inflammatory innate signaling pathways and to have inflammatory as well as regulatory functions during adaptive immune processes.

This study for the first time indicates a protective effect of NLRC5 during intestinal inflammation and discusses a role for this NLR member in the establishment of intestinal tolerance. Up to now investigations on an aberrant activation of intestinal effector lymphocytes during colitis concentrated

on the impact of $CD4^+$ regulatory T cells, while here an important role of regulatory $CD8^+$ T cells is presumed.
Based on the here presented data, functional defects in NLRC5 are presumed to account for a decreased clearance of infected and malignant cells and to impair the establishment of immunological tolerance. Accordingly, mutations in *NLRC5* might favor severe infectious and inflammatory diseases as well as cancer.

Future experiments are needed to further investigate the role of NLRC5 for peripheral tolerance as well as for the course of infectious diseases and tumor development. Manipulating MHC class I surface expression e.g. via its transcriptional regulator NLRC5 could be a powerful therapeutical tool for diverse medical conditions as infections, chronic inflammations, tumors or even for transplantational medicine.

7 ZUSAMMENFASSUNG

Das komplexe Immunsystem der Säugetiere umfasst diverse synergistische Mechanismen um den Organismus vor der konstanten Bedrohung durch potentiell schädliche Umwelteinflüsse zu schützen, aber auch um eine Toleranz gegenüber harmlosen Einflüssen zu etablieren. Um die Ursache von Krankheiten zu verstehen und neue Behandlungsstrategien entwickeln zu können, ist es unumgänglich diese Vielfalt an Immunmechanismen aufzudecken und zu erforschen.

In dieser Arbeit wurde NLRC5, ein Mitglied aus der Familie der NOD-ähnlichen Rezeptoren, untersucht. NLRs werden überwiegend als zytoplasmatische Pathogen-erkennende Rezeptoren (PRRs) eingeordnet, die eine angeborene Immunantwort gegen Pathogen-assoziierte fremde oder Gefahren-assoziierte endogene molekulare Strukturen initiieren. Ein Ligand für NLRC5 wurde bisher noch nicht identifiziert, trotzdem wird von einer immunologischen Funktion des Proteins ausgegangen. Anfänglich wurde ein Einfluss von NLRC5 auf die Expression von Interferonen und NF-κB Zielgenen sowie auf die Produktion von IL-1β berichtet. Dieser Einfluss wird jedoch kontrovers diskutiert. Außerdem konnte gezeigt werden, dass NLRC5 diverse Gemeinsamkeiten mit dem NLR Protein CIITA hat. CIITA ist der Ko-Transaktivator für die Transkription MHC II-kodierender *HLA* Gene und somit essenziel für adaptive Immunprozesse. Analog dazu wurde für NLRC5 beschrieben, dass es die Transkription von MHC I kodierenden *HLA* Genes initiiert.

Diese Studie sollte untersuchen inwieweit NLRC5 zu angeborenen oder erworbenen Immunprozessen beiträgt. Dazu wurden *Nlrc5*-defiziente (Ko) Mäuse generiert. Diese waren lebensfähig und fertil unter spezifisch-pathogenfreien Lebensbedingungen. Sie wiesen keine erkennbaren Immundefekte auf.

NLRC5 wurde vor allem in Immungeweben exprimiert und durch IFNɣ induziert. In Übereinstimmung mit seiner Rolle als transkriptioneller Regulator war die Oberflächenexpression von MHC I in *Nlrc5* Ko Mäusen stark vermindert. Trotzdem bestand eine verbleibende MHC I Expression, die abhängig vom untersuchten Zelltyp war. Darüber hinaus war MHC I weiterhin induzierbar. Dies deuted auf die Existenz weiterer MHC I-regulierender Mechanismen. Es wird angenommen, dass einer dieser Mechanismen die transkriptionelle Aktivierung von MHC I-kodierenden Genen durch CIITA ist.

Die stark reduzierten MHC I Spiegel in *Nlrc5*-defizienten Mäusen beeinträchtigten die Generation von $CD8^+$ T Lymphozyten. Die MHC II^+ Zellpopulation war hingegen vergrößert, was sich jedoch nicht auf die Anzahl $CD4^+$ T Lymphozyten auswirkte. Neben diesen Einflüssen auf das adaptive Immunsystem wirkte sich NLRC5 auch auf die Signalwege der angeborenen Immunität aus. Das Protein war entscheidend an der Induktion von Typ I und II Interferonen sowie der Produktion von IL-1β beteiligt.

Aufgrund der verminderten Anzahl $CD8^+$ T Lymphozyten und der beeinträchtigten Produktion von IFNɣ und IL-1β wurde hier ursprünglich angenommen, dass *Nlrc5* Ko Mäuse weniger empfänglich für die Induktion einer intestinalen Entzündung sind. Im Gegensatz dazu konnte in dieser Arbeit in DSS-induzierten Kolitismodellen gezeigt werden, dass *Nlrc5*-defiziente Mäuse ein verstärktes Krankheitsbild entwickeln. Der ausgeprägtere Phänotyp korrelierte mit einer gesteigerten epithelialen Destruktion und der erhöhten Produktion inflammatorischer Zytokine. Es kam hingegen nicht zu einem vermehrten Influx von Entzündungszellen in das Kolon.

Verschiedene Mechanismen werden hier diskutiert, die versuchen den unerwarteten Schweregrad der DSS-induzierten Kolitis in *Nlrc5*-defizienten Mäusen zu erklären. Es wird angenommen, dass der verstärkte intestinale Epithelschaden *Nlrc5*-defizienter Mäuse durch eine anormale Aktivierung lokaler T Lymphozyten ausgelöst wird. Die reduzierte Expression von MHC I-Molekülen und eine verringerte $CD8^+$ regulatorische T Zellpopulation als auch verminderten IFNγ Spiegel können die Ausbildung

einer angemessenen intestinalen Toleranz beeinträchtigen. Dies begünstigt eine anormale Aktivierung mukosaler Lymphozyten und führt zur Ausbildung einer intestinalen Entzündung.
Zusammenfassend konnte in dieser Arbeit gezeigt werden, dass NLRC5 an pro-inflammatorischen Signalwege der angeborenen Immunität beteiligt ist und sowohl inflammatorische als auch regulatorische Funktionen in adaptiven Immunprozessen hat. Diese Studie deutet zum ersten Mal auf einen protektiven Effekt von NLRC5 bei entzündlichen Darmerkrankungen hin und impliziert eine Rolle bei der Ausbildung der intestinalen Toleranz. Untersuchungen zur anormalen Aktivierung reifer intestinaler Lymphozyten während einer Kolitis konzentrierten sich bisher auf den Einfluss $CD4^+$ regulatorischer T Zellen. Hier wird hingegen eine wichtige Rolle für die $CD8^+$ regulatorische T Zellpopulation impliziert.
Basierend auf den hier gezeigten Daten wird angenommen, dass funktionelle Defekte in NLRC5 zu einer verminderten Beseitigung infizierter und maligner Zellen führen, sowie die Ausbildung der immunologischen Toleranz beeinträchtigen. Dementsprechend könnten Mutationen im *NLRC5* Gen schwere Infektions- und Entzündungskrankheiten sowie die Entstehung von Tumoren begünstigen.

Es bedarf zukünftiger Experimente um die Rolle von NLRC5 in der peripheren Toleranz als auch im Verlauf von Infektionskrankheiten und in der Tumorentstehung zu untersuchen. Eine gezielte Einflussnahme auf die MHC I Expression an der Zelloberfläche z.B. über den transkriptionellen Regulator NLRC5, wäre ein wirksames therapeutisches Werkzeug für diverse medizinische Indikationen wie beispielsweise Infektionen, chronische Entzündungen, Tumore oder auch in der Transplantationsmedizin.

8 APPENDIX

8.1 BIBLIOGRAPHY

Allen, I.C., TeKippe, E.M., Woodford, R.-M.T., Uronis, J.M., Holl, E.K., Rogers, A.B., Herfarth, H.H., Jobin, C., and Ting, J.P.-Y. (2010). The NLRP3 inflammasome functions as a negative regulator of tumorigenesis during colitis-associated cancer. J. Exp. Med. *207*, 1045–1056.

Arai, Y., Takanashi, H., Kitagawa, H., and Okayasu, I. (1998). Involvement of interleukin-1 in the development of ulcerative colitis induced by dextran sulfate sodium in mice. Cytokine *10*, 890–896.

Aravind, L., Dixit, V.M., and Koonin, E.V. (2001). Apoptotic molecular machinery: vastly increased complexity in vertebrates revealed by genome comparisons. Science *291*, 1279–1284.

Bär, F., Sina, C., Hundorfean, G., Pagel, R., Lehnert, H., Fellermann, K., and Büning, J. (2013). Inflammatory bowel diseases influence major histocompatibility complex class I (MHC I) and II compartments in intestinal epithelial cells. Clin Exp Immunol *172*, 280–289.

Barnich, N., Aguirre, J.E., Reinecker, H.-C., Xavier, R., and Podolsky, D.K. (2005). Membrane recruitment of NOD2 in intestinal epithelial cells is essential for nuclear factor-{kappa}B activation in muramyl dipeptide recognition. J. Cell Biol. *170*, 21–26.

Benko, S., Magalhaes, J.G., Philpott, D.J., and Girardin, S.E. (2010). NLRC5 limits the activation of inflammatory pathways. J. Immunol *185*, 1681–1691.

Berg, D.F., Bahadursingh, A.M., Kaminski, D.L., and Longo, W.E. (2002). Acute surgical emergencies in inflammatory bowel disease. Am. J. Surg. *184*, 45–51.

Bisping, G., Lügering, N., Lütke-Brintrup, S., Pauels, H.-G., Schürmann, G., Domschke, W., and Kucharzik, T. (2001). Patients with inflammatory bowel disease (IBD) reveal increased induction capacity of intracellular interferon-gamma (IFN-γ) in peripheral CD8+ lymphocytes co-cultured with intestinal epithelial cells. Clinical & Experimental Immunology *123*, 15–22.

Biswas, A., Meissner, T.B., Kawai, T., and Kobayashi, K.S. (2012). Cutting Edge: Impaired MHC Class I Expression in Mice Deficient for Nlrc5/Class I Transactivator. J Immunol *189*, 516–520.

Bland, P. (1988). MHC class II expression by the gut epithelium. Immunol. Today *9*, 174–178.

Boden, E.K., and Snapper, S.B. (2008). Regulatory T cells in inflammatory bowel disease. Curr. Opin. Gastroenterol. *24*, 733–741.

Le Bon, A., and Tough, D.F. (2002). Links between innate and adaptive immunity via type I interferon. Curr. Opin. Immunol. *14*, 432–436.

Braegger, C.P., Nicholls, S., Murch, S.H., Stephens, S., and MacDonald, T.T. (1992). Tumour necrosis factor alpha in stool as a marker of intestinal inflammation. Lancet *339*, 89–91.

Breese, E.J., Michie, C.A., Nicholls, S.W., Murch, S.H., Williams, C.B., Domizio, P., Walker-Smith, J.A., and MacDonald, T.T. (1994). Tumor necrosis factor alpha-producing cells in the intestinal mucosa of children with inflammatory bowel disease. Gastroenterology *106*, 1455–1466.

Brimnes, J., Allez, M., Dotan, I., Shao, L., Nakazawa, A., and Mayer, L. (2005). Defects in CD8+ Regulatory T Cells in the Lamina Propria of Patients with Inflammatory Bowel Disease. J Immunol *174*, 5814–5822.

Bubeník, J. (2003). Tumour MHC class I downregulation and immunotherapy (Review). Oncol. Rep. *10*, 2005–2008.

Bylund-Fellenius, A.C., Landström, E., Axelsson, L.G., and Midtvedt, T. (1994). Experimental Colitis Induced by Dextran Sulphate in Normal and Germfree Mice. Microb Ecol Health Dis *7*, 207–215.

Carvalho, F.A., Nalbantoglu, I., Aitken, J.D., Uchiyama, R., Su, Y., Doho, G.H., Vijay-Kumar, M., and Gewirtz, A.T. (2012). Cytosolic flagellin receptor NLRC4 protects mice against mucosal and systemic challenges. Mucosal Immunol *5*, 288–298.

Chamaillard, M., Hashimoto, M., Horie, Y., Masumoto, J., Qiu, S., Saab, L., Ogura, Y., Kawasaki, A., Fukase, K., Kusumoto, S., et al. (2003a). An essential role for NOD1 in host recognition of bacterial peptidoglycan containing diaminopimelic acid. Nat. Immunol. *4*, 702–707.

Chamaillard, M., Philpott, D., Girardin, S.E., Zouali, H., Lesage, S., Chareyre, F., Bui, T.H., Giovannini, M., Zaehringer, U., Penard-Lacronique, V., et al. (2003b). Gene-environment interaction modulated by allelic heterogeneity in inflammatory diseases. Proc. Natl. Acad. Sci. U.S.A. *100*, 3455–3460.

Chassaing, B., Aitken, J.D., Malleshappa, M., and Vijay-Kumar, M. (2014). Dextran Sulfate Sodium (DSS)-Induced Colitis in Mice. Curr Protoc Immunol *104*, Unit – 15.25.

Chen, G.Y., Shaw, M.H., Redondo, G., and Núñez, G. (2008). The innate immune receptor Nod1 protects the intestine from inflammation-induced tumorigenesis. Cancer Res. *68*, 10060–10067.

Coccia, M., Harrison, O.J., Schiering, C., Asquith, M.J., Becher, B., Powrie, F., and Maloy, K.J. (2012). IL-1β mediates chronic intestinal inflammation by promoting the accumulation of IL-17A secreting innate lymphoid cells and CD4+ Th17 cells. J Exp Med *209*, 1595–1609.

Cui, J., Zhu, L., Xia, X., Wang, H.Y., Legras, X., Hong, J., Ji, J., Shen, P., Zheng, S., Chen, Z.J., et al. (2010). NLRC5 Negatively Regulates the NF-[kappa]B and Type I Interferon Signaling Pathways. Cell *141*, 483–496.

Danese, S., and Fiocchi, C. (2011). Ulcerative colitis. N. Engl. J. Med. *365*, 1713–1725.

Davis, B.K., Roberts, R.A., Huang, M.T., Willingham, S.B., Conti, B.J., Brickey, W.J., Barker, B.R., Kwan, M., Taxman, D.J., Accavitti-Loper, M.-A., et al. (2010). Cutting Edge: NLRC5-Dependent Activation of the Inflammasome. J Immunol.

Dieleman, L.A., Ridwan, B.U., Tennyson, G.S., Beagley, K.W., Bucy, R.P., and Elson, C.O. (1994). Dextran sulfate sodium-induced colitis occurs in severe combined immunodeficient mice. Gastroenterology *107*, 1643–1652.

Dostert, C., Pétrilli, V., Van Bruggen, R., Steele, C., Mossman, B.T., and Tschopp, J. (2008). Innate immune activation through Nalp3 inflammasome sensing of asbestos and silica. Science *320*, 674–677.

Dotan, I., Allez, M., Nakazawa, A., Brimnes, J., Schulder-Katz, M., and Mayer, L. (2007). Intestinal epithelial cells from inflammatory bowel disease patients preferentially stimulate CD4+ T cells to proliferate and secrete interferon-γ. American Journal of Physiology - Gastrointestinal and Liver Physiology *292*, G1630–G1640.

Elinav, E., Strowig, T., Kau, A.L., Henao-Mejia, J., Thaiss, C.A., Booth, C.J., Peaper, D.R., Bertin, J., Eisenbarth, S.C., Gordon, J.I., et al. (2011). NLRP6 inflammasome regulates colonic microbial ecology and risk for colitis. Cell *145*, 745–757.

Engelhardt, K.R., and Grimbacher, B. (2014). IL-10 in humans: lessons from the gut, IL-10/IL-10 receptor deficiencies, and IL-10 polymorphisms. Curr. Top. Microbiol. Immunol. *380*, 1–18.

Fais, S., Pallone, F., Squarcia, O., Biancone, L., Ricci, F., Paoluzi, P., and Boirivant, M. (1987). HLA-DR antigens on colonic epithelial cells in inflammatory bowel disease: I. Relation to the state of activation of lamina propria lymphocytes and to the epithelial expression of other surface markers. Clin Exp Immunol *68*, 605–612.

Fais, S., Capobianchi, M.R., Pallone, F., Di Marco, P., Boirivant, M., Dianzani, F., and Torsoli, A. (1991). Spontaneous release of interferon gamma by intestinal lamina propria lymphocytes in Crohn's disease. Kinetics of in vitro response to interferon gamma inducers. Gut *32*, 403–407.

Fais, S., Capobianchi, M.R., Silvestri, M., Mercuri, F., Pallone, F., and Dianzani, F. (1994). Interferon expression in Crohn's disease patients: increased interferon-gamma and -alpha mRNA in the intestinal lamina propria mononuclear cells. J. Interferon Res. *14*, 235–238.

Forcione, D.G., Sands, B., Isselbacher, K.J., Rustgi, A., Podolsky, D.K., and Pillai, S. (1996). An increased risk of Crohn's disease in individuals who inherit the HLA class II DRB3*0301 allele. PNAS *93*, 5094–5098.

Fournier, B.M., and Parkos, C.A. (2012). The role of neutrophils during intestinal inflammation. Mucosal Immunol *5*, 354–366.

Frank, D.N., St Amand, A.L., Feldman, R.A., Boedeker, E.C., Harpaz, N., and Pace, N.R. (2007). Molecular-phylogenetic characterization of microbial community imbalances in human inflammatory bowel diseases. Proc. Natl. Acad. Sci. U.S.A. *104*, 13780–13785.

Fuss, I.J., Neurath, M., Boirivant, M., Klein, J.S., de la Motte, C., Strong, S.A., Fiocchi, C., and Strober, W. (1996). Disparate CD4+ lamina propria (LP) lymphokine secretion profiles in inflammatory bowel disease. Crohn's disease LP cells manifest increased secretion of IFN-gamma, whereas ulcerative colitis LP cells manifest increased secretion of IL-5. J. Immunol. *157*, 1261–1270.

Gadola, S.D., Moins-Teisserenc, H.T., Trowsdale, J., Gross, W.L., and Cerundolo, V. (2000). TAP deficiency syndrome. Clin Exp Immunol *121*, 173–178.

Garbi, N., Tan, P., Diehl, A.D., Chambers, B.J., Ljunggren, H.-G., Momburg, F., and Hämmerling, G.J. (2000). Impaired immune responses and altered peptide repertoire in tapasin-deficient mice. Nat Immunol *1*, 234–238.

Garrett, W.S., Lord, G.M., Punit, S., Lugo-Villarino, G., Mazmanian, S.K., Ito, S., Glickman, J.N., and Glimcher, L.H. (2007). Communicable ulcerative colitis induced by T-bet deficiency in the innate immune system. Cell *131*, 33–45.

Geppert, T.D., and Lipsky, P.E. (1985). Antigen presentation by interferon-gamma-treated endothelial cells and fibroblasts: differential ability to function as antigen-presenting cells despite comparable Ia expression. J. Immunol. *135*, 3750–3762.

Gersemann, M., Becker, S., Kübler, I., Koslowski, M., Wang, G., Herrlinger, K.R., Griger, J., Fritz, P., Fellermann, K., Schwab, M., et al. (2009). Differences in goblet cell differentiation between Crohn's disease and ulcerative colitis. Differentiation *77*, 84–94.

Ghosh, S., Chaudhary, R., Carpani, M., and Playford, R. (2006). Interfering with interferons in inflammatory bowel disease. Gut *55*, 1071–1073.

Girardin, S.E., Tournebize, R., Mavris, M., Page, A.L., Li, X., Stark, G.R., Bertin, J., DiStefano, P.S., Yaniv, M., Sansonetti, P.J., et al. (2001). CARD4/Nod1 mediates NF-kappaB and JNK activation by invasive Shigella flexneri. EMBO Rep. *2*, 736–742.

Girardin, S.E., Boneca, I.G., Viala, J., Chamaillard, M., Labigne, A., Thomas, G., Philpott, D.J., and Sansonetti, P.J. (2003). Nod2 is a general sensor of peptidoglycan through muramyl dipeptide (MDP) detection. J. Biol. Chem. *278*, 8869–8872.

Girdlestone, J. (1996). Transcriptional regulation of MHC class I genes. Eur. J. Immunogenet. *23*, 395–413.

Glimcher, L.H., and Kara, C.J. (1992). Sequences and Factors: A Guide to MHC Class-II Transcription. Annual Review of Immunology *10*, 13–49.

Gobin, S.J., Peijnenburg, A., Keijsers, V., and van den Elsen, P.J. (1997). Site alpha is crucial for two routes of IFN gamma-induced MHC class I transactivation: the ISRE-mediated route and a novel pathway involving CIITA. Immunity *6*, 601–611.

Gobin, S.J., Keijsers, V., van Zutphen, M., and van den Elsen, P.J. (1998a). The role of enhancer A in the locus-specific transactivation of classical and nonclassical HLA class I genes by nuclear factor kappa B. J. Immunol. *161*, 2276–2283.

Gobin, S.J., Peijnenburg, A., van Eggermond, M., van Zutphen, M., van den Berg, R., and van den Elsen, P.J. (1998b). The RFX complex is crucial for the constitutive and CIITA-mediated transactivation of MHC class I and beta2-microglobulin genes. Immunity *9*, 531–541.

Gobin, S.J., van Zutphen, M., Woltman, A.M., and van den Elsen, P.J. (1999). Transactivation of classical and nonclassical HLA class I genes through the IFN-stimulated response element. J. Immunol. *163*, 1428–1434.

Gobin, S.J., van Zutphen, M., Westerheide, S.D., Boss, J.M., and van den Elsen, P.J. (2001). The MHC-specific enhanceosome and its role in MHC class I and beta(2)-microglobulin gene transactivation. J. Immunol. *167*, 5175–5184.

Greegor, D.H. (1971). Occult blood testing for detection of asymptomatic colon cancer. Cancer *28*, 131–134.

Hall, L.J., Faivre, E., Quinlan, A., Shanahan, F., Nally, K., and Melgar, S. (2011). Induction and activation of adaptive immune populations during acute and chronic phases of a murine model of experimental colitis. Dig. Dis. Sci. *56*, 79–89.

Hampe, J., Cuthbert, A., Croucher, P.J., Mirza, M.M., Mascheretti, S., Fisher, S., Frenzel, H., King, K., Hasselmeyer, A., MacPherson, A.J., et al. (2001). Association between insertion mutation in NOD2 gene and Crohn's disease in German and British populations. Lancet *357*, 1925–1928.

Hampe, J., Franke, A., Rosenstiel, P., Till, A., Teuber, M., Huse, K., Albrecht, M., Mayr, G., De La Vega, F.M., Briggs, J., et al. (2007). A genome-wide association scan of nonsynonymous SNPs identifies a susceptibility variant for Crohn disease in ATG16L1. Nat. Genet. *39*, 207–211.

Hans, W., Schölmerich, J., Gross, V., and Falk, W. (2000a). The role of the resident intestinal flora in acute and chronic dextran sulfate sodium-induced colitis in mice. Eur J Gastroenterol Hepatol *12*, 267–273.

Hans, W., Schölmerich, J., Gross, V., and Falk, W. (2000b). Interleukin-12 induced interferon-g increases inflammation in acute dextran sulfate sodium induced colitis in mice. European Cytokine Network *11*, 67–74.

Hartman, I.Z., Kim, A., Cotter, R.J., Walter, K., Dalai, S.K., Boronina, T., Griffith, W., Lanar, D.E., Schwenk, R., Krzych, U., et al. (2010). A reductionist cell-free major histocompatibility complex class II antigen processing system identifies immunodominant epitopes. Nat. Med. *16*, 1333–1340.

Harton, J.A., Cressman, D.E., Chin, K.-C., Der, C.J., and Ting, J.P.-Y. (1999). GTP Binding by Class II Transactivator: Role in Nuclear Import. Science *285*, 1402–1405.

Hershberg, R.M., and Mayer, L.F. (2000). Antigen processing and presentation by intestinal epithelial cells – polarity and complexity. Immunology Today *21*, 123–128.

Herzer, K., Falk, C.S., Encke, J., Eichhorst, S.T., Ulsenheimer, A., Seliger, B., and Krammer, P.H. (2003). Upregulation of Major Histocompatibility Complex Class I on Liver Cells by Hepatitis C Virus Core Protein via p53 and TAP1 Impairs Natural Killer Cell Cytotoxicity. J. Virol. *77*, 8299–8309.

Hogan, P.G., Chen, L., Nardone, J., and Rao, A. (2003). Transcriptional regulation by calcium, calcineurin, and NFAT. Genes Dev. *17*, 2205–2232.

Hommes, D.W., Mikhajlova, T.L., Stoinov, S., Štimac, D., Vucelic, B., Lonovics, J., Zákuciová, M., D'Haens, G., Van Assche, G., Ba, S., et al. (2006). Fontolizumab, a humanised anti-interferon γ antibody, demonstrates safety and clinical activity in patients with moderate to severe Crohn's disease. Gut *55*, 1131–1137.

Hugot, J.P., Chamaillard, M., Zouali, H., Lesage, S., Cézard, J.P., Belaiche, J., Almer, S., Tysk, C., O'Morain, C.A., Gassull, M., et al. (2001). Association of NOD2 leucine-rich repeat variants with susceptibility to Crohn's disease. Nature *411*, 599–603.

Human Protein Atlas (2015). Tissue expression of HLA-B - Summary - The Human Protein Atlas.

Ikeda, H., Old, L.J., and Schreiber, R.D. (2002). The roles of IFN gamma in protection against tumor development and cancer immunoediting. Cytokine Growth Factor Rev. *13*, 95–109.

Inohara, N., Koseki, T., Lin, J., del Peso, L., Lucas, P.C., Chen, F.F., Ogura, Y., and Núñez, G. (2000). An induced proximity model for NF-kappa B activation in the Nod1/RICK and RIP signaling pathways. J. Biol. Chem. *275*, 27823–27831.

Inohara, N., Ogura, Y., Fontalba, A., Gutierrez, O., Pons, F., Crespo, J., Fukase, K., Inamura, S., Kusumoto, S., Hashimoto, M., et al. (2003). Host recognition of bacterial muramyl dipeptide mediated through NOD2. Implications for Crohn's disease. J. Biol. Chem. *278*, 5509–5512.

Ito, R., Shin-Ya, M., Kishida, T., Urano, A., Takada, R., Sakagami, J., Imanishi, J., Kita, M., Ueda, Y., Iwakura, Y., et al. (2006). Interferon-gamma is causatively involved in experimental inflammatory bowel disease in mice. Clin Exp Immunol *146*, 330–338.

Itoh-Lindstrom, Y., Piskurich, J.F., Felix, N.J., Wang, Y., Brickey, W.J., Platt, J.L., Koller, B.H., and Ting, J.P. (1999). Reduced IL-4-, lipopolysaccharide-, and IFN-gamma-induced MHC class II expression in mice lacking class II transactivator due to targeted deletion of the GTP-binding domain. J. Immunol. *163*, 2425–2431.

Itzkowitz, S.H., Present, D.H., and Crohn's and Colitis Foundation of America Colon Cancer in IBD Study Group (2005). Consensus conference: Colorectal cancer screening and surveillance in inflammatory bowel disease. Inflamm. Bowel Dis. *11*, 314–321.

Janeway, C. (2005). Immunobiology: the immune system in health and disease (New York: Garland Science).

Janeway, C.A. (1989). Approaching the Asymptote? Evolution and Revolution in Immunology. Cold Spring Harb Symp Quant Biol *54*, 1–13.

Jiang, H., and Chess, L. (2000). The specific regulation of immune responses by CD8+ T cells restricted by the MHC class Ib molecule, Qa-1. Annu. Rev. Immunol. *18*, 185–216.

Jones, D.A., and Takemoto, D. (2004). Plant innate immunity - direct and indirect recognition of general and specific pathogen-associated molecules. Curr. Opin. Immunol. *16*, 48–62.

Jostins, L., Ripke, S., Weersma, R.K., Duerr, R.H., McGovern, D.P., Hui, K.Y., Lee, J.C., Philip Schumm, L., Sharma, Y., Anderson, C.A., et al. (2012). Host-microbe interactions have shaped the genetic architecture of inflammatory bowel disease. Nature *491*, 119–124.

Kanazawa, N., Okafuji, I., Kambe, N., Nishikomori, R., Nakata-Hizume, M., Nagai, S., Fuji, A., Yuasa, T., Manki, A., Sakurai, Y., et al. (2005). Early-onset sarcoidosis and CARD15 mutations with constitutive nuclear factor-kappaB activation: common genetic etiology with Blau syndrome. Blood *105*, 1195–1197.

Kanneganti, T.-D., Body-Malapel, M., Amer, A., Park, J.-H., Whitfield, J., Franchi, L., Taraporewala, Z.F., Miller, D., Patton, J.T., Inohara, N., et al. (2006a). Critical role for Cryopyrin/Nalp3 in activation of caspase-1 in response to viral infection and double-stranded RNA. J. Biol. Chem. *281*, 36560–36568.

Kanneganti, T.-D., Ozören, N., Body-Malapel, M., Amer, A., Park, J.-H., Franchi, L., Whitfield, J., Barchet, W., Colonna, M., Vandenabeele, P., et al. (2006b). Bacterial RNA and small antiviral compounds activate caspase-1 through cryopyrin/Nalp3. Nature *440*, 233–236.

Karimuddin, Gilles (2015). Surgery for Abdominal/Intestinal Crohn's Disease.

Kaser, A., Zeissig, S., and Blumberg, R.S. (2010). Inflammatory Bowel Disease. Annual Review of Immunology *28*, 573–621.

Kawai, T., and Akira, S. (2010). The role of pattern-recognition receptors in innate immunity: update on Toll-like receptors. Nat Immunol *11*, 373–384.

Kobayashi, Y. (2006). Neutrophil infiltration and chemokines. Crit. Rev. Immunol. *26*, 307–316.

Koboziev, I., Karlsson, F., and Grisham, M.B. (2010). Gut-associated lymphoid tissue, T cell trafficking, and chronic intestinal inflammation. Annals of the New York Academy of Sciences *1207*, E86–E93.

Komatsu, M., Kobayashi, D., Saito, K., Furuya, D., Yagihashi, A., Araake, H., Tsuji, N., Sakamaki, S., Niitsu, Y., and Watanabe, N. (2001). Tumor Necrosis Factor-α in Serum of Patients with Inflammatory Bowel Disease as Measured by a Highly Sensitive Immuno-PCR. Clinical Chemistry *47*, 1297–1301.

Kuenzel, S., Till, A., Winkler, M., Häsler, R., Lipinski, S., Jung, S., Grötzinger, J., Fickenscher, H., Schreiber, S., and Rosenstiel, P. (2010). The Nucleotide-Binding Oligomerization Domain-Like Receptor NLRC5 Is Involved in IFN-Dependent Antiviral Immune Responses. J Immunol *184*, 1990–2000.

Kufer, T.A., Kremmer, E., Adam, A.C., Philpott, D.J., and Sansonetti, P.J. (2008). The pattern-recognition molecule Nod1 is localized at the plasma membrane at sites of bacterial interaction. Cell. Microbiol. *10*, 477–486.

Kumar, H., Pandey, S., Zou, J., Kumagai, Y., Takahashi, K., Akira, S., and Kawai, T. (2011). NLRC5 deficiency does not influence cytokine induction by virus and bacteria infections. J. Immunol *186*, 994–1000.

Kwon, K.H., Murakami, A., Hayashi, R., and Ohigashi, H. (2005). Interleukin-1β targets interleukin-6 in progressing dextran sulfate sodium-induced experimental colitis. Biochemical and Biophysical Research Communications *337*, 647–654.

Laemmli, U.K. (1970). Cleavage of structural proteins during the assembly of the head of bacteriophage T4. Nature *227*, 680–685.

Li, L., Xu, T., Huang, C., Peng, Y., and Li, J. (2014). NLRC5 Mediates Cytokine Secretion in RAW264.7 Macrophages and Modulated by the JAK2/STAT3 Pathway. Inflammation 1–13.

Ligumsky, M., Simon, P.L., Karmeli, F., and Rachmilewitz, D. (1990). Role of interleukin 1 in inflammatory bowel disease--enhanced production during active disease. Gut *31*, 686–689.

Lippert, H. (2003). Lehrbuch Anatomie. In Lehrbuch Anatomie: 183 Tabellen, (München; Jena: Urban und Fischer), p. 316.

Lowry, O.H., Rosebrough, N.J., Farr, A.L., and Randall, R.J. (1951). Protein measurement with the Folin phenol reagent. J. Biol. Chem. *193*, 265–275.

Mahida, Y.R., Wu, K., and Jewell, D.P. (1989). Enhanced production of interleukin 1-beta by mononuclear cells isolated from mucosa with active ulcerative colitis of Crohn's disease. Gut *30*, 835–838.

Mähler, M., Bristol, I.J., Leiter, E.H., Workman, A.E., Birkenmeier, E.H., Elson, C.O., and Sundberg, J.P. (1998). Differential susceptibility of inbred mouse strains to dextran sulfate sodium-induced colitis. Am. J. Physiol. *274*, G544–G551.

Malmgaard, L. (2004). Induction and Regulation of IFNs During Viral Infections. Journal of Interferon & Cytokine Research *24*, 439–454.

Marguerat, S., MacDonald, H.R., Kraehenbuhl, J.P., and van Meerwijk, J.P. (1999). Protection from radiation-induced colitis requires MHC class II antigen expression by cells of hemopoietic origin. J. Immunol. *163*, 4033–4040.

Mariathasan, S., Weiss, D.S., Newton, K., McBride, J., O'Rourke, K., Roose-Girma, M., Lee, W.P., Weinrauch, Y., Monack, D.M., and Dixit, V.M. (2006). Cryopyrin activates the inflammasome in response to toxins and ATP. Nature *440*, 228–232.

Martin, B., Banz, A., Bienvenu, B., Cordier, C., Dautigny, N., Bécourt, C., and Lucas, B. (2004). Suppression of CD4+ T Lymphocyte Effector Functions by CD4+CD25+ Cells In Vivo. J Immunol *172*, 3391–3398.

Martin, B.K., Chin, K.C., Olsen, J.C., Skinner, C.A., Dey, A., Ozato, K., and Ting, J.P. (1997). Induction of MHC class I expression by the MHC class II transactivator CIITA. Immunity *6*, 591–600.

Martinon, F., and Tschopp, J. (2004). Inflammatory caspases: linking an intracellular innate immune system to autoinflammatory diseases. Cell *117*, 561–574.

Martinon, F., and Tschopp, J. (2005). NLRs join TLRs as innate sensors of pathogens. Trends in Immunology *26*, 447–454.

Martinon, F., Burns, K., and Tschopp, J. (2002). The Inflammasome: A Molecular Platform Triggering Activation of Inflammatory Caspases and Processing of proIL-β. Molecular Cell *10*, 417–426.

Martinon, F., Pétrilli, V., Mayor, A., Tardivel, A., and Tschopp, J. (2006). Gout-associated uric acid crystals activate the NALP3 inflammasome. Nature *440*, 237–241.

Mayer, L., and Eisenhardt, D. (1990). Lack of induction of suppressor T cells by intestinal epithelial cells from patients with inflammatory bowel disease. J. Clin. Invest. *86*, 1255–1260.

Mayer, L., Eisenhardt, D., Salomon, P., Bauer, W., Plous, R., and Piccinini, L. (1991). Expression of class II molecules on intestinal epithelial cells in humans. Differences between normal and inflammatory bowel disease. Gastroenterology *100*, 3–12.

McDermott, M.F. (2002). Genetic clues to understanding periodic fevers, and possible therapies. Trends Mol Med *8*, 550–554.

MedlinePlus Splenomegaly: MedlinePlus Medical Encyclopedia.

Medscape (2014). Splenomegaly.

Meissner, T.B., Li, A., Biswas, A., Lee, K.-H., Liu, Y.-J., Bayir, E., Iliopoulos, D., van den Elsen, P.J., and Kobayashi, K.S. (2010). NLR family member NLRC5 is a transcriptional regulator of MHC class I genes. Proc. Natl. Acad. Sci. U.S.A *107*, 13794–13799.

Meissner, T.B., Li, A., Liu, Y.-J., Gagnon, E., and Kobayashi, K.S. (2012a). The nucleotide-binding domain of NLRC5 is critical for nuclear import and transactivation activity. Biochemical and Biophysical Research Communications *418*, 786–791.

Meissner, T.B., Liu, Y.-J., Lee, K.-H., Li, A., Biswas, A., Van Eggermond, M.C.J.A., Van Den Elsen, P.J., and Kobayashi, K.S. (2012b). NLRC5 Cooperates with the RFX Transcription Factor Complex To Induce MHC Class I Gene Expression. J Immunol.

Mempel, T.R., Pittet, M.J., Khazaie, K., Weninger, W., Weissleder, R., von Boehmer, H., and von Andrian, U.H. (2006). Regulatory T cells reversibly suppress cytotoxic T cell function independent of effector differentiation. Immunity *25*, 129–141.

Miceli-Richard, C., Lesage, S., Rybojad, M., Prieur, A.M., Manouvrier-Hanu, S., Häfner, R., Chamaillard, M., Zouali, H., Thomas, G., and Hugot, J.P. (2001). CARD15 mutations in Blau syndrome. Nat. Genet. *29*, 19–20.

Mogensen, T.H. (2009). Pathogen Recognition and Inflammatory Signaling in Innate Immune Defenses. Clinical Microbiology Reviews *22*, 240–273.

Moore, C.B., Bergstralh, D.T., Duncan, J.A., Lei, Y., Morrison, T.E., Zimmermann, A.G., Accavitti-Loper, M.A., Madden, V.J., Sun, L., Ye, Z., et al. (2008). NLRX1 is a regulator of mitochondrial antiviral immunity. Nature *451*, 573–577.

Morgan, D.A., Ruscetti, F.W., and Gallo, R. (1976). Selective in vitro growth of T lymphocytes from normal human bone marrows. Science *193*, 1007–1008.

Muhlethaler-Mottet, A., Otten, L.A., Steimle, V., and Mach, B. (1997). Expression of MHC class II molecules in different cellular and functional compartments is controlled by differential usage of multiple promoters of the transactivator CIITA. EMBO J *16*, 2851–2860.

Muller, A.F., and Toghill, P.J. (1995). Hyposplenism in gastrointestinal disease. Gut *36*, 165–167.

Müller, S., Lory, J., Corazza, N., Griffiths, G.M., Z'graggen, K., Mazzucchelli, L., Kappeler, A., and Mueller, C. (1998). Activated CD4+ and CD8+ cytotoxic cells are present in increased numbers in the intestinal mucosa from patients with active inflammatory bowel disease. Am J Pathol *152*, 261–268.

Müller, U., Steinhoff, U., Reis, L.F., Hemmi, S., Pavlovic, J., Zinkernagel, R.M., and Aguet, M. (1994). Functional role of type I and type II interferons in antiviral defense. Science *264*, 1918–1921.

Muñoz-Planillo, R., Kuffa, P., Martínez-Colón, G., Smith, B.L., Rajendiran, T.M., and Núñez, G. (2013). K^+ efflux is the common trigger of NLRP3 inflammasome activation by bacterial toxins and particulate matter. Immunity *38*, 1142–1153.

Neefjes, J., Jongsma, M.L.M., Paul, P., and Bakke, O. (2011). Towards a systems understanding of MHC class I and MHC class II antigen presentation. Nat Rev Immunol *11*, 823–836.

Neerincx, A., Lautz, K., Menning, M., Kremmer, E., Zigrino, P., Hösel, M., Büning, H., Schwarzenbacher, R., and Kufer, T.A. (2010). A role for the human nucleotide-binding domain, leucine-rich repeat-containing family member NLRC5 in antiviral responses. J. Biol. Chem *285*, 26223–26232.

Neerincx, A., Rodriguez, G.M., Steimle, V., and Kufer, T.A. (2012). NLRC5 Controls Basal MHC Class I Gene Expression in an MHC Enhanceosome-Dependent Manner. J Immunol.

Neerincx, A., Jakobshagen, K., Utermöhlen, O., Büning, H., Steimle, V., and Kufer, T.A. (2014). The N-Terminal Domain of NLRC5 Confers Transcriptional Activity for MHC Class I and II Gene Expression. J Immunol *193*, 3090–3100.

Nell, S., Suerbaum, S., and Josenhans, C. (2010). The impact of the microbiota on the pathogenesis of IBD: lessons from mouse infection models. Nat. Rev. Microbiol. *8*, 564–577.

Neurath, M.F. (2014). Cytokines in inflammatory bowel disease. Nat. Rev. Immunol. *14*, 329–342.

Ni, J., Chen, S.F., and Hollander, D. (1996). Effects of dextran sulphate sodium on intestinal epithelial cells and intestinal lymphocytes. Gut *39*, 234–241.

Nicklas, W., Baneux, P., Boot, R., Decelle, T., Deeny, A.A., Fumanelli, M., Illgen-Wilcke, B., and FELASA (Federation of European Laboratory Animal Science Associations Working Group on Health Monitoring of Rodent and Rabbit Colonies) (2002). Recommendations for the health monitoring of rodent and rabbit colonies in breeding and experimental units. Lab. Anim. *36*, 20–42.

Noguchi, M., Hiwatashi, N., Liu, Z., and Toyota, T. (1995). Enhanced interferon-gamma production and B7-2 expression in isolated intestinal mononuclear cells from patients with Crohn's disease. J. Gastroenterol. *30 Suppl 8*, 52–55.

Obermeier, F., Kojouharoff, G., Hans, W., Schölmerich, J., Gross, V., and Falk, W. (1999). Interferon-gamma (IFN-γ)- and tumour necrosis factor (TNF)-induced nitric oxide as toxic effector molecule in chronic dextran sulphate sodium (DSS)-induced colitis in mice. Clin Exp Immunol *116*, 238–245.

Ogura, Y., Bonen, D.K., Inohara, N., Nicolae, D.L., Chen, F.F., Ramos, R., Britton, H., Moran, T., Karaliuskas, R., Duerr, R.H., et al. (2001). A frameshift mutation in NOD2 associated with susceptibility to Crohn's disease. Nature *411*, 603–606.

Ohkusa, T. (1985). [Production of experimental ulcerative colitis in hamsters by dextran sulfate sodium and changes in intestinal microflora]. Nihon Shokakibyo Gakkai Zasshi *82*, 1327–1336.

Okada, Y., Maeda, N., Takakura, S., Miyata, K., and Koshiba, M. (2011). Tacrolimus ameliorates dextran sulfate sodium-induced colitis in mice: implication of interferon-γ and interleukin-1β suppression. Biol. Pharm. Bull. *34*, 1823–1827.

Okayasu, I., Hatakeyama, S., Yamada, M., Ohkusa, T., Inagaki, Y., and Nakaya, R. (1990). A novel method in the induction of reliable experimental acute and chronic ulcerative colitis in mice. Gastroenterology *98*, 694–702.

Okazaki, K., Morita, M., Nishimori, I., Sano, S., Toyonaga, M., Nakazawa, Y., Yamamoto, Y., and Yamamoto, Y. (1993). Major histocompatibility antigen-restricted cytotoxicity in inflammatory bowel disease. Gastroenterology *104*, 384–391.

Park, J.-H., Kim, Y.-G., McDonald, C., Kanneganti, T.-D., Hasegawa, M., Body-Malapel, M., Inohara, N., and Núñez, G. (2007). RICK/RIP2 mediates innate immune responses induced through Nod1 and Nod2 but not TLRs. J. Immunol. *178*, 2380–2386.

Pereira, J.L.R., Hughes, P.L.E., and Young, H.L. (1987). Spleen size in patients with inflammatory bowel disease. Dis Colon Rectum *30*, 403–409.

Perse, E, M., and Cerar, A. (2012). Dextran Sodium Sulphate Colitis Mouse Model: Traps and Tricks. BioMed Research International *2012*.

Podolsky, D.K. (2002). Inflammatory Bowel Disease. New England Journal of Medicine *347*, 417–429.

Powrie, F., Leach, M.W., Mauze, S., Menon, S., Barcomb Caddle, L., and Coffman, R.L. (1994). Inhibition of Thl responses prevents inflammatory bowel disease in scid mice reconstituted with CD45RBhi CD4+ T cells. Immunity *1*, 553–562.

Ranjan, P., Singh, N., Kumar, A., Neerincx, A., Kremmer, E., Cao, W., Davis, W.G., Katz, J.M., Gangappa, S., Lin, R., et al. (2014). NLRC5 interacts with RIG-I to induce a robust antiviral response against influenza virus infection. Eur. J. Immunol. n/a – n/a.

Rawlings, J.S., Rosler, K.M., and Harrison, D.A. (2004). The JAK/STAT signaling pathway. Journal of Cell Science *117*, 1281–1283.

Reinecker, H.C., Steffen, M., Witthoeft, T., Pflueger, I., Schreiber, S., MacDermott, R.P., and Raedler, A. (1993). Enhanced secretion of tumour necrosis factor-alpha, IL-6, and IL-1 beta by isolated lamina propria mononuclear cells from patients with ulcerative colitis and Crohn's disease. Clin. Exp. Immunol. *94*, 174–181.

Reith, W., LeibundGut-Landmann, S., and Waldburger, J.-M. (2005). Regulation of MHC class II gene expression by the class II transactivator. Nat Rev Immunol *5*, 793–806.

Reits, E., Griekspoor, A., Neijssen, J., Groothuis, T., Jalink, K., van Veelen, P., Janssen, H., Calafat, J., Drijfhout, J.W., and Neefjes, J. (2003). Peptide diffusion, protection, and degradation in nuclear and cytoplasmic compartments before antigen presentation by MHC class I. Immunity *18*, 97–108.

Rennick, D.M., Fort, M.M., and Davidson, N.J. (1997). Studies with IL-10-/- mice: an overview. J. Leukoc. Biol. *61*, 389–396.

Rioux, J.D., Xavier, R.J., Taylor, K.D., Silverberg, M.S., Goyette, P., Huett, A., Green, T., Kuballa, P., Barmada, M.M., Datta, L.W., et al. (2007). Genome-wide association study identifies new susceptibility loci for Crohn disease and implicates autophagy in disease pathogenesis. Nat. Genet. *39*, 596–604.

Robbins, G.R., Truax, A.D., Davis, B.K., Zhang, L., Brickey, W.J., and Ting, J.P.-Y. (2012). Regulation of Class I Major Histocompatibility Complex (MHC) by Nucleotide-Binding Domain, Leucine-Rich Repeat-Containing (NLR) Proteins. J. Biol. Chem.

Round, J.L., and Mazmanian, S.K. (2009). The gut microbiota shapes intestinal immune responses during health and disease. Nat. Rev. Immunol. *9*, 313–323.

Rozen, P., Flatau, E., Schujman, E., and Gefel, A. (1977). Variability of splenomegaly in Crohn's disease. Am. J. Gastroenterol. *67*, 498–493.

Ryan, F.P., Smart, R.C., Holdsworth, C.D., and Preston, F.E. (1978). Hyposplenism in inflammatory bowel disease. Gut *19*, 50–55.

Al-Sadi, R.M., and Ma, T.Y. (2007). IL-1β Causes an Increase in Intestinal Epithelial Tight Junction Permeability. J Immunol *178*, 4641–4649.

Saiki, R.K., Scharf, S., Faloona, F., Mullis, K.B., Horn, G.T., Erlich, H.A., and Arnheim, N. (1985). Enzymatic amplification of beta-globin genomic sequences and restriction site analysis for diagnosis of sickle cell anemia. Science *230*, 1350–1354.

Sasaki, T., Hiwatashi, N., Yamazaki, H., Noguchi, M., and Toyota, T. (1992). The role of interferon gamma in the pathogenesis of Crohn's disease. Gastroenterol. Jpn. *27*, 29–36.

Satsangi, J., Wolstencroft, R.A., Cason, J., Ainley, C.C., Dumonde, D.C., and Thompson, R.P. (1987). Interleukin 1 in Crohn's disease. Clin. Exp. Immunol. *67*, 594–605.

Schroder, K., Hertzog, P.J., Ravasi, T., and Hume, D.A. (2004). Interferon-γ: an overview of signals, mechanisms and functions. Journal of Leukocyte Biology *75*, 163–189.

Seifert, U., Bialy, L.P., Ebstein, F., Bech-Otschir, D., Voigt, A., Schröter, F., Prozorovski, T., Lange, N., Steffen, J., Rieger, M., et al. (2010). Immunoproteasomes preserve protein homeostasis upon interferon-induced oxidative stress. Cell *142*, 613–624.

Shapiro, A.L., Viñuela, E., and Maizel, J.V. (1967). Molecular weight estimation of polypeptide chains by electrophoresis in SDS-polyacrylamide gels. Biochem. Biophys. Res. Commun. *28*, 815–820.

Sheikh, S.Z., Matsuoka, K., Kobayashi, T., Li, F., Rubinas, T., and Plevy, S.E. (2010). Cutting edge: IFN-gamma is a negative regulator of IL-23 in murine macrophages and experimental colitis. J. Immunol. *184*, 4069–4073.

Shinoda, M., Shin-Ya, M., Naito, Y., Kishida, T., Ito, R., Suzuki, N., Yasuda, H., Sakagami, J., Imanishi, J., Kataoka, K., et al. (2010). Early-stage blocking of Notch signaling inhibits the depletion of goblet cells in dextran sodium sulfate-induced colitis in mice. J. Gastroenterol. *45*, 608–617.

Siegmund, B., Rieder, F., Albrich, S., Wolf, K., Bidlingmaier, C., Firestein, G.S., Boyle, D., Lehr, H.A., Loher, F., Hartmann, G., et al. (2001a). Adenosine kinase inhibitor GP515 improves experimental colitis in mice. J. Pharmacol. Exp. Ther. *296*, 99–105.

Siegmund, B., Lehr, H.-A., Fantuzzi, G., and Dinarello, C.A. (2001b). IL-1β-converting enzyme (caspase-1) in intestinal inflammation. Proc Natl Acad Sci U S A *98*, 13249–13254.

Singer, D.S., and Devaiah, B.N. (2013). CIITA and its dual roles in MHC gene transcription. Front. Immunol. *4*, 476.

Spilianakis, C., Papamatheakis, J., and Kretsovali, A. (2000). Acetylation by PCAF Enhances CIITA Nuclear Accumulation and Transactivation of Major Histocompatibility Complex Class II Genes. Mol. Cell. Biol. *20*, 8489–8498.

Staehli, F., Ludigs, K., Heinz, L.X., Seguín-Estévez, Q., Ferrero, I., Braun, M., Schroder, K., Rebsamen, M., Tardivel, A., Mattmann, C., et al. (2012). NLRC5 Deficiency Selectively Impairs MHC Class I- Dependent Lymphocyte Killing by Cytotoxic T Cells. J Immunol *188*, 3820–3828.

Steimle, V., Siegrist, C.A., Mottet, A., Lisowska-Grospierre, B., and Mach, B. (1994). Regulation of MHC class II expression by interferon-gamma mediated by the transactivator gene CIITA. Science *265*, 106–109.

Stokkers, P., Reitsma, P., Tytgat, G., and van Deventer, S.J.H. (1999). HLA-DR and -DQ phenotypes in inflammatory bowel disease: a meta-analysis. Gut *45*, 395–401.

Strober, W., Fuss, I.J., and Blumberg, R.S. (2002). The Immunology of Mucosal Models of Inflammation1. Annual Review of Immunology *20*, 495–549.

Tanimura, N., Saitoh, S., Matsumoto, F., Akashi-Takamura, S., and Miyake, K. (2008). Roles for LPS-dependent interaction and relocation of TLR4 and TRAM in TRIF-signaling. Biochem. Biophys. Res. Commun. *368*, 94–99.

Thelemann, C., Eren, R.O., Coutaz, M., Brasseit, J., Bouzourene, H., Rosa, M., Duval, A., Lavanchy, C., Mack, V., Mueller, C., et al. (2014). Interferon-γ Induces Expression of MHC Class II on Intestinal Epithelial Cells and Protects Mice from Colitis. PLoS ONE *9*, e86844.

Thomas, K.R., and Capecchi, M.R. (1987). Site-directed mutagenesis by gene targeting in mouse embryo-derived stem cells. Cell *51*, 503–512.

Ting, J.P.-Y., Lovering, R.C., Alnemri, E.S., Bertin, J., Boss, J.M., Davis, B.K., Flavell, R.A., Girardin, S.E., Godzik, A., Harton, J.A., et al. (2008). The NLR Gene Family: A Standard Nomenclature. Immunity *28*, 285–287.

Tlaskalová-Hogenová, H., Tucková, L., Stepánková, R., Hudcovic, T., Palová-Jelínková, L., Kozáková, H., Rossmann, P., Sanchez, D., Cinová, J., Hrncír, T., et al. (2005). Involvement of innate immunity in the development of inflammatory and autoimmune diseases. Ann. N. Y. Acad. Sci. *1051*, 787–798.

Toes, R.E., Nussbaum, A.K., Degermann, S., Schirle, M., Emmerich, N.P., Kraft, M., Laplace, C., Zwinderman, A., Dick, T.P., Müller, J., et al. (2001). Discrete cleavage motifs of constitutive and immunoproteasomes revealed by quantitative analysis of cleavage products. J. Exp. Med. *194*, 1–12.

Tong, Y., Cui, J., Li, Q., Zou, J., Wang, H.Y., and Wang, R.-F. (2012). Enhanced TLR-induced NF-|[kappa]|B signaling and type I interferon responses in NLRC5 deficient mice. Cell Research.

Tresca (2015). How Resection Surgery Can Treat Crohn's Disease.

Triantafilou, K., Kar, S., van Kuppeveld, F.J.M., and Triantafilou, M. (2013). Rhinovirus-Induced Calcium Flux Triggers NLRP3 and NLRC5 Activation in Bronchial Cells. Am. J. Respir. Cell Mol. Biol.

Tschopp, J., Martinon, F., and Burns, K. (2003). NALPs: a novel protein family involved in inflammation. Nat. Rev. Mol. Cell Biol. *4*, 95–104.

Villani, A.-C., Lemire, M., Fortin, G., Louis, E., Silverberg, M.S., Collette, C., Baba, N., Libioulle, C., Belaiche, J., Bitton, A., et al. (2009). Common variants in the NLRP3 region contribute to Crohn's disease susceptibility. Nat Genet *41*, 71–76.

Wagner, R.N., Proell, M., Kufer, T.A., and Schwarzenbacher, R. (2009). Evaluation of Nod-Like Receptor (NLR) Effector Domain Interactions. PLoS ONE *4*, e4931.

Waldner, M.J., Wirtz, S., Becker, C., Seidel, D., Tubbe, I., Cappel, K., Hähnel, P.S., Galle, P.R., Schuler, M., and Neurath, M.F. (2010). Perforin deficiency attenuates inflammation and tumor growth in colitis-associated cancer. Inflamm. Bowel Dis. *16*, 559–567.

Wang, Y.M., and Alexander, S.I. (2009). CD8 regulatory T cells: What's old is now new. Immunol Cell Biol *87*, 192–193.

Wang, X., Kuivaniemi, H., Bonavita, G., Mutkus, L., Mau, U., Blau, E., Inohara, N., Nunez, G., Tromp, G., and Williams, C.J. (2002). CARD15 mutations in familial granulomatosis syndromes: a study of the original Blau syndrome kindred and other families with large-vessel arteritis and cranial neuropathy. Arthritis Rheum. *46*, 3041–3045.

Westendorf, A.M., Fleissner, D., Groebe, L., Jung, S., Gruber, A.D., Hansen, W., and Buer, J. (2009). CD4+Foxp3+ regulatory T cell expansion induced by antigen-driven interaction with intestinal epithelial cells independent of local dendritic cells. Gut *58*, 211–219.

Williams, T.M., Leeth, R.A., Rothschild, D.E., Coutermarsh-Ott, S.L., McDaniel, D.K., Simmons, A.E., Heid, B., Cecere, T.E., and Allen, I.C. (2015). The NLRP1 Inflammasome Attenuates Colitis and Colitis-Associated Tumorigenesis. J Immunol 1402098.

Wirtz, S., Neufert, C., Weigmann, B., and Neurath, M.F. (2007). Chemically induced mouse models of intestinal inflammation. Nat. Protocols *2*, 541–546.

Xavier, R.J., and Podolsky, D.K. (2007). Unravelling the pathogenesis of inflammatory bowel disease. Nature *448*, 427–434.

Yan, Y., Kolachala, V., Dalmasso, G., Nguyen, H., Laroui, H., Sitaraman, S.V., and Merlin, D. (2009). Temporal and Spatial Analysis of Clinical and Molecular Parameters in Dextran Sodium Sulfate Induced Colitis. PLoS ONE *4*, e6073.

Yao, Y., Wang, Y., Chen, F., Huang, Y., Zhu, S., Leng, Q., Wang, H., Shi, Y., and Qian, Y. (2012). NLRC5 regulates MHC class I antigen presentation in host defense against intracellular pathogens. Cell Research.

Yossef, R., Rosental, B., Appel, M.Y., Hershkovitz, O., and Porgador, A. (2012). Upregulation of MHC class I expression following dengue virus infection: the mechanism at the promoter level. Expert Rev Anti Infect Ther *10*, 285–287.

Zaki, M.H., Boyd, K.L., Vogel, P., Kastan, M.B., Lamkanfi, M., and Kanneganti, T.-D. (2010). The NLRP3 inflammasome protects against loss of epithelial integrity and mortality during experimental colitis. Immunity *32*, 379–391.

Zaki, M.H., Vogel, P., Malireddi, R.K.S., Body-Malapel, M., Anand, P.K., Bertin, J., Green, D.R., Lamkanfi, M., and Kanneganti, T.-D. (2011). The NOD-like receptor NLRP12 attenuates colon inflammation and tumorigenesis. Cancer Cell *20*, 649–660.

Zenewicz, L.A., Antov, A., and Flavell, R.A. (2009). CD4 T-cell differentiation and inflammatory bowel disease. Trends in Molecular Medicine *15*, 199–207.

Pflanzentoxine - Chemgapedia.

M. R. The Nobel Prize in Physiology or Medicine 2007.

8.2 FIGURE DIRECTORY

Fig. 1-1: Tripartite NLR structure 13
Fig. 1-2: Generation and presentation of antigenic peptides 18
Fig. 3-1: *NLRC5* expression in human and murine tissues 39
Fig. 3-2: NLRC5 protein levels and its induction in human cell lines 40
Fig. 3-3: Spleen weight in *Nlrc5* ko mice 41
Fig. 3-4: Structure of secondary lymphoid organs in *Nlrc5* ko mice 42
Fig. 3-5: Immune cell populations in the spleen of *Nlrc5*-deficient mice 43
Fig. 3-6: MHC class I expression on murine *Nlrc5*-deficient macrophages 44
Fig. 3-7: MHC class I expression on murine *Nlrc5*-deficient lymphocytes 45
Fig. 3-8: Identification and analysis of MHC class I (H-2Kb) expressing lymphocyte subpopulations 46
Fig. 3-9: MHC class II expression on *Nlrc5*-deficient leukocytes 47
Fig. 3-10: Surfacial MHC class I expression on murine lymphocytes upon stimulation 48
Fig. 3-11: Induction of *Ifnb* in stimulated *Nlrc5*-deficient primary cell cultures 49
Fig. 3-12: Activation of *Nlrc5*-deficient splenocytes & induction of IFN□□ by LPS 50
Fig. 3-13: Induction and secretion of IL-1β in stimulated *Nlrc5*-deficient primary cells 52
Fig. 3-14: Induction of pro-inflammatory mediators in stimulated *Nlrc5*-deficient BMDMs 53
Fig. 3-15: Treatment of experimental animals to induce acute DSS colitis 54
Fig. 3-16: Survival during the course of acute DSS colitis 54
Fig. 3-17: DAI – A combined score of body weight, stool consistency and fecal occult blood 55
Fig. 3-18: Colon shortening during acute colitis 56
Fig. 3-19: Infiltration of inflammatory cells and epithelial damage in the colon during acute colitis 58
Fig. 3-20: Depletion of mucin-containing goblet cells in murine colon during acute colitis 59
Fig. 3-21: Cytokine expression in murine colon during acute colitis 60
Fig. 3-22: Serum cytokine levels during acute colitis 61
Fig. 3-23: Murine spleen weight during acute colitis 62
Fig. 3-24: Expression of myeloperoxidase during acute colitis 62
Fig. 3-25: Expression of *Cd8* and *Cd4* in murine spleens during acute colitis 63
Fig. 3-26: Treatment of experimental animals to induce chronic DSS colitis 64
Fig. 3-27: Survival during the course of chronic DSS colitis 64
Fig. 3-28: Body weight changes and diarrhea score 65
Fig. 3-29: Colon shortening during chronic colitis 66
Fig. 3-30: Infiltration of inflammatory cells and epithelial damage in the colon during chronic colitis 67
Fig. 3-31: Lymphatic tissue in murine colons upon repeated DSS treatment 68
Fig. 3-32: Cytokine expression in murine colon during chronic colitis 68
Fig. 3-33: Serum cytokine levels during chronic colitis 69
Fig. 3-34: Murine spleen weight during chronic colitis 70
Fig. 3-35: Expression of myeloperoxidase during chronic colitis 70
Fig. 3-36: Expression of *Cd8* and *Cd4* in murine spleen and colon during chronic colitis 71

8.3 TABLE DIRECTORY

Tab. 1: NLR subfamilies classified by effector domain homology....10
Tab. 2: *Nlrc5* knockout strategy....23
Tab. 3: Animal experiment license numbers....24
Tab. 4: *Nlrc5* Genotyping Primer Sequences....24
Tab. 5: Genotyping of *Nlrc5*$^{-/-}$ mice....24
Tab. 6: Cultured immortal and primary cell lines....26
Tab. 7: Cell culture media....27
Tab. 8: List of utilized stimuli....28
Tab. 9: Enzyme-linked immunosorbent assays....29
Tab. 10: Endpoint PCR....32
Tab. 11: Reverse Transcription....33
Tab. 12: TaqMan Assay Procedure....34
Tab. 13: TaqMan Assays obtained from Life Technologies™....34
Tab. 14: Self-casted polyacrylamide gels....35
Tab. 15: Antibody List....36
Tab. 16: Self-arranged buffers....37
Tab. 17: Tissue cDNA panels obtained from Clontech....38
Tab. 18: Software used for data analyses and presentation....38

8.4 ABBREVIATIONS

AD	Acidic activation domain; also: acidic transactivation or acidic domain
AIM2	Absent in melanoma 2
ALR	AIM2-like receptors
APC	Antigen presenting cell
APC + antibody	Allophycocyanin
ASC	Apoptosis-associated speck-like protein containing a CARD
BIR	Baculoviral inhibitory repeat-like domain
BLS	Bare lymphocyte syndrome
BMDC	Bone marrow-derived dendritic cells
BMDM	Bone marrow-derived macrophages
bp	Base pair
BSA	Bovine serum albumin
CARD	Caspase activation and recruitment domain
CD	Crohn´s disease; Morbus Crohn
CD + number	Cluster of differentiation
cDNA	Complementary DNA
CIITA	MHC class II transactivator
CLIP	Class II associated li peptide
CLR	C-type lectin receptors
CMV	Cytomegalovirus
DAMP	Danger-associated molecular pattern
DC	Dendritic cell
DMEM	Dulbecco's Minimal Essential Medium
DNA	Deoxyribonucleic acid
dsRNA	Double stranded RNA
DSS	Dextran sulfate sodium
DSZM	German Collection of Microorganisms and Cell cultures (Deutsche Sammlung von Mikroorganismen und Zellkulturen)
EDTA	Ethylenediaminetetraacetic acid
ES	Embryonic stem cell
FCS	Fetal calf serum
FELASA	Federation European Laboratory Animal Science Association
FITC	Fluorescein isothiocyanate
FRET	Förster or fluorescence resonance energy transfer
FSC	Forward scatter
GALT	Gut-associated lymphoid tissue
GAPDH	Glyceraldehyde 3-phosphate dehydrogenase
GAS	IFNɣ activation sequence
gDNA	Genomic DNA
GM-CSF	Granulocyte macrophage colony-stimulating factor
GWAS	Genome-wide association study
HE	Hematoxylin and eosin
HEPES	4-(2-hydroxyethyl)-1-piperazineethanesulfonic acid
HET-E	incompatibility locus protein from Podospora anserina
HLA	Human leukocyte antigen
HRP	Horseradish peroxidase
HSV-1	Herpes simplex virus 1
hu	Human
IBD	Inflammatory bowel disease
IEC	intestinal epithelial cells
IFN	Interferon
IFNAR	Type I interferon receptor
IgG	Immunoglobulin G
IKKα/IKKβ	IκB kinase heterodimer
IL	Interleukin
Iono	Ionomycin

IRF	Interferon regulatory factor
ISG	Interferone stimulated gene
ISRE	Interferon-specific response element
IVC	Individually ventilated cages
IκB	Inhibitor of NF-κB
KC	Keratinocyte-derived chemokine; CXCL1
LMP2	Low-molecular-mass protein 2
LPS	Lipopolysaccharid
LRR	Leucine-rich repeat
MALT	Mucosa-associated lymphoid tissue
MAPK	Mitogen-activated protein kinases
M-CSF	Macrophage-colony stimulating factor
MDA5	Melanoma differentiation associated gene 5
MIP1a	Macrophage inflammatory protein 1 alpha ; CCL3
MMLV	Moloney Murine Leukemia Virus
MMM	Mouse Macrophage Medium
MPO	Myeloperoxidase
mRNA	Messenger ribonucleic acid
ms	Mouse
MyD88	Myeloid differentiation primary response gene 88
Mϕ	Macrophage
NACHT	Acronym: NAIP, CIITA, HET-E, TP1
NAIP	Neuronal apoptosis inhibitor protein
NBD	Nucleotide-binding domain
NDV	Newcastle disease virus
NFDM	Non fat dry milk
NF-κB	Nuclear factor 'kappa-light-chain-enhancer' of activated B-cells
NK cell	Natural killer cell
NKT cell	Natural killer T cell
NLR	NBD and LRR-containing gene family
NLRA	NLR family, AC domain containing
NLRB	NLR family, BIR domain containing
NLRC	NLR family, CARD domain containing
NLRP	NLR family, PYD domain containing
NLS	Nuclear localization signal
NOD	Nucleotide-binding and oligomerization domain
number + h	Hour(s)
o/n	Overnight
OAS	Oligoadenylate syntethase
PAF	Platelet-activating factor
PAGE	Polyacrylamid gel electrophoresis
PAMP	Pathogen-associated microbial pattern
PBMC	Peripheral blood mononuclear cell
PBS	Phosphate-buffered saline
PCR	Polymerase chain reaction
PE	R-Phycoerythrin
PHA	Phytohemagglutinin
PI	Propidium iodide
PMA	Phorbol 12-myristate 13-acetate
poly(I:C)	Polyinosinic acid-polycytidylic acid; synthetic dsRNA
PRR	Pattern recognition receptors
PYD	Pyrin domain
RANTES	Regulated on Activation, Normal T cell Expressed and Secreted
rh	Recombinant human
RIG-I	Retinoic Acid-Inducible Gene 1
RLR	Retinoic Acid-Inducible Gene 1-Like Receptor
rm	Recombinant murine
RNA	Ribonucleic acid
ROS	Reactive oxygen species

RPMI	Roswell Park Memorial Institute medium
RT PCR	Reverse transcription PCR
RT-qPCR	Real Time quantitative PCR
SDS	Sodium dodecyl sulfate
SEM	Standard Error of the Mean
SeV	Sendai virus
SPF	Specific pathogen-free
SSC	Sideward scatter
ssRNA	Single stranded RNA
TAE	Tris base / acetic acid / EDTA buffer
TAP	Transporter-associated with peptide binding
tapasin	TAP-associated glycoprotein
Taq	Polymerase initially found in *Thermus aquaticus*
TCR	T cell receptor
TEMED	N,N,N′,N′-Tetramethylethylenediamine
TGF-β	Transforming growth factor beta
TIR	TOLL/IL1 receptor
TLR	Toll-like receptor
TNBS	2,4,6-Trinitrobenzenesulfonic acid
TNFα	Tumor necrosis factor alpha
TP1	Telomerase-associated protein
Treg	Regulatory T cell
TRIF	TIR-domain-containing adapter inducing interferon-β
Tris	Tris(hydroxymethyl)aminomethane
UC	Ulcerative colitis; Colitis ulcerosa
VHH	Victor Hensen House (animal facility)
VSV	Vesicular stomatitis virus
ZTH	Central animal facility
β2M	Beta-2-microglobulin